Inhibition of glucose uptake in NK cells enhances their serial killing capacity

Dissertation

submitted to the

Faculty of Chemistry and Biological Chemistry

at the Technische Universität Dortmund

for the degree of

Doctor of Natural Sciences

Thesis by Lea Katharina Picard (born in Siegen)

Referees Prof. Dr. Carsten Watzl

Prof. Dr. Dr. Philipp Zimmer

Für meine Eltern

1 Table of content

2 Acknowledgements

Zuerst möchte ich mich bei Prof. Carsten Watzl für die Möglichkeit bedanken hier meine Doktorarbeit zu schreiben. Ich danke dir für deine Betreuung, dein Vertrauen in mich und meine Arbeit, für die Möglichkeiten, die du mir gegeben hast und deine stets offene Tür.

Ein weiteres Danke an Prof. Philipp Zimmer für die Begutachtung meiner Dissertation als Zweitgutachter.

Ein Dankeschön auch an Prof. Silvia Capellino, die immer ein offenes Ohr für mich hatte und stets mit Ratschlägen zur Seite stand.

Ein sehr herzliches und besonderes Danke geht an:

Alex	Elena	Leonie	Mina	Peter
Biene	Isabel	Maren	Natalie	Sarah
Doris U.	Jens	Martin	Nicole	Vivian
Doris T	Lejla	Mia	Nora	

Euch möchte ich von Herzen für diese unglaublich schönen 3 ¾ Jahre DANKEN. Ihr wart immer mit einem offenen Ohr, mit Ratschlägen, Tipps und Tricks zur Stelle und habt mich immer gerne ins Labor kommen lassen. Dazu zählt eben nicht nur die Arbeit, sondern auch die gemeinsamen Pausen (mit und ohne Kaffee), Süßigkeiten und die gemeinsamen Gespräche. Ich habe viel gelernt...auch abseits des Labors. Es war eine unglaublich schöne, lehrreiche, lustige und wertvolle Zeit mit Euch und ich bin sehr froh meine Doktorandenzeit mit Euch erlebt zu haben.

Ebenso möchte ich mich auch bei meinen Eltern, meiner Familie und meinen Freunden bedanken. Ihr habt mich immer unterstützt und habt mich immer wissen lassen, dass ich alles machen und schaffen kann. Felix, dir danke ich dafür, dass du mich auch in den stressigen Zeiten ertragen, mich unterstützt und aufgebaut hast.

Jedem einzelnen von Euch sage ich ein herzliches Dankeschön für Eure Worte, Eure Zeit, Eure Nerven und Euren Humor.

3 Abstract

Glucose-transporter (GLUT)-inhibitors, like Glutor and Glupin, effectively inhibit the proliferation of different tumor cells, making them potential candidates for cancer therapies. Therefore, assessing the impact of GLUT-inhibitors on NK cell function is crucial, as these cells play an important role in anti-tumor response. Seahorse analysis of the energetic phenotype of NK cells treated with Glutor or Glupin showed decreased glycolysis. To further examine the effect of both inhibitors on NK cell effector functions, resting or pre-activated human NK cells were stimulated through CD16 in the presence or absence of Glutor or Glupin. This acute inhibition of the GLUT had no significant effect on NK cell cytotoxicity, cytokine secretion or killing capacity against tumor cells. To analyze possible long-term effects, we cultured freshly isolated NK cells for 3 weeks in the presence or absence of Glutor or Glupin. We could detect a lack of proliferation in case of Glutor-treatment, whereas Glupin-treated NK cells displayed a delayed proliferation. Analysis of various surface receptors showed that long-term treatment with Glutor or Glupin led to an altered NK cell phenotype compared to the control. Furthermore, we examined the cytotoxic and immunoregulatory function of these NK cells: Long-term treatment with Glutor reduced the degranulation and IFN-γ secretion after stimulation via CD16 or NKp30. Interestingly, Glupin did not affect degranulation in comparison to the control cells, whereas the IFN-γ secretion was significantly diminished after stimulation via CD16 or NKp30. Furthermore, the serial-killing capacity of long-term treated NK cells with Glupin was higher than that of control cells. Experiments regarding the usage of other fuels, like glutamine or fatty acids, revealed that NK cells did not use fatty acids to fulfil their functions and that glutamine seems to be not responsible for this increased serial killing capacity. RNA-sequencing data together with the analysis of NAD^+/NADH concentrations of Glupin-treated NK cells suggests a possible role of CD38 and NAD^+ in the serial killing capacity of NK cells. Further, RNA-sequencing of Glutor-treated NK cells displayed a cell cycle arrest, which could explain the lack of proliferation. These data identify Glupin as a suitable candidate for cancer therapy.

4 Zusammenfassung

Glukose-Transporter (GLUT)-Inhibitoren wie Glutor und Glupin hemmen wirksam die Vermehrung verschiedener Tumorzellen, was sie zu potenziellen Kandidaten für Krebstherapien macht. Daher ist es von entscheidender Bedeutung, die Auswirkungen von GLUT-Inhibitoren auf die NK-Zell Funktion zu untersuchen, da diese Zellen eine wichtige Rolle bei der Krebsbekämpfung spielen. Die Analyse des energetischen Phänotyps von NK-Zellen, die mit Glutor oder Glupin behandelt wurden, zeigte eine reduzierte glykolytische Kapazität. Um die Wirkung der beiden Inhibitoren auf die Effektor-Funktionen von NK-Zellen weiter zu untersuchen, wurden ruhende oder voraktivierte NK-Zellen in An- oder Abwesenheit von Glutor oder Glupin über CD16 stimuliert. Diese akute Hemmung der GLUT hatte keine signifikanten Auswirkungen auf die Zytotoxizität der NK-Zellen oder deren Zytokin-Freisetzung. Um mögliche Langzeiteffekte zu analysieren, kultivierten wir frisch isolierte NK-Zellen 3 Wochen lang in An- oder Abwesenheit von Glutor oder Glupin. Die Behandlung der NK-Zellen mit Glutor verhinderte die Proliferation, während mit Glupin behandelte NK-Zellen eine verzögerte Proliferation aufwiesen. Die Analyse verschiedener Oberflächenrezeptoren zeigte, dass eine Langzeitbehandlung mit Glutor oder Glupin zu einem veränderten Phänotyp der NK-Zellen im Vergleich zur Kontrolle führte. Außerdem untersuchten wir die zytotoxische und immunregulatorische Funktion dieser NK-Zellen: Die Langzeitbehandlung mit Glutor führte zu einer erniedrigten Degranulation und IFN-γ Sekretion nach Stimulation über CD16 oder NKp30. Interessanterweise wirkte sich Glupin nicht negativ auf die Degranulation aus, während die IFN-γ Sekretion nach Stimulation über CD16 oder NKp30 signifikant vermindert war. Darüber hinaus zeigte sich eine erhöhte serial-killing Kapazität von Glupin-langzeitbehandelten NK-Zellen. Experimente zur Verwendung anderer Nährstoffe, wie Glutamin oder Fettsäuren, ergaben, dass NK-Zellen keine Fettsäuren zur Ausübung ihrer Funktionen verwenden und dass Glutamin nicht für diese erhöhte serial-killing Kapazität verantwortlich zu sein scheint. Die RNA-Sequenzierungsdaten in Verbindung mit der Analyse der NAD^+/NADH-Konzentrationen von mit Glupin behandelten NK-Zellen deuten auf eine mögliche Rolle von CD38 und NAD^+ bei der serial-killing Kapazität von NK-Zellen hin. Darüber hinaus zeigte die RNA-Sequenzierung von mit Glutor behandelten NK-Zellen einen Zellzyklus-Stillstand, was die fehlende Proliferation erklären könnte. Diese Daten weisen Glupin als einen geeigneten Kandidaten für die Krebstherapie aus.

5 Introduction

5.1 NK cells

Natural killer (NK) cells are part of the innate immune system and account for 5 to 15 % of the lymphocytes in peripheral blood (Freud and Caligiuri 2006). Unlike T and B lymphocytes, they do not have a clonotypic antigen receptor, but possess germline-encoded receptors to regulate their functions (Watzl 2014). NK cells can be classified based on their expression of CD56 and CD16 and the absence of CD3. According to the expression levels of CD56 and CD16, NK cells can be further divided into $CD56^{bright}CD16^{-}$ NK cells and the more mature $CD56^{dim}CD16^{+}$ NK cell population. In addition, the $CD56^{dim}CD16^{+}$ NK cell population can be subdivided into $CD56^{dim}CD57^{-}CD62L^{+}CD94/NKG2A^{+}$ and the more mature $CD56^{dim}CD57^{+}CD62L^{-}CD94/NKG2A^{-}$ NK cells (Caligiuri 2008; Luetke-Eversloh et al. 2013). CD57 expression reflects differentiated NK cells with a high cytotoxic capacity (Nielsen et al. 2013), while the expression of CD62L and CD94/NKG2A is indicative of an intermediate stage of NK cell differentiation (Juelke et al. 2010). The maturation of NK cells occurs in bone marrow, but also in secondary lymphoid tissues (Caligiuri 2008; Luetke-Eversloh et al. 2013). Due to their cytotoxic function, NK cells play an important role in killing transformed or infected cells (Long et al. 2013). NK cells use two main modes of cytotoxicity: 1) induction of death-receptor mediated apoptosis via the interaction of Fas-ligand (FasL) or tumor necrosis factor (TNF)-related apoptosis-inducing ligand (TRAIL) and the corresponding receptors on the target cell and 2) the directed release of lytic granules containing granzymes and perforin towards the target cell. Based on these capabilities, it is possible for some NK cells to kill not only one tumor cell but several tumor cells in a row, which is referred to as “serial killing” (Prager and Watzl 2019). In addition, they have an immunoregulatory function. They can produce cytokines and chemokines such as interferon-gamma (IFN-γ), TNF-α or interleukin (IL-) 10 which affect cells of the innate and adaptive immune system (Cooper et al. 2001). For example, they can activate macrophages via IFN-γ signalling, which is associated with increased expression of hypoxia-inducible factor-1 alpha (HIF1α) and IL-1ß (Wang et al. 2018).

5.2 NK cell activation

The functions of NK cells are controlled by a close interplay of activating and inhibitory receptors. Whether the NK cell kills the target cell or not, is determined by the transmitted signals. Both activating and inhibitory receptors transmit their signal via intracellular motifs or adapter molecules. Transformed or infected cells increase the surface expression of ligands for activating receptors on NK cells. In contrast, healthy cells express major histocompatibility complex (MHC) class 1 proteins, which can be recognized by the inhibitory receptors on NK cells, inducing inhibitory signaling (Long et al. 2013; Watzl 2014). This recognition of healthy cells is referred to as self-recognition. In the case of the binding of activating ligands, this leads to activation of the NK cell if the activating signals predominate compared to the inhibitory signals. Loss or downregulation of MHC class 1 on infected or transformed cells leads to reduced inhibitory signaling in the NK cell and consequently to activation associated with lysis of the target cell, also referred to as the missing self-theory (Raulet 2006).

There are several families of activating receptors. Natural cytotoxicity receptors (NCRs) as well as the fragment crystallizable (Fc)-receptor CD16 (FcγRIIIA) associate with partner chains, which contain an immunoreceptor tyrosine-based activation motif (ITAM) (Figure 1) (Chiesa et al. 2006; Watzl and Long 2010). CD16 associates with FcεRIγ and CD3zeta chains and is capable of efficiently activating resting NK cells in the absence of other stimuli (Lanier et al. 1991; Watzl and Long 2010). Further, CD16 is responsible for the induction of antibody mediated cellular cytotoxicity (ADCC) (Bryceson et al. 2006; Srpan et al. 2018). NCRs include NKp30, NKp44 as well as NKp46. Resting NK cells express only NKp30 and NKp46 on their surface, whereas activated NK cells express all three forms (Chester et al. 2015). NKp30 and NKp46 associate with FcεRIγ and CD3zeta chains, while NKp44 associates with DAP12 (Watzl 2014). In contrast to CD16, NCRs and all other receptors are unable to induce NK cell activation in the absence of co-activating signals (Bryceson et al. 2006). Activation of NK cells via the ITAM signaling pathway starts with the Src-family kinases-mediated phosphorylation of ITAM. (Figure 1). This induces recruitment of the kinases spleen tyrosine kinase (Syk) as well as Zeta-chain-associated protein kinase 70 (ZAP70), resulting in the phosphorylation of transmembrane adapter molecules such as Linker for activation of T cells (LAT) or cytosolic adapter molecules like SH2 domain-

containing leukocyte protein of 76 kDa (SLP-76). These adapter molecules can then initiate downstream signal transduction via recruitment, phosphorylation, and activation of phosphatidyl inositol 3-OH kinase (PI3K), phospholipase C (PLC)γ- 1 and 2, and Vav guanine nucleotide exchange factor 2 and 3 (Vav 2 and 3) (Figure 1) (Watzl 2014).

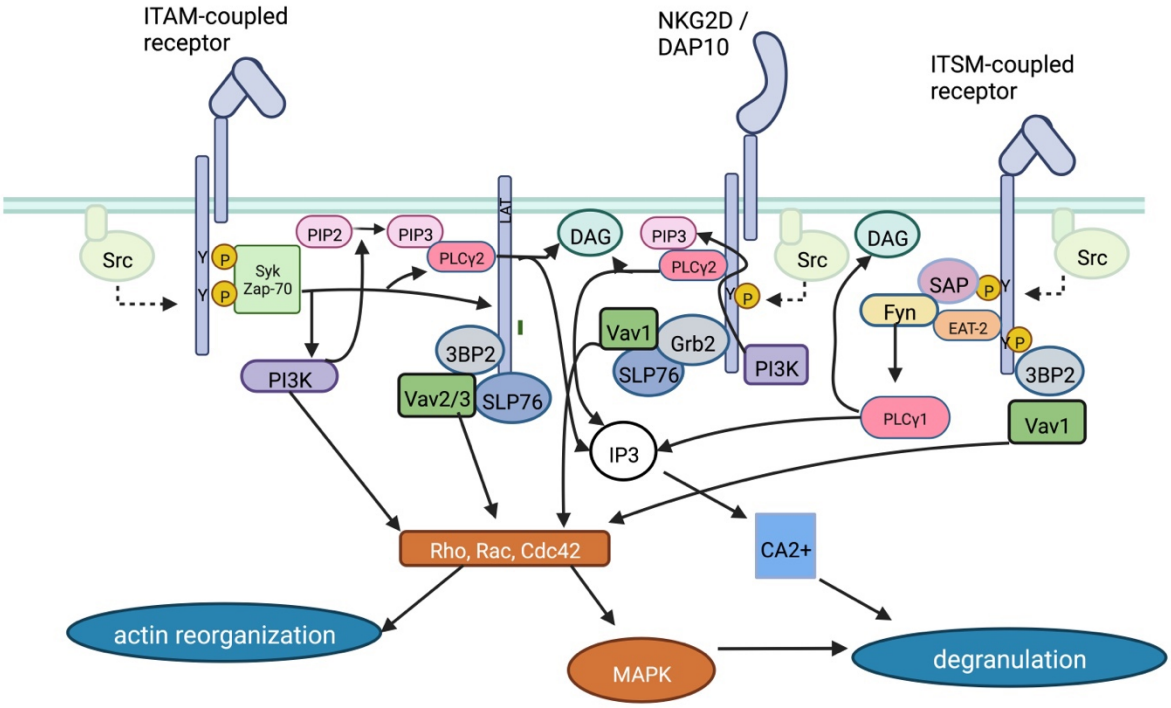

Figure 1: Signaling pathways of activating receptors

Schematic illustration of signaling pathways of the activating human NK cell receptors. CD16 and NKp30 couple to ITAM-containing partner chains. NKG2D couples to DAP10, containing a YINM motif. 2B4 possess ITSM-signaling motifs in its cytoplasmic tail. Modified from Watzl 2014

The activating receptor NK group member D (NKG2D) belongs to the C-type lectin superfamily and recognizes MHC 1-chain-related protein A or B (MICA, MICB) and UL16 binding protein (ULBP) 1, 2, 3, or 4, whose expression is upregulated on stressed, transformed or infected cells (Chester et al. 2015). The signaling adapter of NKG2D is DAP10, that contains the YINM tyrosine-based signaling motif. Upon ligand binding, YINM is phosphorylated by Src-family kinases and can either recruit Vav1 via the adapter growth factor receptor-bound protein 2 (Grb2) or it can bind PI3K (Watzl and Long 2010). Both 2B4 and CD2-like receptor-activating cytotoxic cell (CRACC), among a few others, belong to the signaling lymphocyte activation molecule (SLAM)-related receptor family and have immunoreceptor tyrosine-based switch motifs (ITSM) in their

cytoplasmic part (Watzl 2014). This motif is phosphorylated by Src-family kinases and afterwards recruits the small SH2-domain-containing adapter molecules SLAM-associated protein (SAP) or Ewing's sarcoma-associated transcript-2 (EAT-2) (Figure 1). SAP recruits the Src-family kinase Fyn, which results in the phosphorylation and activation of Vav1 and PLC-γ1, whereas EAT-2 transmits positive signals via a tyrosine residue in its carboxy-terminal part. In addition, EAT-2 can also transmit inhibitory signals (Watzl and Urlaub 2012; Watzl 2014). Furthermore, activation of the NK cell can also occur via cytokine receptors. Thus, the binding of IL-12 to the IL-12 receptor on the NK cells leads to the recruitment of Janus kinase 2 (JAK2) and the subsequent phosphorylation of the transcription factor signal transducer and activator of transcription 4 (STAT4). The phosphorylated form of STAT4 translocate to the nucleus and induces the transcription of IFN-γ (Wang et al. 2000). Once activated, the NK cells undergo a metabolic transition that affects the functions as well as the proliferation of the NK cells (Gardiner 2019).

5.3 Metabolism

Metabolism can be divided biochemically into catabolism and anabolism. Catabolism describes the conversion of metabolic substrates into energy, while anabolism is the process by which new molecules are generated using energy. However, in addition to this classical biochemical definition, immune metabolism provides a direct link to immune cell functions. Immune metabolism depends on glycolysis and oxidative phosphorylation (OxPhos). Both metabolic pathways are linked by the tricarboxylic acid (TCA) cycle and require glucose, which is an important fuel for cells. Glycolysis and OxPhos differ in energy production: OxPhos builds 34 adenosine triphosphate (ATP) molecules from one glucose molecule, while glycolysis generates two ATP molecules from one glucose molecule. OxPhos is thus more efficient than glycolysis in energy supply, but glycolysis serves to generate precursors that are required for the biosynthesis of effector molecules and facilitate the survival of rapidly proliferating cells. In addition, glycolysis allows faster processing of glucose, resulting in faster availability of ATP than OxPhos (Gardiner 2019).

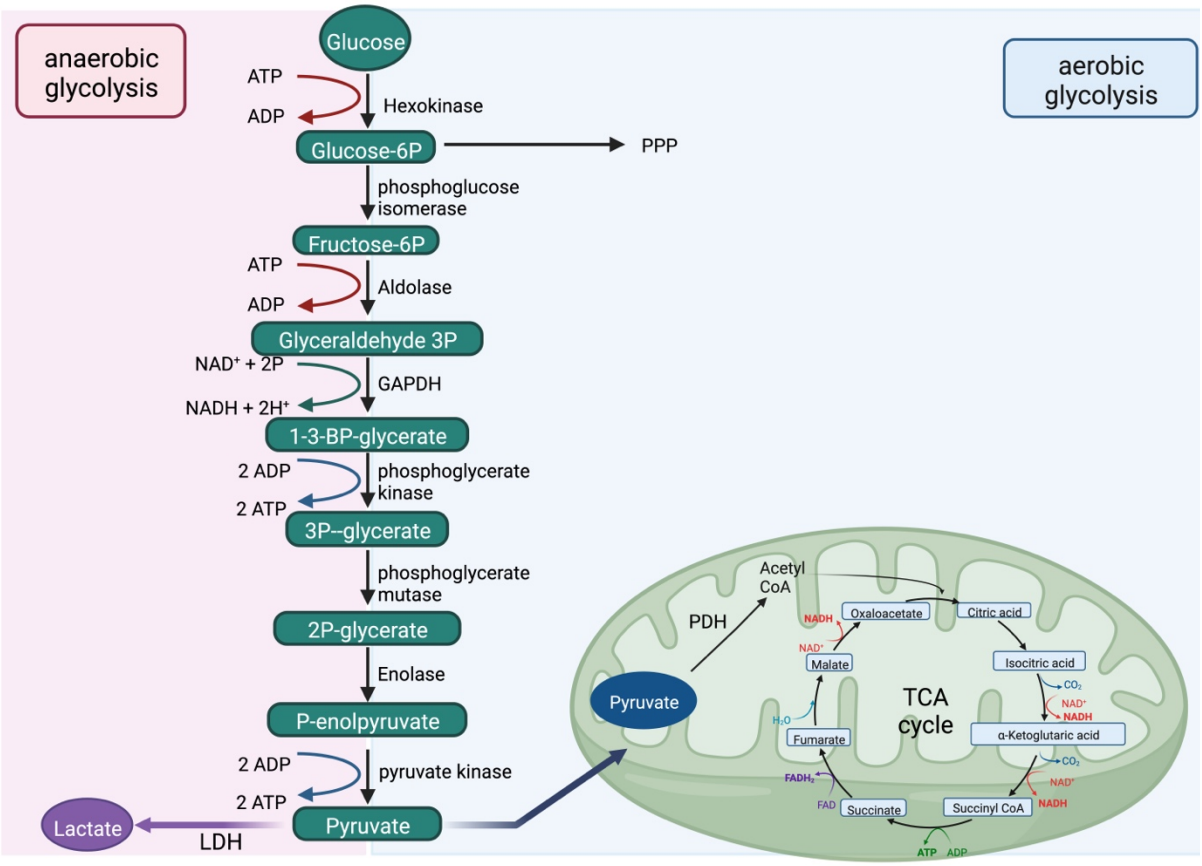

Figure 2: schematic illustration of glycolysis and TCA-cycle

Glucose is metabolized into pyruvate via glycolysis. Further use of pyruvate is dependent on the availability of oxygen. In anaerobic conditions pyruvate is converted into lactate by the lactate-dehydrogenase (LDH) in the cytoplasm. In the presence of oxygen, pyruvate is transported into the mitochondria and converted to acetyl-CoA, which can enter the TCA-cycle to generate energy. In addition to using glucose for glycolysis, it can also be used in the pentose phosphate pathway (PPP) after conversion into Glucose-6-phosphate (G6P).

Glycolysis occurs in the cytoplasm and begins with the transport of glucose into the cell via glucose transporters. Hexokinases (HK) convert glucose to glucose-6-phosphate (G6P), which in turn can be fed into various metabolic pathways. During glycolysis (Figure 2), G6P is converted to pyruvate in a series of enzymatic reactions, which produce two molecules of pyruvate, ATP and NADH. The subsequent use of pyruvate is dependent on the presence of oxygen (O_2). The absence of oxygen leads to the oxidation of pyruvate to lactate and nicotinamide adenine dinucleotide (NAD^+). In the presence of oxygen, pyruvate is transported into the mitochondria and converted by the pyruvate dehydrogenase (PDH) into CO_2 and acetyl-CoA, which is then fed into the TCA cycle and subsequently citrate is formed. In a series of enzymatic reactions, the reducing equivalents NADH and dihydroflavin adenine dinucleotide ($FADH_2$) are produced. Both are involved in the electron transport chain (ETC), where they are required to transfer electrons to complex I and complex II. The ETC (Figure 3) consists

of 5 complexes: NADH dehydrogenase (C I), succinate dehydrogenase (C II), ubiquinol cytochrome C reductase (C III), cytochrome C oxidase (C IV), and ATP synthase (C V) (Martínez-Reyes and Chandel 2020). The resulting mitochondrial membrane potential is used by the ATP synthase to produce ATP in in the presence of oxygen and this process is known as oxidative phosphorylation (OxPhos) (Li et al. 2021).

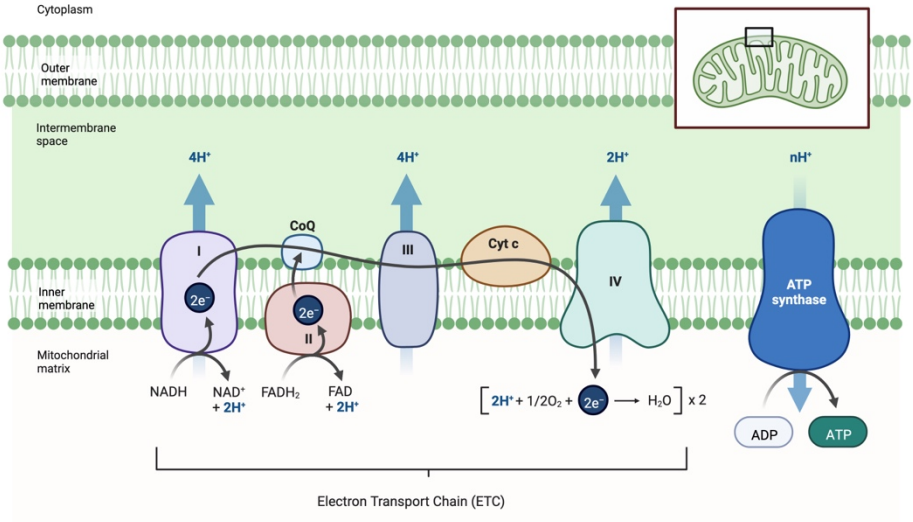

Figure 3: electron transport chain

Schematic illustration of the electron transport chain anchored in the mitochondria. The ETC consists of five complexes (CI to CV) and the two free electron carriers, CoQ and cyt c. NADH and FADH2 donate electrons to CI and CII, accordingly, thereby reducing CoQ to CoQH2. CoQH2 is in turn oxidized by CIII, and the electrons donated to cyt c. The reduced cyt c is then oxidized by CIV, reducing the oxygen molecule as the terminal electron acceptor. During oxidative phosphorylation, protons accumulate in the intermembrane space via CI, CIII, and CIV, which are essential for CV to drive ATP synthesis. Modified from Li et al 2021 and created with BioRender.

Citrate is not only used in the TCA cycle, but it can also be transported to the cytosol via the citrate-malate transporter solute carrier family 25 member 1 (SLC25A1). In the cytosol, citrate is converted by the ATP citrate lyase (ACLY) to oxaloacetate and acetyl-CoA. Subsequently, oxaloacetate is converted to malate and transported back to the mitochondria. This results in the transfer of electrons from the cytoplasm to the mitochondria and the generation of cytosolic NAD^+. Moreover, acetyl-CoA regulates gene expression by controlling acetylation reactions and is involved in lipid synthesis pathways (Guillerey and Smyth 2017). NAD^+ acts as a coenzyme in many redox reactions and is also an important cofactor for non-redox NAD^+-dependent enzymes. Thus, NAD^+ links cellular metabolism and signaling transduction. NAD^+ can be converted by the NAD^+ glycohydrolases, such as CD38 as well as the protein deacylase family of sirtuins and poly ADP ribose polymerase (PARPs). To keep the intracellular NAD^+ level stable, NAD^+ is continually synthesized, catabolized and recycled in the cell. CD38 is a multifunctional ectoenzyme that hydrolyses NAD^+ to nicotinamide (NAM) and adenosine diphosphate ribose (ADPR) through its

glycohydrolase activity or processes NAD^+ to NAM and cyclicADPR through its ADP-ribosyl cyclase activity. The enzymatic activity of CD38 triggers $Ca2^+$ signaling and regulates key cellular processes such as immune cell activation, metabolism and survival (Covarrubias et al. 2021).

In addition to glycolysis, G6P can also be used in the pentose phosphate pathway (PPP). The PPP generates ribose, which is required for the synthesis of RNA, DNA and nicotinamide adenine dinucleotide phosphate (NADPH), which is needed for fatty acid (FA) synthesis (Werner et al. 2016). Beside glucose, also glutamine and fatty acids are important for cellular metabolism (Poznanski and Ashkar 2019). Both feed into the TCA cycle in the mitochondria. Glutamine is converted by glutamate-dehydrogenase into α-ketoglutarate (α-KG), which enters the TCA cycle (Yang et al. 2014). Fatty acids are converted via fatty acid oxidation (FAO) into acetyl-CoA, which feeds into the TCA cycle (Gardiner 2019). Mitochondria play a central role in the metabolism of a cell since both the TCA cycle and the ETC are anchored in the mitochondria. Thus, the mitochondrial mass can be a marker for the metabolic state of a cell since activation of lymphocytes goes ahead with an increased mitochondrial mass. But mitochondrial mass is per se no indicator for functionality. Functionality of mitochondria can be displayed by its structure, due to fusion and fission, which is known to affect mitochondrial functions (Gardiner 2019). Zheng et al demonstrate that tumor-infiltrating NK cells display small, fragmented mitochondria, which is correlated with impaired cytotoxicity and NK cell loss (Zheng et al. 2019).

5.4 NK cell metabolism and function

The metabolic pathways described above are not used to similar extent by all cells, so it is assumed that the particular metabolic pattern supports the specialized functions of the individual cell. Two major metabolic pathways are known to be involved in NK cell activation and proliferation: OxPhos and glycolysis (Mah et al. 2017). While resting mature NK cells mainly rely on OxPhos, activated mature NK cells upregulate OxPhos and glycolysis. The use of OxPhos alone in resting cells ensures a sufficient energy supply without the need to provide additional energy for synthesis of effector molecules. Increased rates of OxPhos and glycolysis upon activation of NK cells by cytokines such as IL-2, IL-12, and IL-15 result in increased energy production and synthesis of molecules essential for effector functions of the cell (Donnelly et al. 2014; Schafer et

al. 2019; Gardiner 2019). In contrast, the metabolic requirements for the IFN-γ production in resting murine NK cells depend on the type of activation. Keppel et al. demonstrated that IFN-γ production of murine NK cells relied on glycolytic and oxidative metabolism when activated through NK cell receptors, whereas activation by cytokines like IL-12 and IL-18 did not depend on glycolysis or OxPhos (Keppel et al. 2015). Inhibition of glycolysis by 2-desoxy-D-glucose (2-DG) results in a decreased killing-capacity and proliferation of IL-15 primed murine NK cells, as well as in a reduced expression of granzyme B and IFN-γ (Mah et al. 2017). Furthermore, increased OxPhos is necessary to support both cytotoxicity and IFN-γ production, whereas glycolysis seems to be less important for NK cell degranulation. However, limiting the rate of glycolysis diminished the IFN-γ production in $CD56^{bright}$ NK cells (Keating et al. 2016). In addition to this activity-based classification, $CD56^{dim}$ and $CD56^{bright}$ NK cells also exhibit differences in their metabolic profile: the metabolic response of $CD56^{bright}$ NK cells to IL-2 or IL-12/IL-15 stimulation is higher, and they show higher mammalian target of rapamycin (mTOR) activity than $CD56^{dim}$ NK cells. In this regard, $CD56^{bright}$ NK cells upregulate the expression of nutrient receptors such as the glucose transporter GLUT-1, the amino acid transporters SLC1A5, SLC7A5 and SLC3A2 (CD98), and the transferrin receptor (CD71) during stimulation with cytokines such as IL-2, IL-12 and IL-15 (Keating et al. 2016; Jensen et al. 2017). On the other hand, $CD56^{dim}$ NK cells display higher rates of glycolysis and OxPhos, as well as increased mitochondrial mass in comparison to $CD56^{bright}$ NK cells (Surace et al. 2021). In addition to glucose as the main energy fuel, glutamine also plays an important role in NK cell metabolism. Glutamine is fed into the TCA cycle via glutaminolysis. The availability of glutamine is essential for NK cell metabolism and effector functions as it contributes to maintain levels of the transcription factor cMyc (Loftus et al. 2018). In contrast, the extent to which fatty acids play a role in NK cell metabolism is not yet known. Previous studies with etomoxir, an inhibitor of the carnitine palmitoyltransferase-1 (CPT1), showed that this treatment had no effect on IFN-γ production by cytokine- or receptor-activated NK cells (Keppel et al. 2015). Further, an increased lipid metabolism due to an increased exposure to fatty acids is associated with impaired NK cell function (Kobayashi et al. 2020). Thus, glucose as well as glutamine seem to be the most important nutrients for NK cells to fulfil their normal functions.

5.5 Regulation of NK cell metabolism

Mammalian target of rapamycin (mTOR), an important metabolic regulator of NK cells, is a serine-threonine kinase which forms two structurally and functionally different complexes: mTOR complex 1 (mTORC1) and mTOR complex 2 (mTORC2). mTORC1 consists of mTOR, regulatory associated protein of mTOR (Raptor), mammalian LST8/G-protein β-subunit like protein (mLST8/GβL) and lethal with sec thirteen 8 (LST8) as core components. Activation of mTOR leads to phosphorylation of eukaryotic translation initiation factor 4E (eIF-4E) binding protein (4E-BP1) and protein S6 kinase 1 (S6K1), which regulate protein translation (Takahara et al. 2020). mTORC1 signaling can be upregulated in both human and mouse NK cells through stimulation with cytokines. (Gardiner 2019). To date, it is known that mTORC1 is involved in the regulation of metabolism and is thus important for NK cell function and development. In mouse models, mTORC1 activity has been shown to play an important role in NK cell development and activation-induced metabolic and functional responses in mature NK cells. Pharmacological inhibition of mTORC1 by rapamycin leads to a reduction in mitochondrial mass and membrane potential, resulting in impaired effector functions (Figure 4). Furthermore, mTORC1 activity is important for increased glycolysis, and inhibition of mTOR leads to a diminished IFN-γ secretion and Granzyme B expression. In addition to mTOR, sterol regulatory element-binding protein (SREBP) and cMyc also play important roles in regulating metabolism. However, the optimal activity of SREBP and the initial induction of cMyc depend on mTOR (Assmann et al. 2017; Loftus et al. 2018). SREBP plays an important role in fatty acid and cholesterol synthesis in T cells (Kidani et al. 2013; Angela et al. 2016). In contrast, in cytokine-stimulated NK cells SREBP activity is important for increased rates of glycolysis and OxPhos. In this context, SREBP supports the activity of the citrate-malate shuttle (CMS), which transports glucose-derived citrate from the mitochondria to the cytosol. The activity of the shuttle in turn leads to the production of mitochondrial NADH, which leads to increased OxPhos in NK cells. Inhibition of SREBP activation results in decreased glycolysis and OxPhos, diminished IFN-γ production, and reduced cytotoxicity against tumor cells. These data further suggest that SREBP is not as important for the TCA cycle but rather for the citrate-malate shuttle (Assmann et al. 2017) (Figure 4).

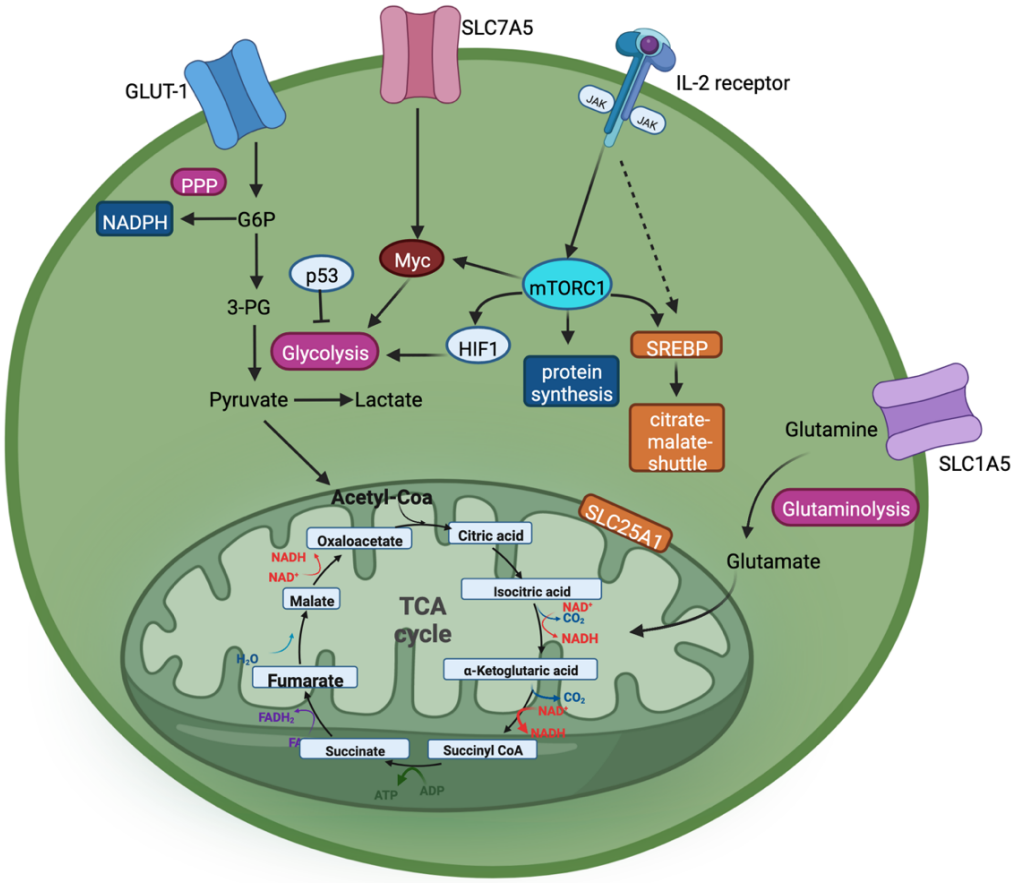

Figure 4: Regulation of NK cell metabolism

NK cell metabolism is regulated by the key regulator mTORC1. mTORC1 is activated by IL-2 signaling and is necessary for the initial induction of cMyc and for optimal SREBP activity. Further cMyc protein levels can be sustained by amino acids (uptake of amino acids via SLC7A5). cMyc regulates the expression of the metabolic machinery and supports glycolysis. SREBP activity can be increased by IL-2 signaling and SREBP itself regulates the metabolic configuration of NK cells by the citrate-malate-shuttle. Beside the regulation of cMyc and SREBP, mTORC1 controls the protein synthesis.

cMyc controls the expression of the metabolic machinery in NK cells and is also required for increased expression of glucose transporters and glycolytic enzymes to support glycolysis. Furthermore, cMyc is required for mitogenesis to provide the increased mitochondrial mass needed to support high OxPhos rates. cMyc expression depends on the availability of amino acids, which are required to maintain high cMyc translation rates to compensate for continuous cMyc degradation. Glutamine, for example, is important for cMyc signaling, because it facilitates amino acid uptake by the L-type amino acid transporter SLC7A5 (Loftus et al. 2018).

5.6 Glucose transporters

Being a large, polar molecule, glucose cannot enter the cell simply by diffusion. Therefore, a large family of structurally related transport proteins known as glucose transporters allows glucose to enter the cell. There are two main types of glucose transporters: sodium-glucose-linked transporters (SGLTs) and glucose transporters with facilitated diffusion (GLUTs). SGLTs are 14-transmembrane spanning proteins that symport glucose along with sodium ions. SGLTs are encoded by the solute carrier 5 A (SLC5A) gene. Up to 6 different SGLTs (SGLT1-6) are known to be expressed primarily by cells of the small intestinal mucosa (Navale and Paranjape 2016). GLUTs are 12-transmembrane-spanning proteins that allow glucose to enter the cell. They are encoded by the solute carrier 2A genes (SLC2A). In humans, up to 14 different GLUTs are known, which differ in their tissue distribution and affinity for glucose and other hexoses.

Table 1: Glucose transporter expression

Name (gene)	Class	Mainly expressed by
GLUT-1 (SLC2A1)	1	somatic cells
GLUT-2 (SLC2A2)	1	hepatocytes, enterocytes
GLUT-3 (SLC2A3)	1	neurons, b-cells of the pancreas
GLUT-4 (SLC2A4)	1	adipocytes, muscle cells
GLUT-5 (SLC2A5)	2	intestine and testis
GLUT-6 (SLC2A6)	3	brain, spleen, peripheral leukocytes
GLUT-7 (SLC2A7)	2	small intestine and colon
GLUT-8 (SLC2A8)	3	adult testis and placenta
GLUT-9 (SLC2A9)	2	spleen
GLUT-10 (SLC2A10)	3	liver, pancreas
GLUT-11 (SLC2A11)	2	heart- and skeletal muscle cells
GLUT-12 (SLC2A12)	3	muscle cells
GLUT-13 (SLC2A13)	3	glial cells
GLUT-14 (SLC2A14)	1	testis

GLUTs have been divided into three subclasses based on sequence similarities: GLUT-1 to GLUT-4 and GLUT-14 belong to Class 1 and are distinguished by their expression profile and affinity for glucose. GLUT-1, GLUT-3 and GLUT-4 have a high affinity for glucose, whereas GLUT-2 has a low affinity for glucose and is active only in the state of hyperglycemia (Thorens and Mueckler 2010). GLUT-5, GLUT-7, GLUT-9,

and GLUT-11 belong to Class 2, whereas GLUT-6, GLUT-8, GLUT-10, GLUT-12, and GLUT-13 belong to Class 3 (Table 1) (Navale and Paranjape 2016). To date, NK cells are known to predominantly express GLUT-1 (Thorens and Mueckler 2010) and to a lesser extent GLUT-3 and GLUT-4 (Terrén et al. 2019).

5.7 NK cells and tumor

NK cells play an essential role in combating tumor cells. As described above, this function is regulated by NK cell metabolism. Tumor cells also depend on glucose metabolism. Otto Warburg discovered several decades ago that tumor cells have a high metabolic demand. However, instead of using OxPhos, tumor cells prefer anaerobic glycolysis despite the availability of oxygen. This phenomenon is referred to as the Warburg effect (Warburg 1925). The intensive use of anaerobic glycolysis leads to increased production of lactate. To prevent cellular acidification, tumor cells upregulate the expression of the lactate transporter MCT4 (Ganapathy et al. 2009). The increased lactate content in the tumor environment acts in two ways. On the one hand, there are tumor cells that import lactate as a major energy source (Semenza 2008; Feron 2009). On the other hand, lactate directly decreases the cytotoxic activity of NK cells (Husain et al. 2013). To overcome inefficient energy production by anerobic glycolysis, tumor cells increase their rate of glycolysis 20- to 30-fold compared with healthy cells. This is accompanied by the upregulation of glucose transporters and consequently increased glucose uptake (Airley and Mobasheri 2007; Ganapathy et al. 2009). Therefore, cancer cells have mainly upregulated GLUT-1 and, to a lesser extent, GLUT-3 (Ganapathy et al. 2009; Krzeslak et al. 2012). Excessive uptake of glucose by tumor cells results in greatly reduced availability of glucose for immune cells. As mentioned earlier, NK cell activity depends on increased glycolysis (Gardiner 2019). Increased GLUT-1 expression is associated with an increased proliferation index and a lower degree of differentiation, and therefore with increased malignant potential, invasiveness, and poor prognosis in various cancer cell types (Krzeslak et al. 2012). Based on these findings, targeted interference with tumor cell metabolism could be a potential therapeutic approach. Therefore, Waldmann et al. have synthesized several glucose transporter inhibitors. The most potent GLUT-inhibitors are Glutor and Glupin. Both are glucose uptake inhibitors that inhibit glycolysis, leading to a stop in proliferation in various cancer cell lines. They differ in their targets: Glupin acts

selectively on GLUT-1 and GLUT-3, while Glutor acts selectively on GLUT-1, GLUT-2, and GLUT-3. The inhibition of GLUT-3 by both Glutor and Glupin was stronger than that of GLUT-1 (Reckzeh et al. 2019; Ceballos et al. 2019). However, in addition to these promising data, the effect of Glupin or Glutor on NK cells is equally important because these cells also express GLUT-1 and -3 and play an important role in killing cancer cells. Therefore, we wanted to know whether Glupin or Glutor affect the ability of NK cells to proliferate, kill target cells, secrete cytokines and chemokines, and whether NK cells change their phenotype in the absence of glucose availability. Therefore, we treated primary human NK cells with Glupin or Glutor and analyzed their functions, phenotype, and proliferation.

6 Materials and Methods

6.1 Primary antibodies

Table 2: primary antibodies

Name (clone)	conjugate	Dilution/ Final conc.	source
Hexokinase 1 (EPR10134(B))	PE	1:800	Abcam (Cambridge, UK)
CD16 (3G8)	PE-Dazzle	1:100	BioLegend (San Diego, CA, USA)
CD57 (HNK-1)	AF647	1:200	
KLRG1 (2F1)	BV510	1:50	
HLA-DR (L243)	BV605	1:100	
NKp30 (P30-15)	APC-Fire750	1:100	
NKp44 (P44-8)	PerCP-Cy5.5	1:100	
NKp46 (9E2)	BV421	1:50	
Granzyme B (GB11)	AF647	1:200	
Perforin (dG9)	FITC	1:100	
CD18 (TS1/18)	AF700	1:800	
CD107a (H4A3)	PE-Cy5	1:50	
2B4 (C1.7)	FITC	1:200	
CD11a (HI111)	AF488	1:2000	
TRAIL (N2B2)	PE-Cy7	1:50	
41BB (4B4-1)	BV421	1:50	
Tim-3 (F38-2E2)	APC-Fire 750	1:50	
CTLA-4 (BNI3)	PE-Dazzle	1:100	
CD18 (TS1/18)	AF700	1:800	
CD66b (G10F5)	APC	1:200	
CD19 (HIB19)	AF700	1:50	
CD16 (3G8)		2 µg/ml	
NKG2A (Z199)	PE	1:100	Beckman Coulter (Brea, CA, USA)
CD98 (REA387)	PE	1:100	Miltenyi Biotec (Bergisch Gladbach, Germany)
cMyc (SH1-26E7.1.3)	FITC	1:50	
CD36 (REA760)	VioGreen	1:50	
CD71 (REA902)	APC	1:50	

Name (clone)	conjugate	Dilution/ Final conc.	source
CD62L (DREG 56)	PE-Cy7	1:200	BD Bioscience (San Jose, CA, USA)
KLRB1 (NKR-3G10)	BUV661	1:100	
TIGIT (741182)	BV786	1:100	
DNAM-1 (DX11)	AF647	1:100	
NKG2C (134591)	BUV496	1:50	
PD-1 (EH12.1)	AF647	1:400	
CD27 (M-T271)	PerCP-Cy5.5	1:50	
CD11c (B-ly6)	PE	1:100	
CD38 (HB7)	BUV395	1:100	
CD3 (UCHT1)	BUV563	1:200	
CD56 (B159) CD56 (NCAM16.2)	BUV805 BV421	1:4000 1:100	
2B4 (C1.7)		2 µg/ml	kindly provided by G. Trinchieri, The Wistar Institute, PA, USA
NKp30 (p30-15)		2 µg/ml	produced in our lab
Glut-1 (202915)	PE	1:100	R & D Systems (Minneapolis, MN, USA)
NKG2D (FAB139N)	AF700	1:100	
NKG2D (149810)		2 µg/ml	
Puromycin (12D10)	AF488	1:200	Sigma-Aldrich (St. Louis, MO, USA)
Control IgG (MOPC21)		2 µg/ml	
CD8a (RPA-T8)	AF532	1:200	Thermo Fisher Scientific (Waltham, MA, USA)
pmTOR (MRRBY)	PE-Cy7	1:50	
CD14 (61D3)	FITC	1:50	Santa Cruz Biotechnology (Dallas, TX, USA)

6.2 Cells

Table 3: Cells

Name	origin
Primary NK cells	Whole blood from healthy humans
K562	CML
K562 mbIL15-41BBL (Feeder cells)	CML
HepG2	HCC
MCF7	Breast cancer cell line

6.3 Cytokines

Table 4: Cytokines

Name	Source
Recombinant human IL-2	NIH Cytokine Repository, Frederick MD, USA
Recombinant human IL-12	R&D Systems
Recombinant human IL-15	PAN-Biotech (Aidenbach, Germany)
Recombinant human IL-18	MBL Life Science (Nagoya, Japan)
Recombinant human IL-21	Miltenyi Biotec

6.4 Inhibitors

Table 5: Inhibitors

Name	Source
Glutor	MPI Dortmund (Reckzeh et al. 2019)
Glupin	MPI Dortmund (Ceballos et al. 2019)
CB839	MPI Dortmund
Oligomycin from Streptomyces diastatochromogenes	Sigma-Aldrich
2-Deoxy-D-glucose	
InSolution Etomoxir - CAS 828934-41-4	

6.5 Kits

Table 6: Kits

Name	Source
Glycolysis stress test kit	Agilent Technologies (Santa Clara, CA, USA)
ELISA MAX™ Deluxe Set Human IFN-γ	BioLegend
Legendplex Inflammation Panel 1 Human	
CellTiter-Glo® 2.0 Cell Viability Assay	Promega (Fitchburg, WI, USA)
NAD/NADH-Glo Assay	
Glucose Uptake-Glo (TM) Assay	
RNAeasy Mini Kit	Qiagen (Venlo, Netherlands)
RNase-Free DNase Set	
Malate Assay kit	Sigma-Aldrich
Human Untouched NK cell Isolation Kit	Thermo Fisher Scientific
eBioscience™ Foxp3 / Transcription Factor Staining Buffer Set	

6.6 Devices

Table 7: Devices

Device	Name	Source
Incubator	HERAcell240i CO2 Incubator	Thermo Fisher Scientific
Clean Benches	HERA Safe 2020	
Centrifuge	Heraeus Multifuge 3 S-R	
	Heraeus Megafuge 40R	
	Heraeus Fresco 21 centrifuge	
Flow cytometer	BD LSRFortessa	BD Bioscience
	Cytek® Aurora	Cytek Bioscience Inc. (Fremont, CA, USA)
Gamma counter	Wizard^2 2-Detector Gamma Counter	PerkinElmer (Waltham, MA, USA)
Plate Reader	GloMax® Discover Microplate Reader	Promega
Microscope Heating device Heating insert Incubator CO_2 module Temperature mod. Camera LED light source Objective	Axio observer 7 Heating device Humidity S1 Heating Insert P Lab-Tek™ S1 Incubator PM 2000 RBT CO_2 Module S Temp Module S Axiocam 506 mono Colibri 7 Plan-Apochromat 20x/0.8 DIC(UV)VIS-IR	Zeiss (Jena, Germany) PeCon GmbH (Erbach, Germany) PeCon GmbH PeCon GmbH PeCon GmbH PeCon GmbH Zeiss Zeiss Zeiss
Seahorse analyzer	Agilent Seahorse XFe96 Analyzer	Agilent Technologies
Real-Time Cell Analyzer	xCELLigence	OLS® OMNI Life Science (Bremen, Germany)
Cell counter	CASY Cell Counter & Analyzer	

6.7 Reagents

Table 8: Reagents

Name	**catalog**	**source**
Seahorse XF RPMI medium	103576-100	Agilent Technologies
Seahorse xFe96 FluxPak	102416-100	Agilent Technologies
BD FACSFlow Sheath Fluid	342003	BD Bioscience
BD FACS™ Permeabilizing Solution 2	340973	BD Bioscience
Brilliant Stain Buffer	566349	BD Bioscience
TruCount Absolute Counting Tubes	663028	BD Bioscience
Zombie NIR™ Fixable Viability Kit	423106	BioLegend
Zombie Yellow™ Fixable Viability Kit	423104	BioLegend
7-AAD Viability Staining Solution	420404	BioLegend
Triton^{R} X-100	3051.4	Carl Roth (Karlsruhe, Germany)
Chromium-51	Cr-RA-8 (5 mCi/ml)	Hartmann Analytic (Braunschweig, Germany)
IMDM without Glucose	AL230A-500ML	neoFroxx GmbH (Einhausen, Germany)
E-Plate 16 PET	2801185	OLS® OMNI Life Science
CASYton	05 651 808 001	OLS® OMNI Life Science
Pancoll Human, density 1.077 g/ml	P04-60500	PAN BIOTECH GmbH (Aidenbach, Germany)
Pancoll Human, density 1.119 g/ml	P04-60150	PAN BIOTECH GmbH
Adenosine-5'-triphosphate disodium salt hydrate	A7699-1G	Sigma-Aldrich
ITS Liquid Media Supplement (100×)	I3146-5ML	Sigma-Aldrich
Natriumbutyrate	303410-100G	Sigma-Aldrich
Pentanoate	75054-1ML	Sigma-Aldrich
RNase AWAY	83931-250ML	Sigma-Aldrich
Puromycin-dihydrochlorid from Streptomyces alboniger	P7255-25MG	Sigma-Aldrich
Paraformaldehyde (PFA)		Sigma-Aldrich
DPBS, no calcium, no magnesium	14190169	Thermo Fisher Scientific
Fetal calf serum (FCS)	10270-106	Thermo Fisher Scientific
IMDM	12440061	Thermo Fisher Scientific

Name	**catalog**	**source**
IMDM GlutaMAX™	31980048	Thermo Fisher Scientific
DMEM	41965062	Thermo Fisher Scientific
Penicillin-Streptomycin Solution (10,000 units ea.)	15140130	Thermo Fisher Scientific
TrypLE™ Express Enzyme (1X), phenol red	12605-010	Thermo Fisher Scientific
SYTOX™ Blue dead cell stain	S34857	Thermo Fisher Scientific
LysoTracker™ DeepRed	L12492	Thermo Fisher Scientific
Sodium Pyruvate (100mM)	11360070	Thermo Fisher Scientific
Non-essential amino acids 100x (NEAA)	11140050	Thermo Fisher Scientific
MitoTracker™ Deep Red FM	M22426	Thermo Fisher Scientific
Tris-HCl (pH 7.4)		Carl Roth
Sodium chloride		Applichem (Darmstadt, Germany)
Glycerol		Carl Roth
Sodium fluoride		Sigma-Aldrich
Orthovanadate		Sigma-Aldrich
Phenylmethylsulfonyl fluoride (PMSF)		Sigma-Aldrich
Dimethyl sulfoxide (DMSO)		Avantor (J.T.Baker), Center Valley, PA, USA
RPMI		Thermo Fisher Scientific

6.8 Buffers and media

Table 9: Buffers and media

Name	Ingredients
Dynal buffer	D-PBS + 0.1% BSA + 2 mM EDTA
FACS buffer	D-PBS + 2% FCS
K562 medium (CTL)	DMEM + 10% FCS + 1% penicillin/streptomycin
NK cell medium	IMDM GlutaMAX™ + 10% FCS + 1% penicillin/streptomycin
MCF7 medium	DMEM + 10% FCS + 1% penicillin/streptomycin + 1% Sodium Pyruvate + 0.1% NEAA + 0.1% Insulin
HepG2 medium	DMEM + 10% FCS + 1% penicillin/streptomycin
Lysis buffer	20 mM Tris-HCl (pH 7.4) 150 mM sodium chloride 10% (w/v) Glycerol 10 mM sodium fluoride 2 mM EDTA 0.5% Triton-X100 1mM Orthovanadate 1mM PMSF ddH20, pH=7.3

6.9 Software

Table 10: Software

FlowJo 10.5.3	FlowJo, LLC, Ashland, USA
GraphPad PRISM Version 9	GraphPad, La Jolla, USA
Seahorse analytics	Agilent
GSEA 4.2.3	UC, San Diego, CA, USA
LEGENDplex™ Data Analysis Software Suite	BioLegend
ImageJ 2	Wayne Rasband and contributors, NIH, Maryland, MD, USA
Illustrations were created with BioRender	

6.10 Isolation of peripheral blood mononuclear cells

The purification of PBMCs (peripheral blood mononuclear cells) from whole blood or buffy coats was carried out using density gradient centrifugation. First, 15 ml of Human Pancoll Lymphocyte Separation Medium (LSM, density: 1.077 g/ml) was placed in a 50 ml Tube and 25-30 ml of whole blood or buffy coat, which was diluted with PBS, was layered without mixing the two layers. The samples were centrifuged at 473 x g for 25 minutes. To obtain a clean PBMC layer, this centrifugation step was performed without braking. In the next step, the PBMC layer was removed and transferred to a new tube. Residual LSM was removed by subsequent washing steps (3 times 5 minutes, 473 x g) with DPBS (Dulbecco's Phosphate-Buffered Saline). The cell number and the viability of the cells were determined using the CASY Cell Counter & Analyzer.

6.11 Isolation of PBMC and granulocytes

To isolate both granulocytes and PBMCs, 10 ml of LSM 1.119 g/ml was overlaid with 10 ml of LSM 1.077 g/ml, followed by the addition of a third layer containing whole blood. The samples were then centrifuged at 473 x g for 25 minutes. To obtain a clean granulocytes layer and PBMC layer, this centrifugation step was performed without braking. Next, the PBMC layer as well as the granulocytes layer was removed and transferred to a new 50 ml Tube, followed by 3 washing steps (each 5 minutes, 473 x g) with DPBS. The cell number and the viability of the cells were determined using the CASY Cell Counter & Analyzer

6.12 Isolation of NK cells and cell culture

Human NK cells were isolated from PBMC with the Dynabeads® Untouched™ Human NK Cell-Kit according to the manufacturer's instructions (Invitrogen). For experiments with resting NK cells, isolated NK cells were rested in NK cell medium overnight and then used for experiments. To generate pre-activated NK cells, isolated NK cells were seeded in 96-well round-bottom plates (Nunc) at a density of 1 – 1.5*10^6 mL^{-1} with 30 Gy irradiated feeder cells (K562-mbIL15-41BBL) in medium at a ratio of 2:1 (NK cells:feeder cells) with 200 U/mL IL-2 and 100 ng/mL IL-21 and incubated at 37°C humidified 5% CO_2. On day 8, NK cells were re-stimulated with fresh feeder cells at a ratio of 2:1 (NK cells:feeder cells). In the next weeks, NK cells were counted every 72 h. If cell count was below 3x10^6/ml a medium exchange was performed, if cell count was 3x10^6/ml or higher cells were split to a density of 1.5 – 2 *10^6 mL^{-1} supplemented

with 100 U/mL IL-2. On day 14 recombinant 2.5 ng/mL IL-15 was added and after three weeks NK cells can be used as pre-activated NK cells.

6.13 Short-term treatment

For short-term treatment, resting or pre-activated NK cells were pre-treated with 100 nM Glutor, 100 nM Glupin or 0.1% DMSO for 30 minutes followed by a stimulation for 2 h or 16 h (described in 6.20.2 and 6.21) in the presence of indicated inhibitors or control.

6.14 Long-term treatment

For long-term treatment with 100 nM Glutor, 100 nM Glupin, 0.5 µM CB839 or 0.1% DMSO these substances were added to the culture at day zero and to the fresh medium added to the culture every 72 h.

6.15 Cultivation of cell lines

K562 cells were cultured in K562 medium. MCF7 cells were cultured in MCF7 medium. HepG2 cells were cultured in HepG2 medium. Cells were split 2-3 times a week to $0.3x10^6$/ml depending on growth.

6.16 RTCA analysis

First, 50 µl of medium was added to the e-plate wells and a background measurement was performed. Then $3x10^4$ MCF7 cells or HepG2 cells were seeded in 100 µl medium per well. The measurement was carried out for approx. 16 hours, followed by the addition of NK cells (3750 NK cells) plus medium with or without DMSO (0.1%), Glutor or Glupin (100 nM) in 50 µl. Subsequently, the measurement was started again, and the resistance was measured every 10 minutes over a period of 72 h.

6.17 Cultivation with short-chain fatty acids

Pre-activated NK cells were cultivated with 0.1% DMSO, Pentanoate (2.5 mM, 5 mM, 7.5 mM) or Butyrate (0.5 µM, 0.75 µM, 1 µM) for 72 h, followed by a degranulation-assay against K562 as described in section 6.20.2.

6.18 Inhibition of CPT1

Long-term treated NK cells (100 nM Glupin or 0.1% DMSO) were treated with 1 µM of the CPT1-inhibitor Etomoxir for 24 h, followed by plate-bound stimulation for degranulation-assay (6.20.2) or IFN-γ ELISA (6.21).

6.19 Flow cytometry

6.19.1 Surface staining

1 x 10^5 NK cells were added to v-bottom plates and washed with FACS buffer. This was followed by live-dead staining with zombie NIR in DPBS for 15 min at RT in the dark. After a wash step with FACS buffer, an antibody-cocktail for the activating receptor panel (Table 11) or the functional panel (**Fehler! Verweisquelle konnte nicht gefunden werden.**) was added to the cells and incubated for 15 min at RT in the dark. Cells were washed with FACS buffer, resuspended in 150 µl FACS buffer and measured on a Cytek Aurora flow cytometer. Data were analyzed using FlowJo software, gating for all living $CD56^+$ $CD3^-$ NK cells. Statistical analysis was performed using GraphPad Prism 9.

Table 11: activating receptor panel

antigen	Fluorophore	dilution
CD3	BUV563	200
CD56	BUV805	4000
CD335 (NKp46)	BV421	50
Zombie NIR	Zombie NIR	700
CD244 (2B4)	FITC	200
CD336 (NKp44)	PerCP-Cy5.5	100
CD16	PE-Dazzle	100
CD226 (DNAM-1)	AF647	100
CD314 (NKG2D)	AF700	100
CD337 (NKp30)	APC-Fire750	100

Table 12: functional panel

antigen	Fluorophore	dilution
CD38	BUV395	100
CD159c (NKG2C)	BUV496	50
CD3	BUV563	200
CD161	BUV661	100
CD56	BUV805	4000
CD137 (41BB)	BV421	50
KLRG1	BV510	50
HLA-DR	BV605	100
CD178 (FasL)	BV650	100
TIGIT	BV786	100
CD11a	AF488	2000
CD8	AF532	200
CD27	PerCP-Cy5.5	50
CD159a (NKG2A)	PE	100
CD152 (CTLA-4)	PE-Dazzle	100
CD253 (TRAIL)	PE-Cy7	50
CD279 (PD-1)	AF647	400
CD18	AF700	800
Zombie NIR	Zombie NIR	700
CD366 (TIM-3)	APC-Fire 750	50

6.19.2 Degranulation-Assay

Nunc flat-bottom plates were coated with 2 µg/ml antibodies against CD16, NKp30, NKG2D + 2B4 or with control IgG in PBS overnight at 4°C. $1x10^5$ pre-activated or resting NK cells were pre-treated with 100 nM Glutor, 100 nM Glupin, 0.5 µM CB839 or DMSO (0.1%) in 100 µl NK cell medium for 30 minutes and then stimulated by adding the cells to the prepared plate or with K562 cells (E:T 2:1). The cells were incubated for 2 h (plate-bound stimulation) or 4 h (K562 stimulation) at 37°C and 5% CO_2 in the presence of a CD107a antibody, followed by a surface staining for CD56 (BV421) for 15 min at RT in the dark. Next, NK cells were washed with FACS buffer, resuspended in 150 µl FACS buffer and measured on a BD LSRFortessa flow cytometer. Data were analyzed using FlowJo software, gating on $CD56^+$ $CD107^+$ NK cells followed by statistical analyses using GraphPad Prism 9.

6.19.3 Analysis of Granzyme B and perforin levels

$2x10^5$ pre-treated NK cells were added to a v-bottom-well plate and washed once with FACS buffer. Staining was performed using zombie NIR and anti-CD56 antibody (BV421) in DPBS for 15 min at RT in the dark, followed by a washing step with FACS buffer. Next, cells were fixed using 2 % paraformaldehyde (PFA) (10 min, RT), permeabilized using BD FACS™ Permeabilizing Solution 2 (10 min, RT) and washed once with FACS buffer. Intracellular staining for Granzyme B and Perforin was performed for 30 min at RT in the dark followed by a washing step with FACS buffer, resuspended in 150 µl FACS-buffer and measured on a BD LSRFortessa flow cytometer. Data were analyzed using FlowJo software, gating on living $CD56^+$ NK cells followed by statistical analyses using GraphPad Prism 9.

6.19.4 Analysis of pmTOR and HK1

$2x10^5$ pre-treated NK cells were seeded into a v-bottom-well plate and washed once with FACS buffer. Surface staining was performed using zombie NIR and anti-CD56 antibody (BV421) in PBS for 15 min at RT in the dark, followed by a washing step with FACS buffer. Surface staining, fixation and permeabilization was performed as described in 6.17.3. Intracellular staining for GLUT-1, pmTOR and HK1 was performed for 30 min at RT in the dark followed by a washing step with FACS buffer. Cells were resuspended in 150 µl FACS buffer and measured on a BD LSRFortessa flow cytometer. Data were analyzed using FlowJo software, gating on living $CD56^+$ NK cells followed by statistical using GraphPad Prism 9.

6.19.5 Analysis of cMyc using intracellular staining

$2x10^5$ pre-treated NK cells were seeded into a v-bottom-well plate and washed once with FACS buffer. Staining was performed using zombie NIR and antibodies against CD56 (BV421), CD98 and CD71 in PBS for 15 min at RT in the dark, followed by a washing step with FACS buffer. Next, cells were fixed and permeabilized using the eBioscience™ Foxp3 / Transcription Factor Staining Buffer Set according to the manufacturer's instructions. Intracellular staining for cMyc was performed for 30 min at 4°C in the dark followed by a washing step with FACS buffer. Cells were resuspended in 150 µl FACS buffer and measured on a Cytek Aurora flow cytometer. Data were analyzed using FlowJo software, gating on living $CD56^+$ NK cells followed by statistical analyses using GraphPad Prism 9.

6.19.6 Multiplex-Bead Assay

Supernatants of cultured long-term treated NK cells were collected 24 h after medium exchange and used for multiplex-bead array using Legendplex Human Inflammation Panel 1. The assay was performed according to the manufacturer's instructions (BioLegend) and measured with a BD LSRFortessa flow cytometer. Data were analyzed using the Legendplex software (BioLegend).

6.19.7 Migration-Assay

Supernatants of cultured long-term treated NK cells were collected 24 h after medium exchange and 235 µl of each was added to the lower chamber of the transwell plates (HTS transwell®-96 Permeable Support with 5.0 µm Pore Polycarbonate Membrane, Corning). The transwell inserts were placed into the chamber and 80 µl medium containing $2.5x10^5$ cells (a mixture of previously isolated granulocytes and PBMCs) was added to the insert. After 4 hours of incubation at 37°C and 5% CO_2, a brief incubation at 4°C for 10 min was performed to induce detachment of monocytes. Cells were then removed from the lower chamber, transferred to a v-bottom-well plate, and pelleted by centrifugation. In the next step, cells were resuspended in 50 µl FACS buffer containing an antibody mix for CD3, CD56 (BV421), CD14, CD19, CD66b and CD1c, transferred to TruCount tubes, and incubated for 20 min at RT in the dark. Then, 100 µl FACS buffer was added and measurement of cells was performed using the BD LSRFortessa. Data were analyzed using FlowJo software and absolute cell counts were calculated according to the manufacturer's instructions.

6.19.8 Analysis of mitochondrial mass

Long-term treated NK cells with Glupin (100 nM), DMSO (0.1%) or CB839 (0.5 µM) were stained with 0.1 µM MitoTracker DeepRed in RPMI medium (without FBS) for 15 min at 37°C. Subsequently, cells were washed with DPBS and a staining with anti-CD56 BV421 and Zombie NIR in DPBS was performed (15 min, RT). Fluorescnce intensity of MitoTracker DeepRed was measured using Cytek Aurora flow cytometer. Analysis was performed using FlowJo, gating on living $CD56^+$ NK cells followed by statistical analyses using GraphPad Prism 9.

6.19.9 Proliferation assay

13 x 10^6 freshly isolated NK cells were stained with 0.1 µM CellTracker DeepRed in 10 ml RPMI medium for 15 min at 37°C, followed by a washing step with PBS. Subsequently, 1.5 x 10^6 NK cells were resuspended in 1 ml NK cell medium or IMDM without Glucose with 200 U/mL IL-2 and 100 ng/mL IL-21. NK cells were seeded in 96-well round-bottom plates (Nunc) at a density of 1.5 – 2*10^6 mL^{-1} with 30 Gy irradiated feeder cells (K562-mbIL15-41BBL) at a ratio of 2:1 (NK cells:feeder cells) and incubated in a humidified incubator at 37°C and 5% CO_2. The fluorescence intensity of CellTracker DeepRed was analyzed on days 0, 2 and 4 using flow cytometry (BD LSRFortessa). Analysis was performed using FlowJo, gating on $CD56^+$ NK cells followed by statistical analyses using GraphPad Prism 9.

6.19.10 SCENITH

2x10^5 long-term treated NK cells were seeded in 100 µl IMDM medium/well and incubated in the presence or absence of oligomycin (1 µM), 2-DG (100 mM) or oligomycin + 2-DG for 30 minutes at 37°C and 5% CO_2. Oligomycin inhibits OxPhos, whereas 2-DG inhibits glycolysis. Then 100 µl of IMDM medium containing puromycin (10 µg/ml) was added to each well and incubated for 20 minutes at 37°C and 5% CO_2 (Figure 5). An inhibition of glycolysis or OxPhos impairs protein synthesis, which is associated with a proportional, altered incorporation of puromycin during protein synthesis. (Argüello et al. 2020). These changes can be analyzed via flow cytometry using an anti-puromycin antibody, whose staining intensity is proportional to protein translation. Cells were washed with ice-cold PBS, an Fc block was performed for 5 minutes at 4°C, followed by staining with Zombie NIR, CD56 BV421 and CD16 for 30 min at 4°C. Cells were then washed, fixed and permeabilized with the eBioscience™ Foxp3 / Transcription Factor Staining Buffer Set according to the manufacturer's instructions, followed by intracellular staining with anti-puromycin AF488, anti-pmTOR PE-Cy7 and anti-GLUT-1 for 30 minutes. Finally, cells were washed with FACS buffer and measured on a Cytek Aurora flow cytometer. Data were analyzed using FlowJo software (FlowJo), gating on living $CD56^+$ NK cells followed by statistical analyses using GraphPad Prism 9. Glucose dependence (quantifies how much the translation levels are dependent on glucose oxidation), mitochondrial dependence (quantifies how much translation is dependent on oxidative phosphorylation), glycolytic capacity (maximum capacity to maintain protein synthesis when mitochondrial OXPHOS is

blocked), FAO and AAO capacity (the ability to use fatty acids and amino acids as sources for ATP production in the mitochondria when glucose oxidation is blocked) was calculated as described in table 13. (Argüello et al. 2020).

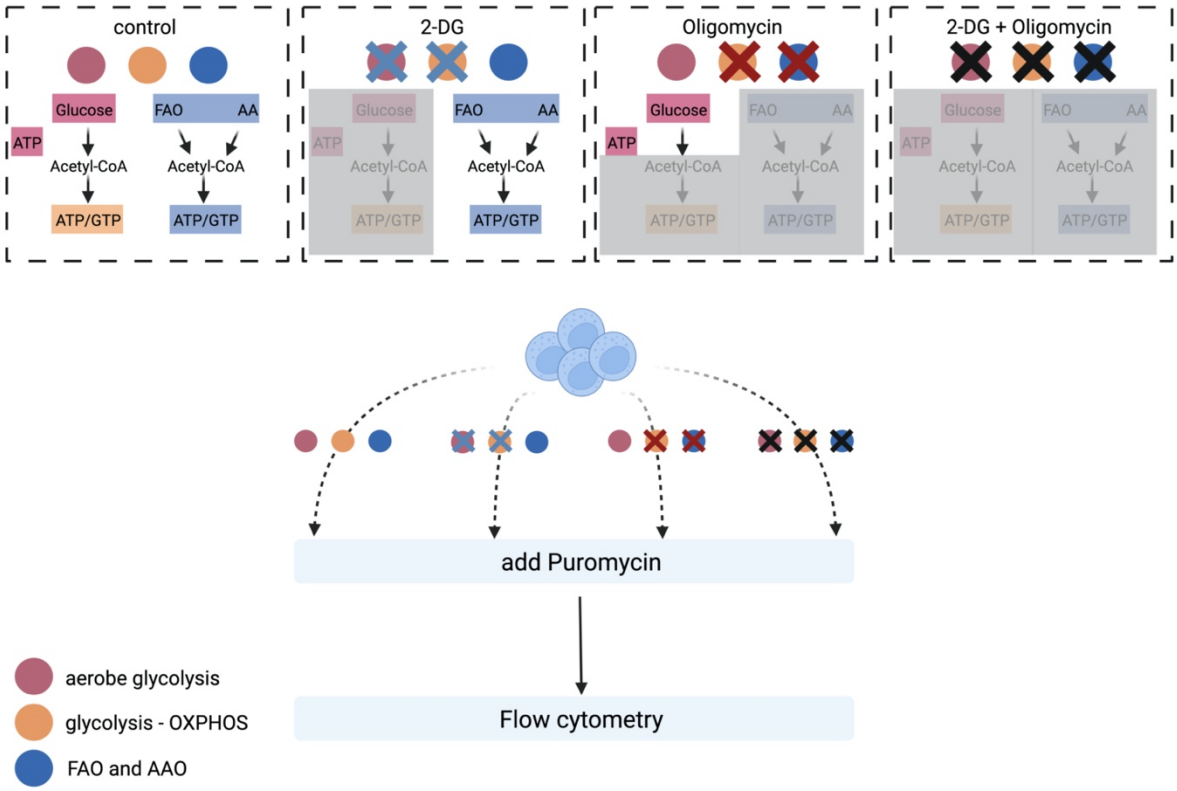

Figure 5: Description of SCENITH

Schematic illustration of SCENITH. NK cells were treated the inhibitor of glycolysis 2-DG, the inhibitor of OxPhos Oligomycin, the combination of 2-DG and Oligomycin or without the inhibitors, followed by the addition of Puromycin, which will be incorporated during protein translation. Subsequently, intracellular staining of Puromycin using anti-Puromycin AF488 was performed and intensity of anti-puromycin AF488 was measured via flow cytometry. Based on the formula below the metabolic capacities and dependencies of the cells can be analyzed.

Table 13: formulas for calculating the metabolic profile

$$Glucose\ dependency\ = \frac{100(Co - DG)}{(Co - DGO)}$$

$$Mitochondrial\ dependency\ = \frac{100\ (Co - O)}{(Co - DGO)}$$

$$Glycolytic\ capacity = (\frac{100(Co - O)}{(Co - DGO)})$$

$$FAO\ and\ AAO\ capacity = (\frac{100(O - DG)}{(O - DGO)})$$

Co: GeoMFI of anti-Puromycin-AF488 upon control treatment
DG: GeoMFI of anti-Puromycin-AF488 upon 2-DG treatment
O: GeoMFI of anti-Puromycin-AF488 upon Oligomycin A treatment
DGO: GeoMFI of anti-Puromycin-AF488 upon DG+O treatment

6.20 ELISA

Resting or pre-activated NK cells were pre-treated with Glutor (100 nM), Glupin (100 nM), CB839 (0.5 µM) or DMSO (0.1%) for 30 minutes and afterwards stimulated via 2 µg/ml plate-bound antibodies against CD16, NKp30, NKG2D + 2B4 or control IgG or via the cytokines IL-12 (0.25 ng/µl) + IL-18 (1.25 ng/µl). After 16 h supernatants were collected, and IFN-γ secretion was analyzed using the ELISA MAX™ Deluxe Set Human IFN-γ from BioLegend according to the manufacturer's instructions. Measurement was done with a GloMax^{R} instrument (Promega) followed by statistical analyses using GraphPad Prism 9. Background measurement of IgG control was excluded for each sample.

6.21 Glucose-uptake Assay

To analyze glucose-uptake of long-term treated NK cells, Glucose uptake-Glo^{TM} Assay (Promega) was performed according to the manufacturer's instructions with 2.5x10^{5} NK cells/well in duplicates. Measurement of luminescent was performed after an incubation of 1 hour using a GloMax^{R} instrument (Promega). Statistical analyses were performed using GraphPad Prism 9.

6.22 NAD/NADH-Assay

Long-term treated NK cells were analyzed for NAD^{+}/NADH concentrations using NAD/NADH-Glo™ Assay (Promega). Assay was performed according to the manufacturer's instructions with 1x10^{5} NK cells/well in duplicates. Measurement was done with a GloMax^{R} instrument. Statistical analyses were performed using GraphPad Prism 9.

6.23 Malate-Assay

To lyse the cells without affecting the nucleus we used nitrogen cavitation. 10x10^{6} NK cells were pelleted and resuspended in 200 µl of Malate-assay buffer. Next, NK cell suspension was added into the pre-cooled cavitation chamber and the chamber was closed. All filling connections were attached, and the pressure was set to 1000 psi. After 5 minutes lysed cells were collected by slowly opening the release valve, followed by a centrifugation step (473 x g, 5 min). Analysis of the Malate concentration was performed using the Malate-Assay kit (Sigma Aldrich) according to the manufacturer's

instructions. Measurement was done with a GloMax^{R} instrument. Statistical analyses were performed using GraphPad Prism 9.

6.24 Seahorse-analysis

The energetic phenotype of pre-activated NK cells was analyzed using the glycolysis stress test kit (Agilent). Experiments were performed according to the manufacturer's instructions. In brief, culture plates were coated with 25 µl poly-l-lysine (10 min, 21°C), followed by the addition of $2.5x10^5$ pre-activated NK cells in 80 µl RPMI without Glucose per well. Cells were incubated for 30 minutes at 37°C without CO_2. In the meantime, injection ports were loaded with 10-fold concentrated substance (final concentration after injection: Port A: 100 nM Glutor, 100 nM Glupin, medium or 0.1% DMSO; Port B: 10 mM Glucose; Port C: 1 µM Oligomycin; Port D: 50 mM 2-DG) and subsequently calibration of the sensors was performed. Lastly, 100 µl RPMI without glucose was added to the cells and measurement using Seahorse XFe96 Analyzer was started. Extracellular acidification rate (ECAR) as well as oxygen consumption rate (OCR) were measured every 3 minutes. After 18 minutes, port A was injected and over the period of 28 minutes, the ECAR and OCR values were measured every 3 minutes. This was followed by the injection of port B and, after an 18-minute measurement period, the injection of port C. After a further 18 minutes, port D was injected followed by an 18-minute measurement. Data were analyzed using the seahorse analytics software (Agilent).

6.25 ^{51}Chromium-release Assay

Cytotoxicity was analyzed using a standard 4 h chromium release assay as previously described (Messmer et al., 2006). In brief, target cells were labelled with ^{51}Cr for 1 h at 37°C and 5% CO_2 on a rotator. Target cells were then washed twice and 5000 targets/well were added to pre-activated NK cells in a 96 u-bottom-well plate (final volume: 200 µl). The NK cells were serially diluted beforehand (1:2), starting with an E:T from 2:1 to 0.25:1 in triplicates. The maximum release was determined by using TritonX-100 for target cell lysis, whereas spontaneous release was determined by the incubation of target cells without NK cells. After 4 hours of incubation, the supernatant was collected and analyzed using the Wizard^2 (Perkin Elmer) gamma counter. The percentage of specific lysis was determined as follows:

$$\frac{experimental\ release - spontaneous\ release}{maximal\ release - spontaneous\ release} * 100\ \%$$

6.26 Serial-killing assays

Assays were performed as described before (Prager et al. 2019). In brief, microchips were equilibrated with 200 µl CTL medium for 1 h at 37°C and 5% CO_2, followed by removing the media and addition of fresh 200 µl CTL medium. Then, 30 µl (30.000 cells) of resuspended MCF7 cells were added and the microchip was placed into the incubator. After 5-10 min, the distribution and amount of tumor cells per well was checked. If there are enough wells with a density of 60-80 tumor cells, the medium was changed to remove cells not yet sedimented. Microchip was incubated for 16 h at 37°C with 5% CO_2 to allow attachment of tumor cells. After 16 h, medium was removed and 200 µl of CTL medium with the dead cell stain SYTOX Blue (1:1000) was added. The microchip was placed into the incubation chamber of the ApoTome System with Axio Observer 7 microscope (Zeiss) equipped with a 20×/0.8 Plan-Apochromat objective and an incubation chamber with environmental control (37 °C, 5% CO_2, humidity device PM S1). Wells with a density of 60-80 tumor cells were selected. Next, long-term treated NK cells were added so that an optimal distribution with about 10-20 NK cells per well was achieved. Time-lapse microscopy was started, and a picture was taken every 3 minutes for 16 h using an Axiocam 506 mono camera. SYTOX Blue was excited using the Colibri 7 LED-module 475 (filter set 38 HE LED) and brightfield was acquired using the TL LED module. Analysis was performed using Image J.

6.27 RNA-Sequencing

$10x10^6$ long-term treated NK cells (21 days) and short-term treated NK cells (72h) were used for RNA Isolation. RNA Isolation was performed using RNAeasy Mini Kit (Qiagen) according to the manufacturer's instructions with an additional step of DNAse treatment. Further analysis regarding purity and RNA-sequencing were performed at the genomics & transcriptomics facility (GTF) at the university hospital Essen.

6.28 Metabolomics

For Metabolomics, $10x10^6$ long-term treated NK cells (21 days) were lysed using 200 µl of lysis buffer (20 min on ice), followed by a centrifugation step (14.800 rpm, 20 min, 4°C). Supernatants were collected and used for metabolomics. Metabolomics were performed by the Metabolomics Innovation Centre (TMIC Canada). They have applied a targeted quantitative metabolomics approach to analyze the samples using a combination of direct injection mass spectrometry with a reverse-phase LC-MS/MS

custom assay. This custom assay, in combination with an ABSciex 4000 QTrap (Applied Biosystems/MDS Sciex) mass spectrometer, can be used for the targeted identification and quantification of up to 143 different endogenous metabolites including amino acids, acylcarnitines, biogenic amines & derivatives, glycerophospholipids, sphingolipids and sugars. The method combines the derivatization and extraction of analytes, and the selective mass-spectrometric detection using multiple reaction monitoring (MRM) pairs. Isotope-labeled internal standards and other internal standards are used for metabolite quantification. The custom assay contains a 96 deep-well plate with a filter plate attached with sealing tape, and reagents and solvents used to prepare the plate assay. First 14 wells were used for one blank, three zero samples, seven standards and three quality control samples. For all metabolites except organic acid, samples were thawed on ice and were vortexed and centrifuged at 13,000 x g. 10 µl of each sample was loaded onto the center of the filter on the upper 96 well plate and dried in a stream of nitrogen. Subsequently, phenyl-isothiocyanate was added for derivatization. After incubation, the filter spots were dried again using an evaporator. Extraction of the metabolites was then achieved by adding 300 µl of extraction solvent. The extracts were obtained by centrifugation into the lower 96-deep well plate, followed by a dilution step with MS running solvent. For organic acid analysis, 150 µl of ice-cold methanol and 10 µl of isotope-labeled internal standard mixture was added to 50 µl of sample for overnight protein precipitation. Then it was centrifuged at 13000 x g for 20 min. 50 µl of supernatant was loaded into the center of wells of a 96-deep-well plate, followed by the addition of 3-nitrophenylhydrazine (NPH) reagent. After incubation for 2 h, BHT stabilizer and water were added before LC-MS injection. Mass spectrometric analysis was performed on an ABSciex 4000 Qtrap® tandem mass spectrometry instrument (Applied Biosystems/MDS Analytical Technologies, Foster City, CA) equipped with an Agilent 1260 series UHPLC system (Agilent Technologies, Palo Alto, CA). The samples were delivered to the mass spectrometer by a LC method followed by a direct injection (DI) method. Data analysis was done using Analyst 1.6.2.

6.29 Statistics

Statistical analyses were performed using GraphPad Prism version 9.

Statistical analysis was performed by Multiple Comparisons: Tukey-Kramer, paired-t test or ONE-Way ANOVA (indicated in the legends).

7 Results

Metabolic regulation of NK cells has a major impact on NK cell function during viral infections but could also influence killing capacity against tumor cells. The newly synthesized anticancer drugs Glutor and Glupin target GLUT-1 and GLUT-3, and in the case of Glutor, GLUT-2. Since NK cells predominantly express GLUT-1, we wanted to investigate whether these inhibitors also affect NK cell metabolism and thereby alter NK cell proliferation and function.

7.1 Short-term treatment

7.1.1 Effect of Glut Inhibitors on energetic phenotype of NK cells

NK cell activity is glucose dependent, and the increased glucose demand upon activation is served by glucose transporters like GLUT-1. Here, we wanted to determine whether NK cells react to the GLUT-inhibitors Glutor and Glupin. To assess the metabolic phenotype of pre-activated NK cells under GLUT-Inhibitor treatment, we used the Seahorse technology to determine changes in the extracellular acidification rate (ECAR) as a measure of glycolysis and changes in the oxygen consumption rate (OCR) as a measure of OxPhos. In the absence of glucose, injection of different concentrations (10 nM, 50 nM, 100 nM, 200 nM) of Glutor or Glupin did not alter basal ECAR values or OCR values. However, in the presence of glucose, a dose-dependent decrease in ECAR values was observed when 50 nM, 100 nM, or 200 nM Glutor was administered, whereas only the two highest concentrations of Glupin (100 nM and 200 nM) resulted in a decrease in ECAR values (Figure 6A). Both inhibitors caused a dose-dependent increase in OCR levels in the presence of glucose suggesting increased OxPhos (Figure 6B). Subsequent inhibition of OxPhos using Oligomycin results in the maximum glycolytic capacity of the cells. NK cells treated with 50 nM, 100 nM, or 200 nM Glutor or with the two highest concentrations of Glupin showed a diminished maximum glycolytic capacity, indicating that these cells cannot acutely compensate for an inhibition of OxPhos via glycolysis. Injection of the glucose-analogue 2-DG caused complete inhibition of glycolysis under all conditions. These data demonstrate that both Glutor and Glupin lead to a specific inhibition of glycolysis in NK cells at concentrations of 100 nM and 200 nM, respectively. Since both inhibitors already exerted an effect on

NK cell metabolism at a concentration of 100 nM, all subsequent experiments were performed with 100 nM Glutor or Glupin.

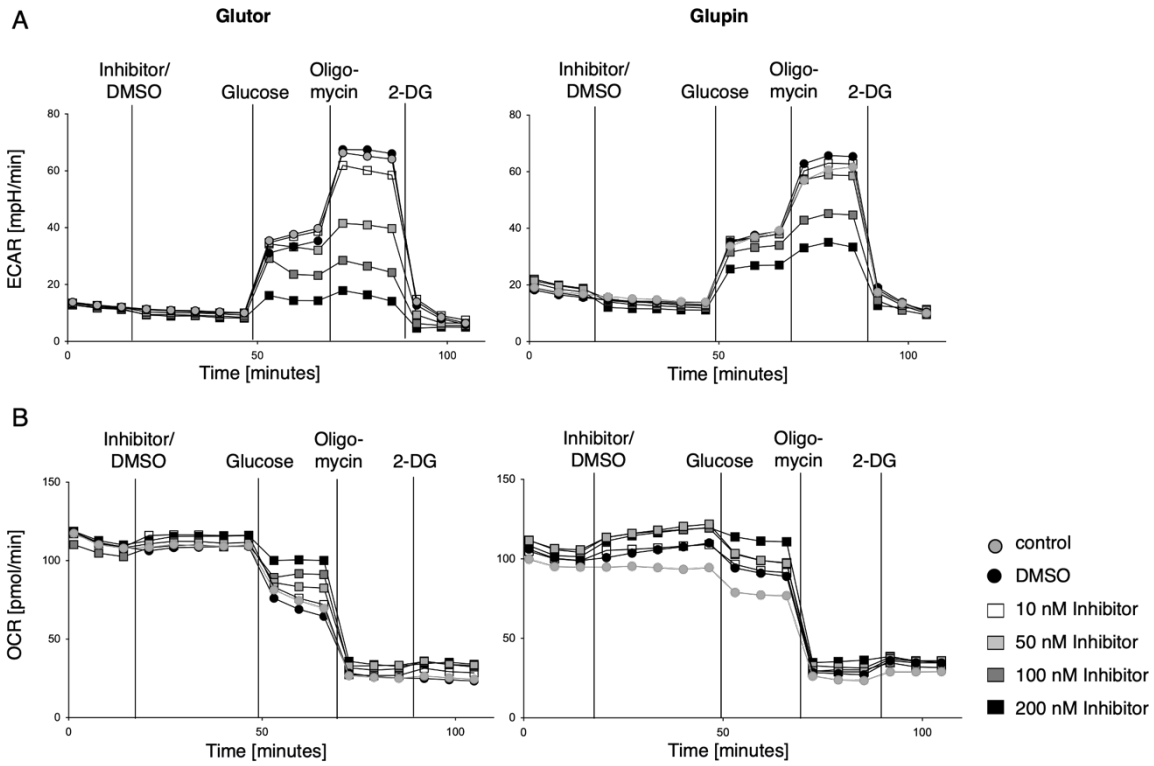

Figure 6: Energetic phenotype of pre-activated NK cells in the presence or absence of Glutor or Glupin

A) ECAR-Levels of pre-activated NK cells before and after addition of indicated concentrations of Glutor (left) or Glupin (right) and DMSO (0.1%) or medium, followed by injection of Glucose, Oligomycin and 2-DG. B) OCR-Levels of pre-activated NK cells before and after addition of indicated concentrations of Glutor (left) or Glupin (right) and DMSO (0.1%) or medium, followed by a second injection of Glucose, a third injection of Oligomycin and a fourth injection of 2-DG. Representative graph of one donor. n=3.

7.1.2 Short-term treatment with Glutor or Glupin did not affect NK cell functions

Since NK cell function is strongly regulated by NK cell metabolism (Gardiner 2019), and both Glutor and Glupin affect NK cell metabolism, we wanted to investigate whether these substances also affect NK cell function. Resting NK cells frequently use OxPhos to fulfill their demands and upregulate glycolysis and OxPhos during their activation. Therefore, we performed short-term inhibitor treatment of resting NK cells and preactivated NK cells because they have different metabolic profiles. We treated resting NK cells or pre-activated NK cells with 100 nM Glutor, 100 nM Glupin or DMSO as a control and analyze CD107a expression to determine degranulation. Treatment with Glutor did not alter the degranulation of resting NK cells as well as pre-activated NK cells compared to control. Similarly, short-term treatment of resting NK cells with Glupin did not alter degranulation compared with control. Similar observations could

be made for pre-activated NK cells. (Figure 7A & B). This indicates that the process of degranulation can occur without additional glucose uptake, at least in the short term.

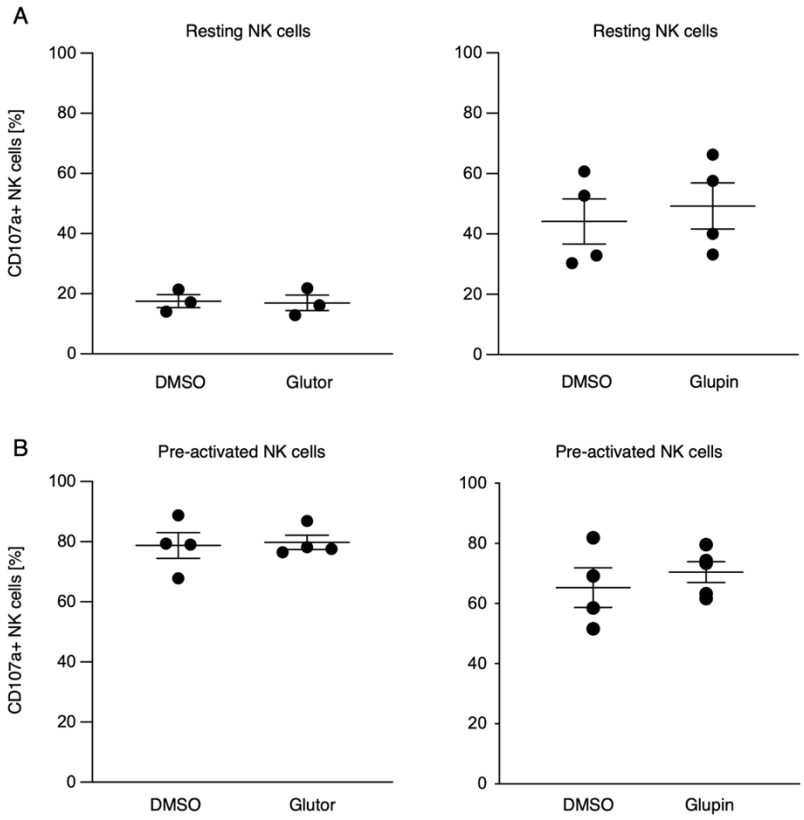

Figure 7: Effect of short-term treatment with Glutor or Glupin on degranulation of resting NK cells or pre-activated NK cells

A) $0.1x10^6$ resting NK cells were pre-treated with 100 nM Glutor (left), 100 nM Glupin (right) or 0.1% DMSO, followed by a stimulation via plate-bound CD16 mAb for 2 hours in the presence of anti-CD107a PE-Cy5. Flow cytometric analysis of CD107a expression on NK cells. B) $0.1x10^6$ pre-activated NK cells were pre-treated with 100 nM Glutor (left), 100nM Glupin (right) or 0.1% DMSO, followed by a stimulation via plate-bound CD16 mAb for 2 hours in the presence of anti-CD107a PE-Cy5. Flow cytometric analysis of CD107a expression on NK cells. n=3-4. Data were pooled from three or four independent experiments. Each experiment was performed with one donor. Data are presented as Mean with SEM.

In addition to cytotoxicity, we were interested in the immunoregulatory function of inhibitor treated NK cells. We analyzed IFN-γ secretion after 16 h stimulation of resting or pre-activated NK cells via plate-bound CD16-mAb in the presence or absence of Glutor or Glupin. The IFN-γ secretion of Glutor-treated resting NK cells or pre-activated NK cells showed no differences in comparison to the control. Short-term treatment of resting NK cells as well as pre-activated NK cells with Glupin showed no differences between Glupin-treatment and control (Figure 8A & B). Thus, short-term blockade of glucose uptake does not appear to have an inhibitory effect on IFN-γ secretion.

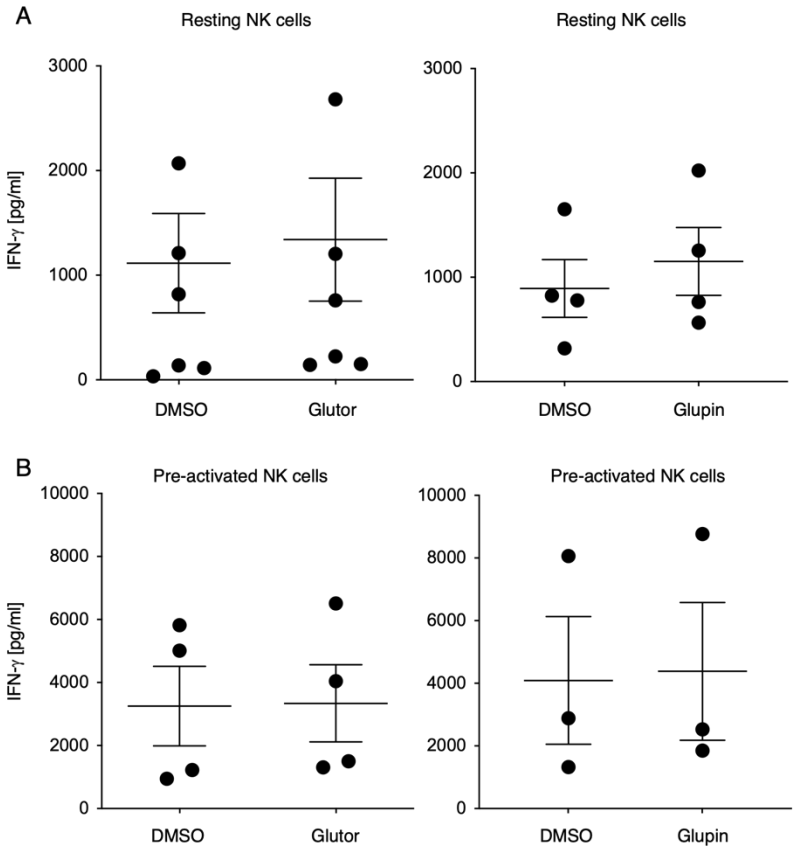

Figure 8: Effect of short-term treatment with Glutor or Glupin on IFN-γ secretion of resting NK cells or pre-activated NK cells

A) $0.1x10^6$ resting NK cells were pre-treated with 100 nM Glutor (left), 100 nM Glupin (right) or 0.1% DMSO, followed by a stimulation via plate-bound CD16 mAb for 16 hours followed by an analysis of IFN-γ secretion in the supernatant. B) $0.1x10^6$ pre-activated NK cells were pre-treated with 100 nM Glutor (left), 100 nM Glupin (right) or 0.1% DMSO, followed by a stimulation via plate-bound CD16 mAb for 16 hours followed by an analysis of IFN-γ secretion in the supernatant. n=3-6. Data were pooled from three or six independent experiments each experiment was performed with one donor. Mean with SEM.

In addition to activation of NK cells via activating receptors, NK cells can also be stimulated by IL-12 and IL-18 to produce large amounts of IFN-γ (Poznanski et al. 2017). We investigated whether this stimulation is influenced by short-term inhibition of GLUT-1 and 3. We could not detect any significant differences between control and NK cells short-term treated by Glutor or Glupin (Figure 9). Therefore, we concluded that NK cell functions are not affected by short-term inhibition of glucose uptake.

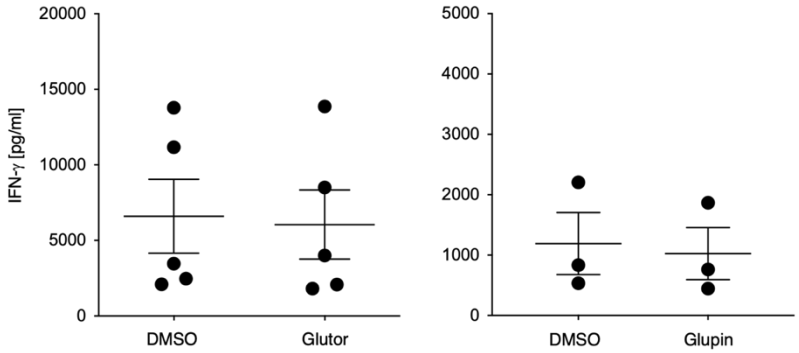

Figure 9: Effect of short-term treatment with Glutor or Glupin on IFN-γ secretion of resting NK cells or pre-activated NK cells

$0.1x10^6$ pre-activated NK cells were pre-treated with 100 nM Glutor (left), 100 nM Glupin (right) or 0.1% DMSO, followed by a stimulation via IL-12 and IL-18 for 16 hours. Analysis of IFN-γ secretion. n=3-5. Data were pooled from three or five independent experiments; each experiment was performed with one donor. Mean with SEM.

7.1.3 No reduced cytotoxic activity against tumor cells during treatment with GLUT-inhibitors

The direct effect of Glutor as well as Glupin on various tumor cell lines has already been investigated. It has been shown that both Glutor and Glupin inhibited the proliferation of different tumor cell lines (Reckzeh et al. 2019; Ceballos et al. 2019). NK cells play a key role in fighting cancer cells. Thus, a decreased killing capacity of NK cells due to Glutor or Glupin application would be detrimental for an anti-cancer drug. We therefore examined the effect of Glutor and Glupin on the interaction between NK cells and tumor cells using an impedance-based analysis assessing proliferation and viability of tumor cells in co-culture with NK cells. We used the breast cancer cell line MCF7 and the hepatocellular carcinoma cell line HepG2. MCF7 cells are sensitive to Glutor, while HepG2 are unaffected by Glutor. In comparison, both seem to be resistant to Glupin at lower concentrations below 500 nM. (Reckzeh et al. 2019; Ceballos et al. 2019). First, we measured the basal cell index of both tumor cell lines during the first 16 h after seeding and then added pre-activated NK cells with or without 100 nM Glutor / 100 nM Glupin or only 100 nM Glutor / 100 nM Glupin to the tumor cells and continued the measurement for additional 72 h. Our analysis confirmed that MCF7 cells are sensitive to 100 nM Glutor, as the cell index (CI) drops significantly. The same could be observed with the addition of NK cells and the combination of NK cells and Glutor leads to an additive decrease in cell index. The addition of 100 nM Glupin did not affect viability and proliferation of MCF7 cells, whereas the addition of NK cells resulted in a decreased cell index. NK cells could still reduce the cell index in the presence of Glupin (Figure 10A). In HepG2, we also observed a decrease in cell index after addition of NK

cells, but there was no decreased value after addition of Glupin or Glutor alone. The combined addition of NK cells and Glupin leads to a decrease in the cell index of HepG2 cells, but based on the previous observation, this effect appears to be due to the NK cells alone (Figure 10B). Furthermore, addition of Glutor has a significant inhibitory effect on the proliferation of MCF7 cells but not on the proliferation of HepG2 cells. Moreover, treatment with Glutor in the presence of NK cells has an additive inhibitory effect on MCF-7 cells. In contrast, both MCF7 cells and HepG2 cells are resistant to 100 nM Glupin, and NK cell function is not negatively affected over the entire duration of Glupin treatment. An additive anti-tumorigenic effect as shown for Glutor and NK cells on MCF7 cells in vitro would be a potential basis for therapeutic approaches targeting these glucose transporters, especially considering the finding that NK cell effector functions are not impaired by the presence of Glutor or Glupin.

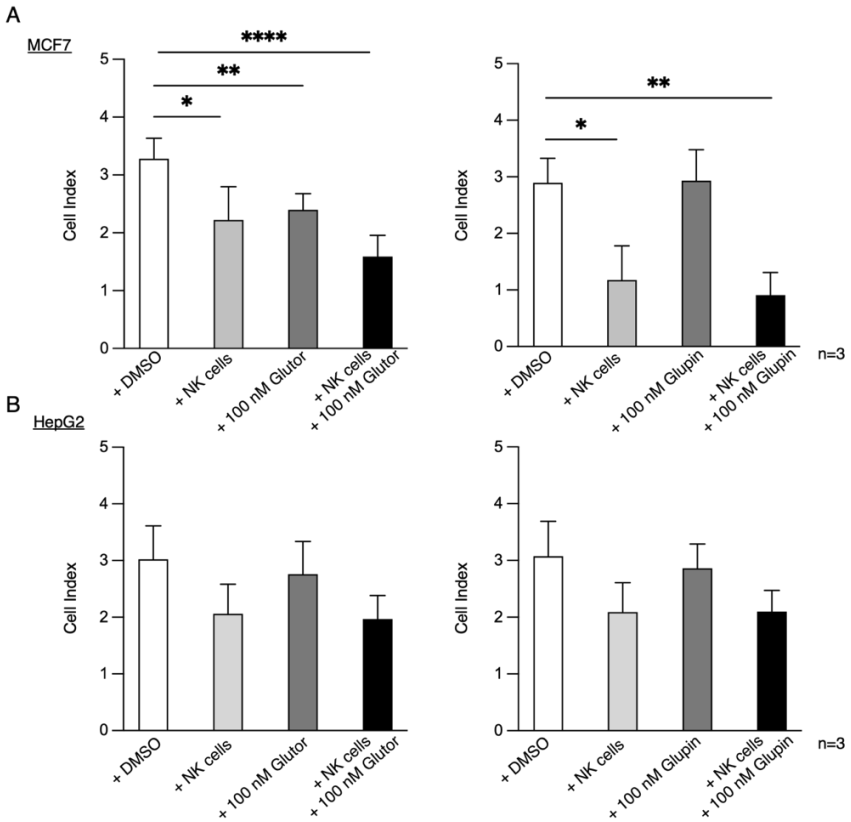

Figure 10: Killing-capacity of pre-activated NK cells during GLUT-inhibition

A) Impedance based analysis of MCF7 (A) or HepG2 (B) cells in the presence or absence of pre-activated NK cells and/ or 100 nM Glutor (left) or 100 nM Glupin (right). Cell Index 72 hours after addition of NK cells and Inhibitors. n=3. Data were pooled from three independent experiments; each experiment was performed with one donor. Mean with SEM. Statistical analysis was performed by Paired t-test. Significant differences are indicated by asterisk *P ≤ 0.05, **P ≤ 0.01, ***P ≤ 0.001, ****P ≤ 0.0001

7.2 Long-term treatment

7.2.1 Effects on proliferation of NK cells during long-term treatment

The previous data show that NK cells can sustain their functions over a short period of time during GLUT inhibition. However, we wanted to investigate in more detail the effects of the prolonged inhibition of glucose uptake with regards to proliferation and function, since a possible therapy with the inhibitors would also have to be continued over a longer period to achieve a successful outcome. Since we could observe effects on the energetic phenotype of the NK cells by addition of 100 nM Glutor or 100 nM Glupin, we decided to use this concentration during the long-term treatment. We used freshly isolated NK cells and treated them for three weeks with 100 nM Glutor or 100 nM Glupin in the presence of feeder cells and the cytokines IL-2, IL-15 and IL-21. First, we performed a proliferation assay, which showed a strong proliferation of control treated NK cells on the fourth day of culture compared to the first and second day (Figure 11). The addition of Glutor (green) resulted in a strongly reduced proliferation similar to glucose-free medium (yellow). Treatment with Glupin (blue) showed a slightly decreased proliferation on day four in comparison to the controls. Based on the findings of Reckzeh et al who showed that tumor cells use glutamine during glucose deprivation (Reckzeh et al. 2019) we are also interested in a possible effect of the glutaminase-inhibitor CB839 (0.5 µM) alone (light violet) or in combination with Glutor (light red) / Glupin (dark red) on proliferation of NK cells. The addition of CD839 alone did not affect proliferation of NK cells on day four, whereas a combination of CB839 with Glutor or Glupin showed a strong decrease in proliferation (Figure 11). This clearly shows the dependence on glucose during proliferation.

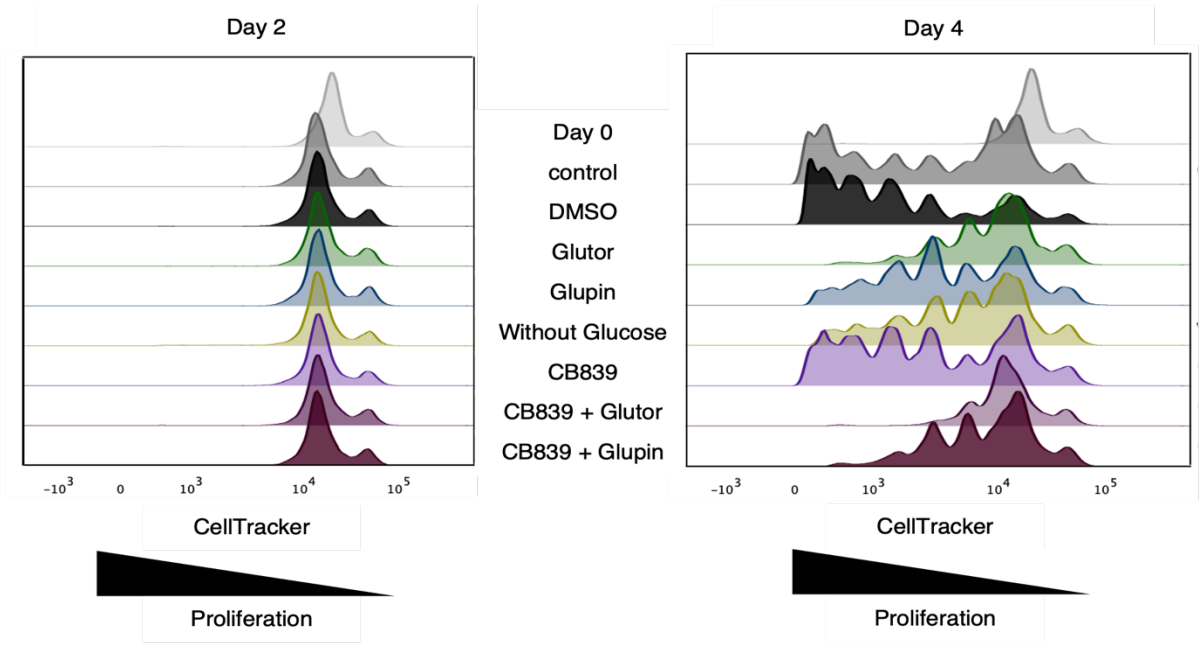

Figure 11: Influence of GLUT-Inhibitors and Glutaminase-Inhibitor on Proliferation of NK cells

Freshly isolated NK cells were stained with CellTracker Deep Red followed by a cultivation of these cells with Feeder cells, IL-2 and IL-21 in the presence or absence of DMSO, 100 nM Glutor, 100 nM Glupin, 0.5 µM CB839, 100 nM Glutor + 0.5 µM CB839 or 100 nM Glupin + 0.5 µM CB839. Medium w/o Glucose was used as a negative control. Flow cytometry analysis of proliferation was performed using fluorescence intensities of CellTracker DeepRed on Day 2 and Day 4. n=?

Since we could already detect differences in the effect of Glutor and Glupin on proliferation on the fourth day, we wanted to investigate the proliferation of NK cells over the entire cultivation period of three weeks. We checked the cell numbers every 72 hours during the first three weeks and were thus able to get an overview of the effect of long-term treatment with Glutor or Glupin on proliferation (Figure 12). The treatment with Glutor resulted in a significantly decreased proliferative capacity of NK cells in comparison to the controls, whereas treatment with Glupin resulted in a delayed proliferation within the first 10 days and increased proliferation afterwards. At the end of the observation period, Glupin-treated NK cells showed similar cell counts as the controls (Figure 12A). These results support the proliferation assay data, indicating that Glutor exerts a stronger effect on NK cells than Glupin. Similarly, the absolute cell numbers of NK cells treated with CB839 alone and in the respective combination with Glutor or Glupin were counted. Treatment of NK cells with CB839 results in a decreased proliferation and the combination of CB839 with Glutor or Glupin enhance this inhibitory effect. However, the viability of the CB839 + Glupin or Glutor treated NK cells decreased severely on day seven, and by day eight, all NK cells were dead (data not shown). Thus, glucose and glutamine are essential for NK cell survival. (Figure 12B).

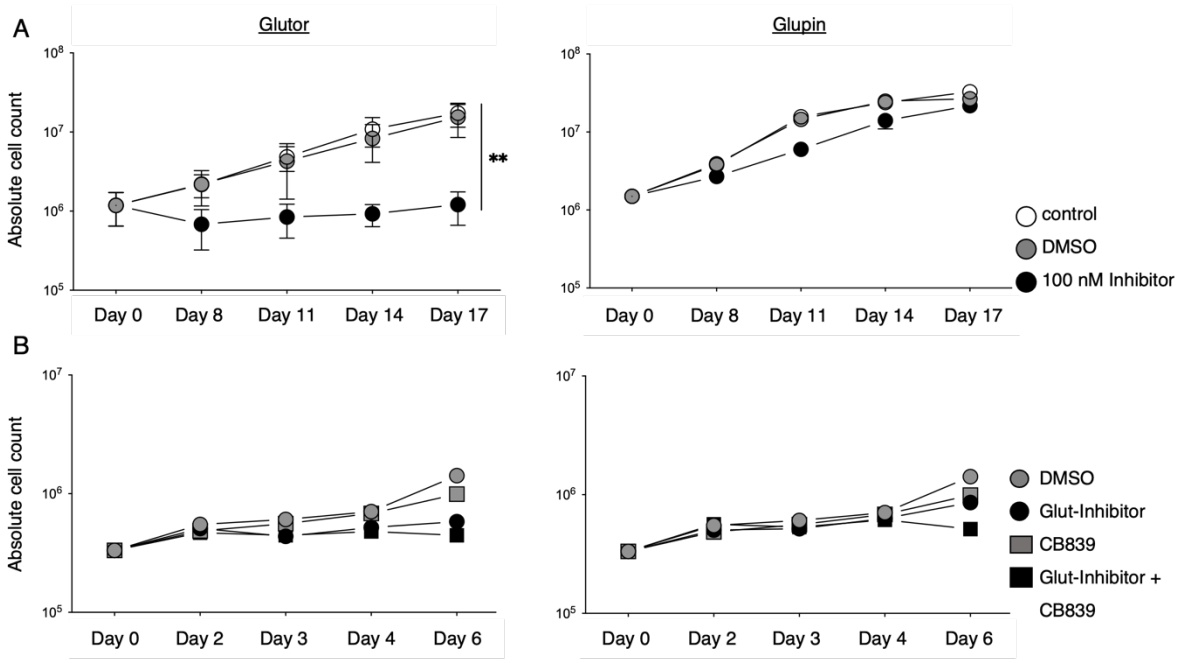

Figure 12: Influence of GLUT-inhibitors and Glutaminase-Inhibitor on absolute cell count

Freshly isolated NK cells were cultivated with feeder cells, IL-2 and IL-21 in the presence or absence of 0.1% DMSO, 100 nM Glutor, 100 nM Glupin, 0.5 µM CB839, 100 nM Glutor + 0.5 µM CB839 or 100 nM Glupin + 0.5 µM CB839. Absolute cell count was calculated at indicated time points. n=4. Data were pooled from four independent experiments each experiment was performed with one donor. Mean with SEM. Statistical analysis was performed by Paired t-test. Significant differences are indicated by asterisk *P ≤ 0.05, **P ≤ 0.01, ***P ≤ 0.001

7.2.2 Metabolic changes of NK cells during long-term treatment

Considering that an effect of Glutor and Glupin on NK cells is already evident within the first seven days, we wanted to investigate the influence of the two inhibitors on the expression levels of important metabolic molecules such as hexokinase-1 (HK1) and phosphorylated mTOR (pmTOR). Based on the changes regarding proliferation during long-term treatment with Glutor or Glupin, we assessed the levels of pmTOR, which plays an important role in regulation of proliferation and activation of NK cells (Donnelly et al. 2014). Treatment with Glutor resulted in a delayed, but extended upregulation of pmTOR levels: levels were lower at day four, but higher at day seven in comparison to the control. A similar trend could be observed for the Glupin-treated NK cells for day four and for day seven (Figure 13A&B). The analysis of the expression levels of HK1, an important enzyme for glycolysis, showed a similar pattern during long-term treatment with Glutor and Glupin. Expression levels were lower on day four, but higher at day seven in comparison to the control. Same trend could be observed for the Glupin-treated NK cells for day four and for day seven (Figure 13A&B). Interestingly, during inhibition of glucose uptake, the expression of HK1 was not downregulated but

upregulated, which may be a compensatory mechanism. Also, the prolonged expression of pmTOR seems to be a mechanism of NK cells to counteract glucose inhibition. And although these processes are observed in both Glutor and Glupin, only Glupin-treated cells manage to proliferate.

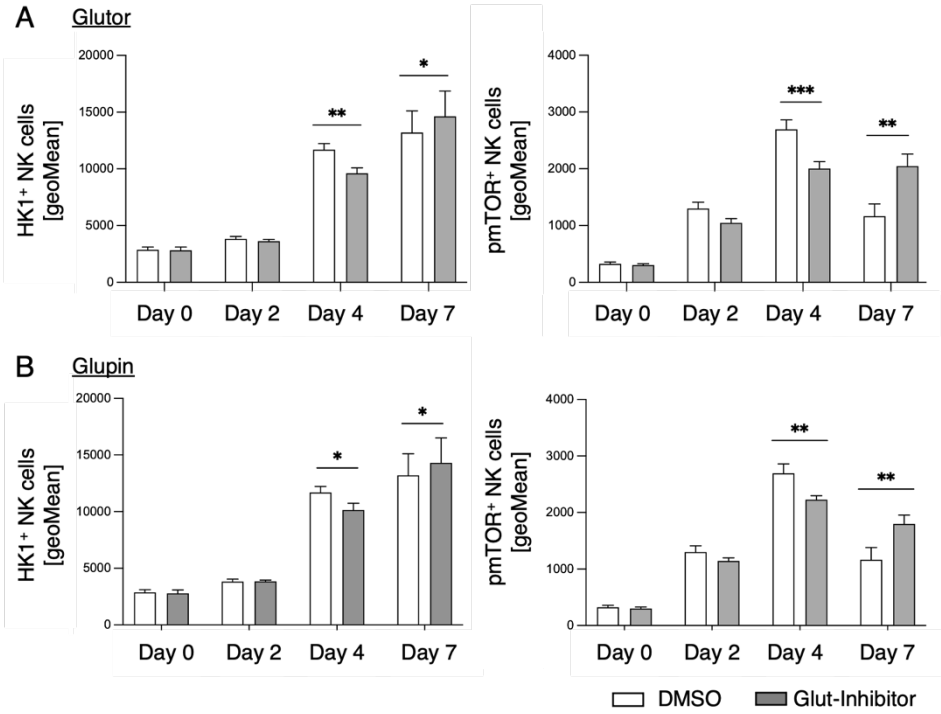

Figure 13: Delayed upregulation of HK1 and pmTOR expression during long-term treatment

Freshly isolated NK cells were cultivated with feeder cells, IL-2 and IL-21 in the presence or absence of DMSO, 100 nM Glutor (A) or 100 nM Glupin (B). Flow cytometry analysis of HK1 expression and pmTOR expression on day 0, day 2, day 4 and day 7. n=6. Data were pooled from three independent experiments each experiment was performed with two donors. Mean with SEM. Statistical analysis was performed by Paired t-test. Significant differences are indicated by asterisk *P ≤ 0.05, **P ≤ 0.01, ***P ≤ 0.001

Since NK cells are metabolically affected by Glupin but continue to proliferate, we wanted to know whether the expression of the nutrient transporters CD71 (transferrin receptor) and CD98 (amino acid transporter) was altered. In addition, we measured expression levels of cMyc, which has a major effect on CD71 expression and is known to control the expression of the metabolic machinery in NK cells. Expression levels of CD71, CD98 and cMyc on day 3, 5 and 21 during treatment with Glupin were measured by flow cytometry (Figure 14). Treatment with Glupin did not change the expression of the transferrin receptor CD71 on days three and five compared to the control. On day 21, the control cells showed a reduced CD71 expression compared to day 3 and 5. This reduction in expression was not observed in the Glupin-treated NK cells, indicating a significant difference between the control cells and the Glupin-treated NK cells in

their CD71 expression. (Figure 14A). A similar trend could be observed for the expression analysis of the amino acid transporter CD98 (Figure 14B). Analysis of cMyc expression at the different time points showed no change in expression levels between Glupin-treated NK cells and control NK cells. (Figure 14C).

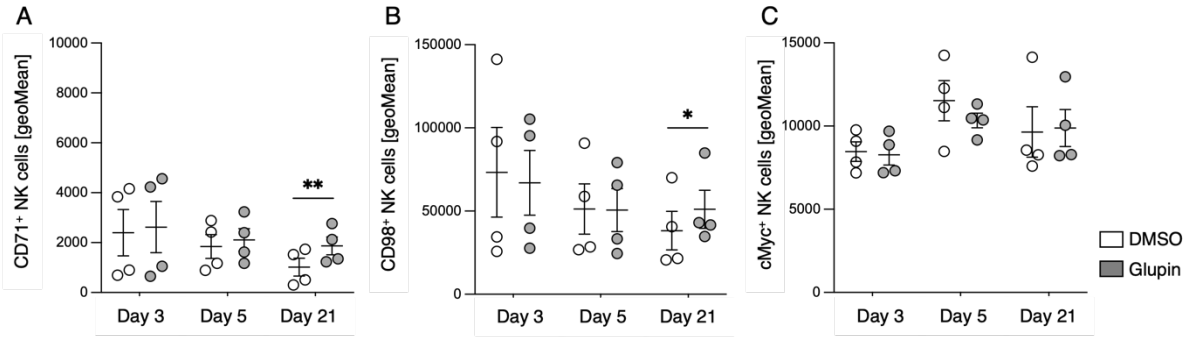

Figure 14: Glupin treatment prevents the downregulation of CD71 and CD98 expression

Freshly isolated NK cells were cultivated with feeder cells, IL-2 and IL-21 in the presence or absence of DMSO or 100 nM Glupin. Flow cytometry analysis of CD71-expression (A), CD98 expression (B) and cMyc expression (C) on day 3, day 5 and day 21. n=4. Data were pooled from three independent experiments each experiment was performed with one or two donors. Mean with SEM. Statistical analysis was performed by Paired t-test. Significant differences are indicated by asterisk *P ≤ 0.05, **P ≤ 0.01, ***P ≤ 0.001

Thus, treatment with Glupin appears to result in sustained enhanced expression of CD98 and CD71, perhaps serving as a counterbalance to inhibition of glucose uptake. Similarly, the effect of Glupin does not appear to be strong enough to also cause a change in cMyc expression, possibly due to incomplete blockade of glucose uptake. Based on these data and the fact that NK cells respond differently to the two GLUT-inhibitors, we wanted to investigate whether we could detect differences in the strength of inhibition of glucose uptake. To investigate this, a glucose uptake assay was performed using long-term treated NK cells in which the uptake of 2-DG was measured. Treatment with Glutor led to a significant reduction in glucose uptake compared to control. This effect was also observed after treatment with Glupin, although in this case the effect was stronger (Figure 15). These data clearly show that both Glutor and Glupin severely inhibit glucose uptake, which raises the question of why Glupin-treated cells show an almost normal proliferation compared to Glutor-treated cells.

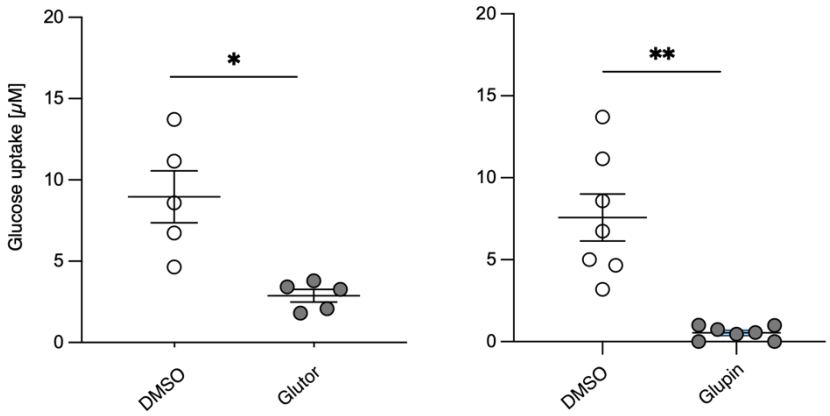

Figure 15: Glucose-uptake was significantly reduced during long-term treatment

$0.25x10^6$ long-term treated NK cells were used for analysis of glucose-uptake using a glucose uptake assay. Uptake was analyzed one hour after addition of 2-DG. n=5-7. Data of 3-4 independent experiments. Each experiment was performed with one or two donors. Mean with SEM. Statistical analysis was performed by Paired t-test. Significant differences are indicated by asterisk *P ≤ 0.05, **P ≤ 0.01, ***P ≤ 0.001

Based on the previous data regarding the changes in proliferation and expression of nutrient transporters and the inhibition of glucose uptake, we now wanted to take a closer look at the metabolic profile of long-term treated NK cells. For this purpose, we used SCENITH, a flow cytometry-based method for analyzing the metabolic profile of cells on single cell level (Argüello et al. 2020). Long-term treated NK cells were incubated with or without the glycolysis-inhibitor 2-DG and the OxPhos inhibitor oligomycin alone or in combination, followed by the addition of puromycin. As shown by Argüello et al, the ATP production and protein synthesis rates of cells are in linear relation. If the NK cell is metabolically dependent on glycolysis or OxPhos, its ATP concentration decreases as well as its protein synthesis, which is accompanied by altered incorporation of puromycin during protein synthesis. These changes can be analyzed via flow cytometry using a fluorescently labelled anti-puromycin antibody. (Argüello et al. 2020). Long-term treatment with Glutor results in a significantly increased mitochondrial dependency, whereas glycolytic capacity was significantly reduced. Glucose dependency as well as FAO and AAO capacity did not change (Figure 16A). A similar trend could be observed for long-term treatment with Glupin: mitochondrial dependency was increased, and glycolytic capacity was diminished. Glucose dependency and FAO and AAO capacity were not affected (Figure 16B). Long-term treatment with Glupin lead to increased mitochondrial dependency, but this increase was even higher in Glutor-treated NK cells.

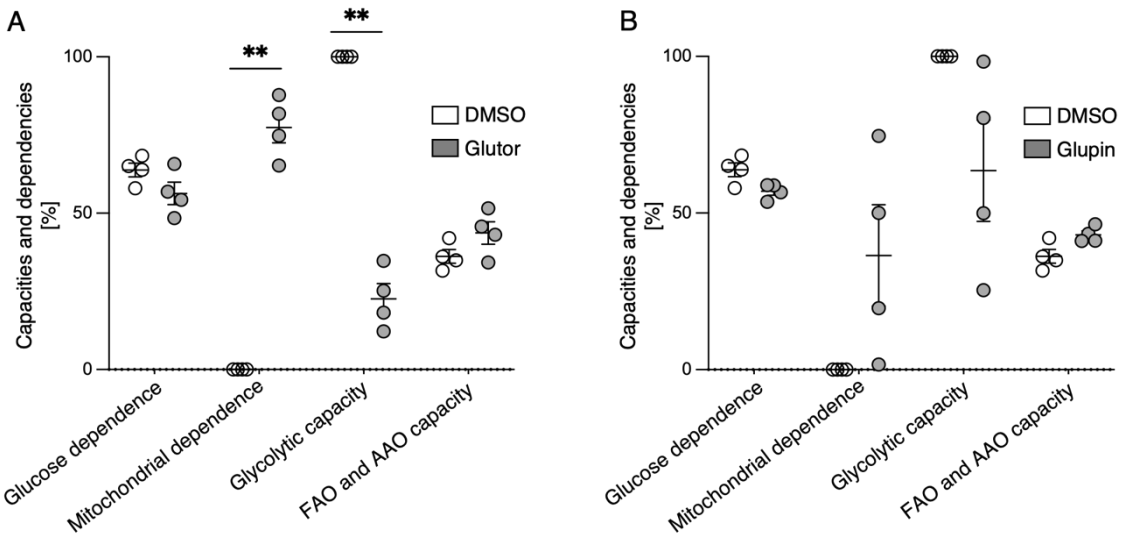

Figure 16: Differences in mitochondrial dependence upon long-term treatment

Long-term treated NK cells (0.1% DMSO, 100 nM Glutor, 100 nM Glupin) were incubated with or without Oligomycin, 2-DG and Oligomycin + 2-DG, followed by the addition of Puromycin. Flow-cytometry analysis of Puromycin expression in these NK cells followed by calculation of glucose dependence, mitochondrial dependence, glycolytic capacity and FAO and AAO capacity. n=4. Data of 3 independent experiments. Each experiment was performed with one or two donors. Mean with SEM. Statistical analysis was performed by Paired t-test. Significant differences are indicated by asterisk *P ≤ 0.05, **P ≤ 0.01, ***P ≤ 0.001

7.2.3 Influence of Glut-Inhibitors on NK cell phenotype

We next wanted to investigate whether these changes in NK cell metabolism also led to changes in NK cell phenotype. We analyzed 21 different surface molecules on long-term treated NK cells using spectral flow cytometry. Inhibition of glucose transporters via Glutor for three weeks led to significantly decreased expression of CD16, CD8, CD62L, TIGIT, 2B4, CD38, CD18 and NKG2C, while KLRB1, KLRG1, and HLA-DR are upregulated. We observed no changes in the expression of TRAIL, CD57, NKp30, NKp46, CD11a, NKG2A, NKG2D, NKp44, DNAM-1 and 41BB (Figure 17A). Glupin treatment significantly increases the expression of HLA-DR, NKp44 and KLRB1, whereas the expression of CD16, CD8, CD57, 2B4 and CD38 was diminished (Figure 17B). Long-term inhibition of glucose uptake thus leads to an altered NK cell phenotype. Glutor and Glupin treated cells show similar tendencies with regards to the up- or downregulation of surface molecules, whereas the long-term treatment with Glutor seems to exert a stronger effect.

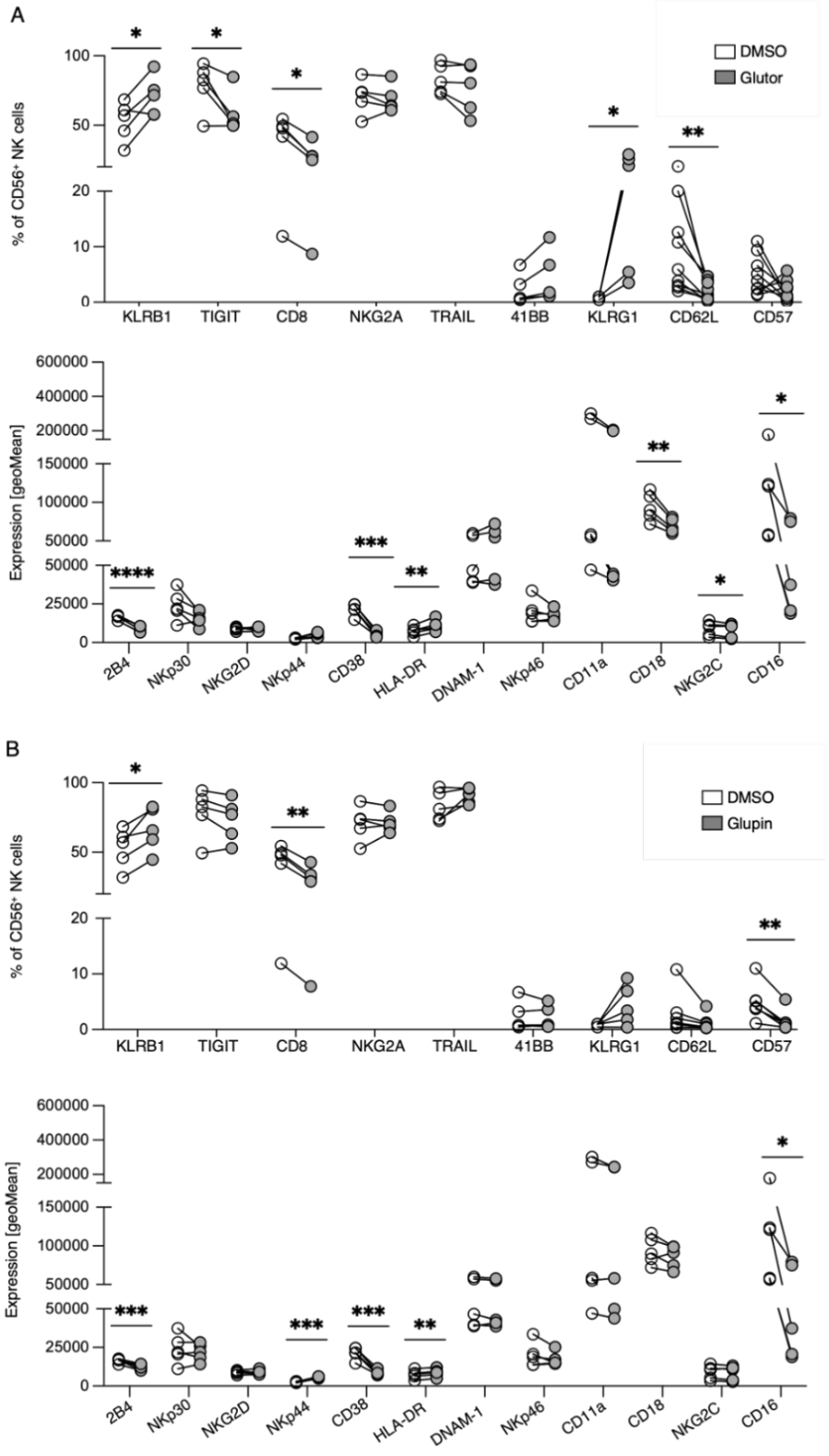

Figure 17: Long-term inhibition of GLUT- 1-3 results in altered NK cell phenotype

NK cells were treated for 3 weeks with 100 nM Glutor (A) or 100 nM Glupin (B) followed by a flow cytometry analysis of the expression of different surface molecules on day 21. n=5-7. Data of 4 independent experiments. Each experiment was performed with one or two donors. Mean with SEM. Statistical analysis was performed by Paired t-test. Significant differences are indicated by asterisk *P ≤ 0.05, **P ≤ 0.01, ***P ≤ 0.001

7.2.4 Effect of Glut-Inhibitors on effector molecules of NK cells

Due to the fact, that glycolysis is important for the synthesis of effector molecules, we were interested in the expression levels of the effector molecules perforin and granzyme B. Perforin levels of Glupin-treated or Glutor-treated NK cells were not affected, whereas granzyme B was significantly increased (Figure 18). Although glycolysis plays an important role in the synthesis of effector molecules, long-term inhibition of glucose uptake does not seem to have a significant negative effect on the synthesis of granzyme B or perforin.

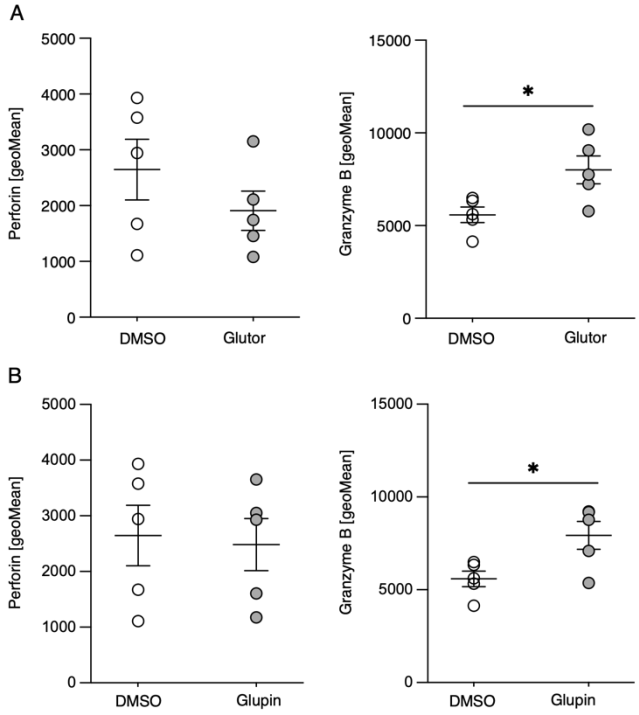

Figure 18: Long-term inhibition of GLUT- 1-3 results in elevated granzyme B Level

NK cells were treated for 3 weeks with 100 nM Glutor (A) or 100 nM Glupin (B) followed by a flow cytometry analysis of perforin and granzyme B expression on day 21. n=5. Data of 3 independent experiments. Each experiment was performed with one or two donors. Mean with SEM. Statistical analysis was performed by Paired t-test. Significant differences are indicated by asterisk *P ≤ 0.05, **P ≤ 0.01, ***P ≤ 0.001

7.2.5 Changes in the cytokine and chemokine profile

It is well known that activation-induced production of cytokines and chemokines is dependent on glycolysis. However, in addition to activation-induced production of cytokines and chemokines, NK cells can also secrete cytokines and chemokines spontaneously. We wanted to investigate the cytokine and chemokine profile after long-term treatment. Therefore, we performed a multiplex bead assay with supernatants of the cultured NK cells to determine the spontaneous secretion of various cytokines and chemokines.

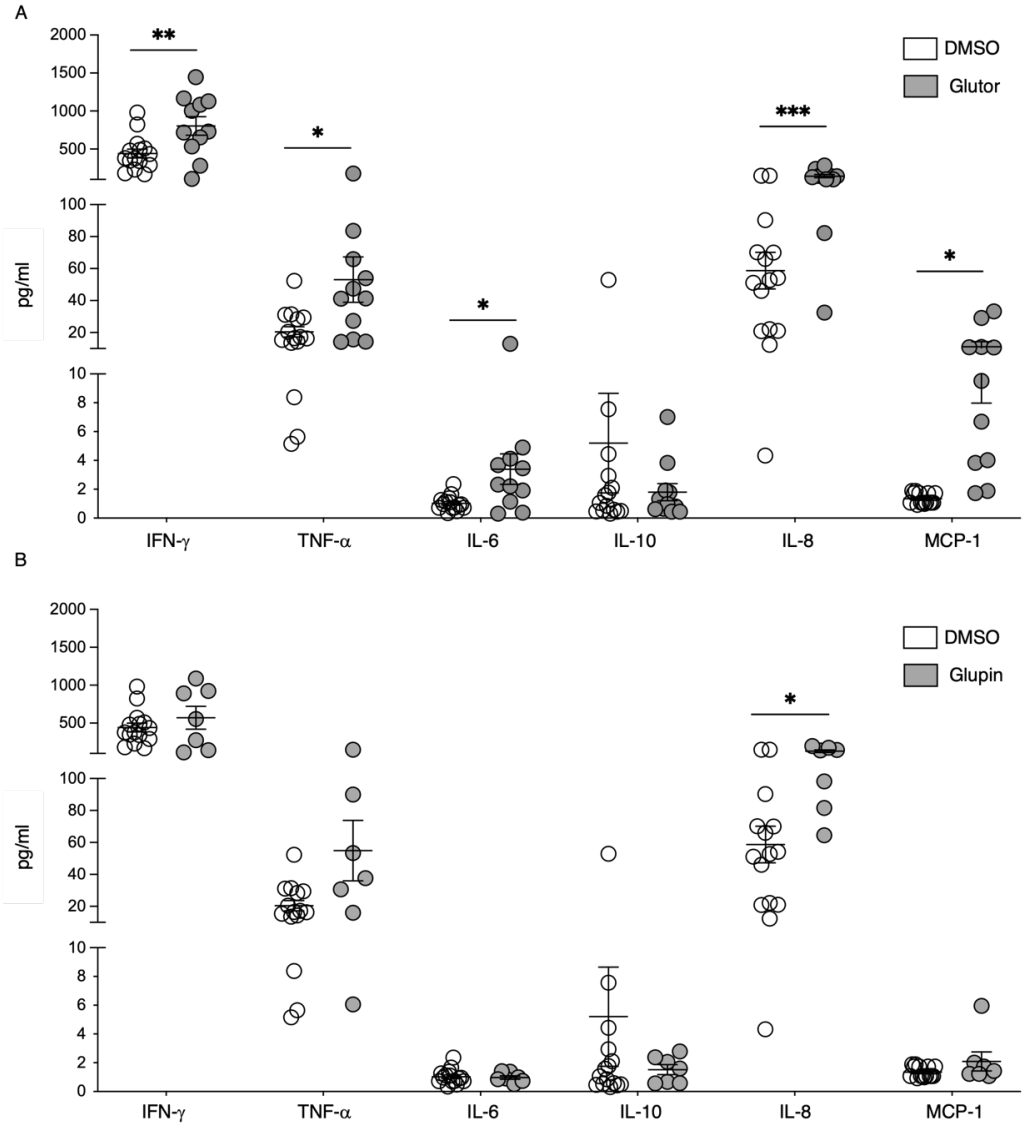

Figure 19: Long-term inhibition of GLUT- 1-3 results in altered cytokine and chemokine profile

Supernatant of long-term treated NK cells (A:Glutor; B:Glupin) were obtained one day after splitting of cultured cells. Spontaneuos secretion of different cytokines and chemokines was analyzed using multiplex-bead assay. n=7-14 donors of 4 independent experiments. Mean with SEM. Statistical analysis was performed by Paired t-test. Significant differences are indicated by asterisk *P ≤ 0.05, **P ≤ 0.01, ***P ≤ 0.001

Glutor-treatment significantly increased the spontaneous secretion of the pro-inflammatory cytokines IFN-γ, TNF-α and IL-6, whereas the anti-inflammatory cytokine IL-10 displayed reduced levels. Also, secretion of the chemokines IL-8 and MCP-1 was significantly increased after long-term treatment with Glutor (Figure 19A). The long-term treatment with Glupin, however, only had a significant effect on IL-8 secretion. For TNF-α, IFN-γ and IL-10 there were tendencies similar to the long-term treatment with Glutor, but no significant changes (Figure 19B). Thus, NK cells are able to spontaneously secrete cytokines and chemokines upon long-term treatment with both Glutor and Glupin. In the case of long-term treatment with Glutor, spontaneous

secretion of pro-inflammatory cytokines and chemokines even seem to be significantly increased.

We wanted to investigate whether this altered chemokine profile leads to an altered migration behavior of the different immune cells. We performed a migration assay using transwell plates and determined the absolute numbers of the cells that migrated towards supernatants of treated NK cells using flow cytometry.

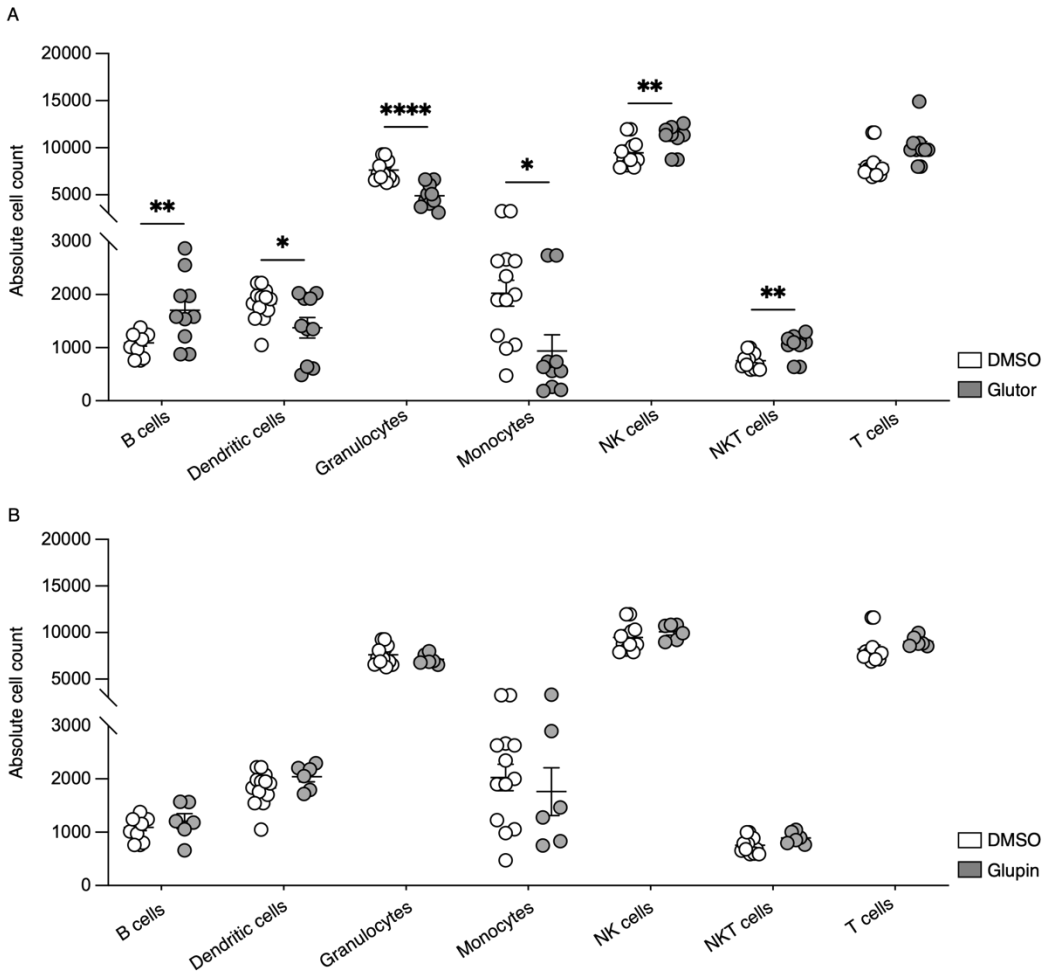

Figure 20: Altered chemokine profile changes migration of immune cells

Supernatants of long-term treated NK cells (A:Glutor; B:Glupin) were obtained one day after splitting of cultured cells and used for the migration assay. PBMCs and granulocytes were isolated from whole blood using density gradient centrifugation. $0.25x10^6$ PBMCs + Granulocytes were seeded into the upper chamber of the transwell and incubated for 4 hours at 37°C, 5% CO_2. Flow cytometry analysis of absolute cell counts of B cells, dendritic cells, granulocytes, monocytes, NK cells, NKT cells and T cells in the lower chamber. n=13 donors of 4 independent experiments. Mean with SEM. Statistical analysis was performed by Paired t-test. Significant differences are indicated by asterisk *P ≤ 0.05, **P ≤ 0.01, ***P ≤ 0.001

The altered chemokine profile of Glutor-treated NK cells resulted in increased migration of B cells, NK cells and NKT cells and decreased migration of dendritic cells, granulocytes, and monocytes. T cells also showed a trend towards increased migration behavior in response to the altered chemokine profile, but these changes were not significant. (Figure 20A). The increased IL-8 level as a result of the Glupin treatment did not lead to any changes in the migration behavior of the various immune cells. (Figure 20B). It may be due to the combination of increased MCP1 and IL-8 that the chemokine profile of Glutor-treated NK cells have a greater effect on the migration of various immune cells than the chemokine profile of Glupin-treated NK cells.

7.2.6 Influence of long-term treatment on NK cell functions

As it is well established that immunoregulatory and cytotoxic functions of NK cells can be modulated by metabolism, we wanted to investigate to what extent long-term treatment with GLUT inhibitors affects NK cell effector functions. Therefore, we determined the IFN-γ secretion of long-term treated NK cells after stimulation via plate-bound antibodies against CD16, NKp30, NKG2D + 2B4 or control IgG for 16 h. Furthermore, we also included stimulation with IL-12 + IL-18 for 16 h. Glutor-treated NK cells showed significantly decreased levels of IFN-γ after stimulation via CD16 and NKp30 as well as via IL-12 + IL-18. The activation via NKG2D + 2B4 showed no alterations in the IFN-γ secretion (Figure 21A). Long-term treatment with Glupin also altered the IFN-γ secretion: NK cells secreted significantly less IFN-γ if they were stimulated via CD16 or NKp30. The stimulation of Glupin-treated NK cells via IL-12 + IL-18 or NKG2D + 2B4 resulted in comparable levels of IFN-γ secretion in comparison to the controls (Figure 21B).

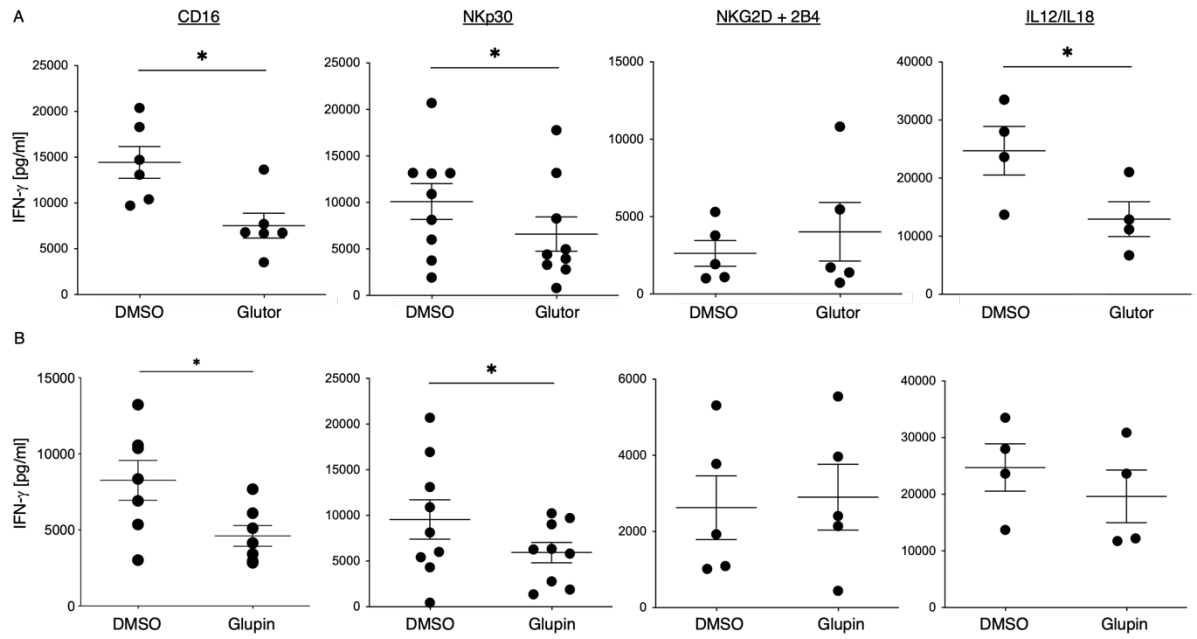

Figure 21: Long-term treatment with Glutor or Glupin decreases IFN-γ secretion of NK cells

A) Long-term treated NK cells (100 nM Glutor) were stimulated via plate-bound CD16 mAb, NKp30 mAb or NKG2D mAb + 2B4 mAb or via IL-12 + IL-18 for 16 hours. IFN-γ secretion was analyzed via ELISA. n=4-9 donors of 4-6 independent experiments. Mean with SEM. Paired t-test. B) Long-term treated NK cells (100 nM Glupin) were stimulated via plate-bound CD16 mAb, NKp30 mAb or NKG2D mAb + 2B4 mAb or via IL-12 + IL-18 for 16 hours. IFN-γ secretion was analyzed via ELISA. n=4-9 donors of 4-6 independent experiments. Mean with SEM. Statistical analysis was performed by Paired t-test. Significant differences are indicated by asterisk *P ≤ 0.05, **P ≤ 0.01, ***P ≤ 0.001

To assess the cytotoxic function of NK cells, we stimulated long-term treated NK cells with plate-bound antibodies against CD16, NKp30 or NKG2D + 2B4 and analyzed CD107a expression after 2 h of incubation by flow cytometry. After long-term treatment with Glutor, activation of NK cells via CD16 or NKp30 led to a significantly lower amount of $CD107a^+$ NK whereas stimulation via NKG2D+2B4 resulted in comparable levels of $CD107a^+$ NK cells (Figure 22A). Long-term treatment with Glupin did not affect the degranulation capacity of NK cells, independent of the different stimulations (Figure 22B). This show that only Glutor affects degranulation of NK cells, whereas the activation-induced secretion of IFN-γ seems to be more sensitive to the inhibition of glucose uptake.

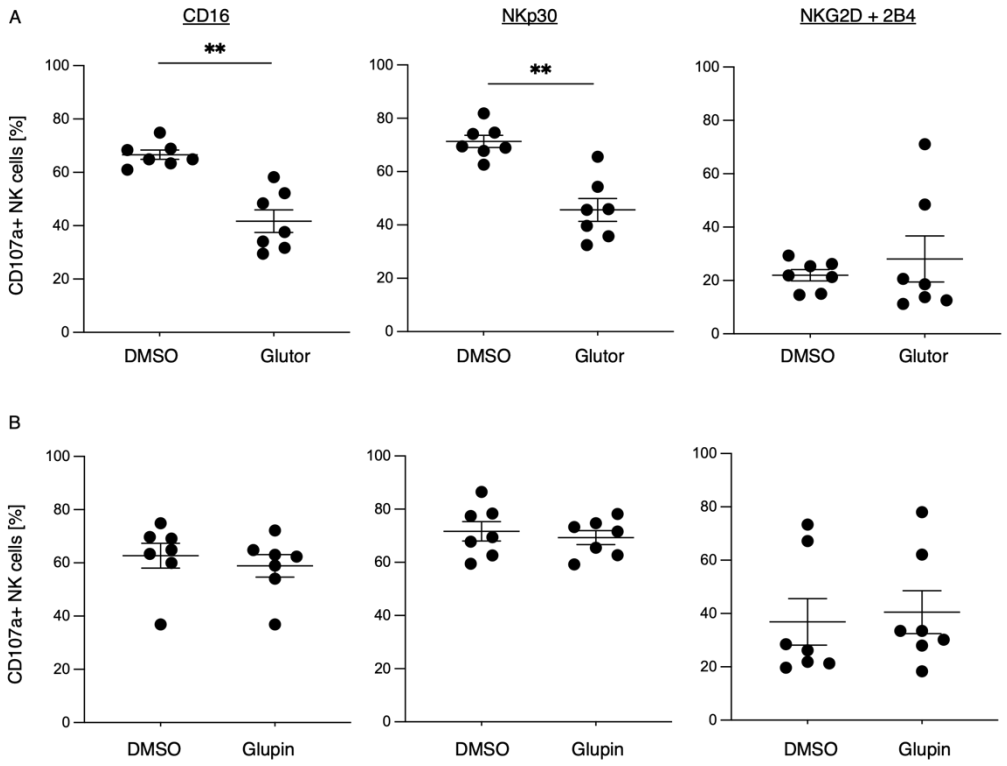

Figure 22: Long-term treatment with Glutor decreases degranulation of NK cells

A) Long-term treated NK cells (100 nM Glutor) were stimulated via plate-bound CD16 mAb, NKp30 mAb or NKG2D mAb + 2B4 mAb for 2 hours in the presence of anti-CD107a PE-Cy5. Flow cytometry analysis of CD107a expression on NK cells. n=7 donors of 4 independent experiments. Mean with SEM. Paired t-test. B) Long-term treated NK cells (100 nM Glupin) were stimulated via plate-bound CD16 mAb, NKp30 mAb or NKG2D mAb + 2B4 mAb for 2 hours in the presence of anti-CD107a PE-Cy5. Flow cytometry analysis of CD107a expression on NK cells. n=7 donors of 4 independent experiments. Mean with SEM. Statistical analysis was performed by Paired t-test. Significant differences are indicated by asterisk *P ≤ 0.05, **P ≤ 0.01, ***P ≤ 0.001

7.2.7 Increased serial-killing capacity of Glupin-treated NK cells

The cytotoxic function of NK cells plays a central role in fighting cancer cells. The previous experiments showed differences between the two inhibitors. On the one hand, both led to increased expression of granzyme B, while on the other hand, cells treated with Glutor showed decreased expression of perforin. Further, in contrast to Glupin, treatment with Glutor led to a decrease in degranulation. Therefore, it is also interesting to investigate whether the killing capacity of NK cells is influenced by a long-term treatment with Glutor or Glupin. Hence, we performed a chromium-release assay with long-term treated NK cells against K562 cells. We observed no changes in the percentage of specific lysis between Glutor-treated NK cells and control NK cells (Figure 23). Also, the long-term treatment with Glupin showed comparable levels of specific lysis in comparison to the control (Figure 23). Thus, the killing capacity within

4 hours does not seem to be limited in such an experimental setup, neither after Glutor nor Glupin treatment.

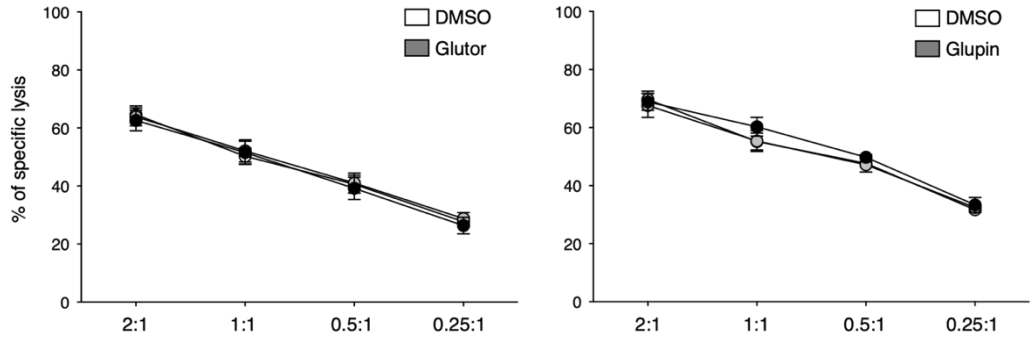

Figure 23: Inhibition of Glucose-transporter1,2 and 3 did not change cytotoxicity

^{52}Cr-release assay of long-term treated NK cells against K562. Percentage of specific lysis after 4 h using chromium-release assay was performed with long-term treated NK cells against K562 cells at different E:T ratios. n=3 donors of 3 independent experiments. Mean with SEM.

Assuming that a chromium release assay has shown the overall killing ability of NK cells, we wanted to investigate the killing ability at the single cell level. NK cells have the ability to kill more than one target cell in a row, which is why they are also called serial killers. We investigated to what extent long-term GLUT inhibition affects the serial killing activity of NK cells. We examined the serial killing capacity of long-term treated NK cells using time-lapse microscopy with a microchip as previously described (Prager et al. 2019). In this assay, individual NK cells are observed over a period of 16 hours and the individual target cell contacts are divided into cytotoxic and non-cytotoxic. In this experiment, each individual cell needs enough energy to keep itself alive for a period of 16 hours and, ideally, to be able to kill one or more tumor cells. Since we could already see a reduction in stimulation-induced IFN-γ secretion after 16 h in inhibitor-treated NK cells, it is now interesting to see to what extent serial killing capacity is affected. We used MCF7 cells as target cells, which are sensitive to Glutor at higher concentrations but resistant to Glupin. Glutor-treated NK cells showed fewer cytotoxic contacts for each target cell contact compared to control NK cells (Figure 24). In addition, the number of kills per NK cell was calculated and showed that the long-term treated NK cells had fewer kills per NK cell. This was also true for the percentage of serial killers (Figure 24A). On the other hand, treatment of the NK cells with Glupin led to an increased cytotoxic activity. They showed more cytotoxic contacts for each target cell contact and the calculations based on these data showed an increased percentage of serial killers and significantly more kills per NK cells (Figure 24B).

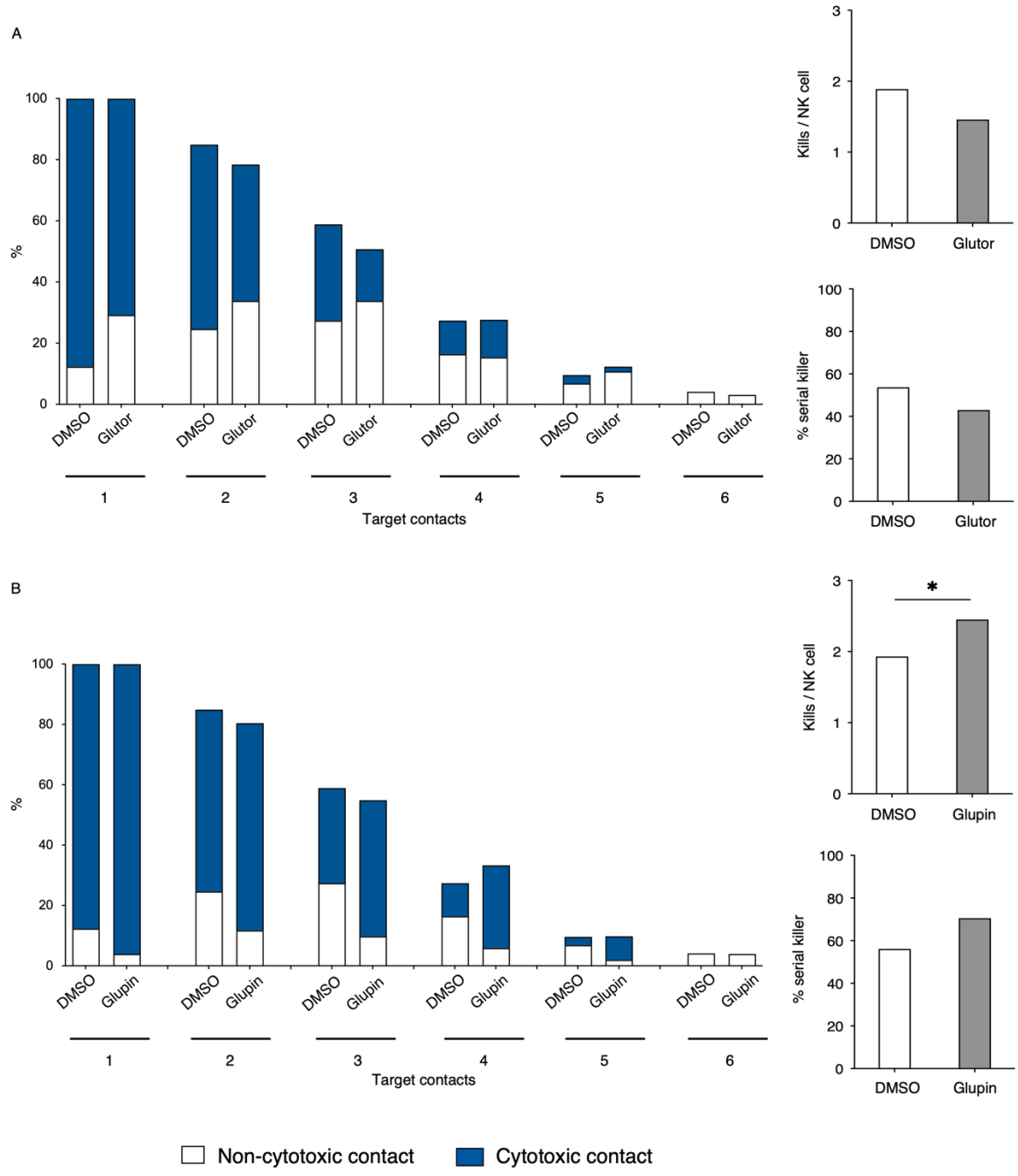

Figure 24: Long-term treatment with Glupin increases serial-killing capacity

Serial killing assay of long-term treated NK cells (A: 100 nM Glutor; B: 100 nM Glupin) as effector cells and MCF7 cells as target cells. Percentage of cytotoxic versus non-cytotoxic contacts was determined for each target cell contact (up to 6 target cell contacts per NK cell were analyzed). Percentage of serial killers and kills per NK cell were calculated. Serial killers were defined as cells which kill more than one target cell. n=63-80 NK cells from 7 donors from 10 independent experiments. Each experiment was performed with one or two donors. Statistical analysis was performed by Multiple Comparisons: Tukey-Kramer. Significant differences are indicated by asterisk *P ≤ 0.05, **P ≤ 0.01, ***P ≤ 0.001

7.2.8 Fatty acid oxidation is not responsible for increased serial-killing capacity

Since Glupin blocks glucose uptake and decreases glycolytic capacity but increases serial killing capacity without limiting NK cell viability, we wanted to investigate whether other fuels such as fatty acids are used for the energy requirements of pre-activated NK cells. It is known that T cells can obtain their energy via short chain fatty acids (SCFA) like butyrate and pentanoate, which leads to a higher cytotoxic activity of these T cells (Luu et al. 2018). Therefore, we used pre-activated NK cells and added different concentrations of butyrate (0.5 µM, 0.75 µM, 1 µM) or pentanoate (2.5 mM, 5 mM, 7.5 mM) to the culture of pre-activated NK cells for three days and determined the expression of CD107a and pmTOR after stimulation with K562 cells. The addition of butyrate did not change the percentage of $CD107a^+$ NK cells in comparison to the control, independent of different concentrations. Also, the expression of pmTOR was not influenced by the addition of different concentrations of butyrate. Similarly, the percentage of $CD107a^+$ NK cells was not altered by the addition of different concentrations of pentanoate in comparison to the control. Furthermore, the expression of pmTOR did not change due to pentanoate treatment (Figure 25). These data indicate, that these two different SCFA are not responsible for the sustained functions of Glupin-treated NK cells. However, in this experimental setup, we tested only these two different SCFA, so we cannot exclude the possibility that Glupin-treated NK cells use other fatty acids to meet their energy needs.

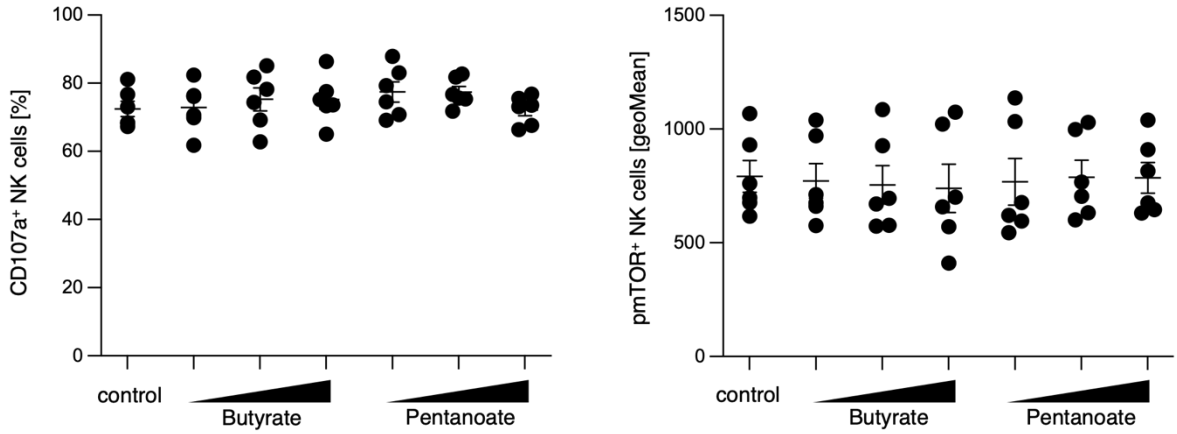

Figure 25:Short-chain fatty acids have no influence on degranulation

Pre-activated NK cells were incubated with different concentrations of the SCFA butyrate (0.5 µM, 0.75 µM, 1 µM) or pentanoate (2.5 mM, 5 mM, 7.5 mM) for 72 h followed by a degranulation-assay against K562 cells (E:T 2:1). CD107a expression and pmTOR expression was analyzed via flow cytometry. n=6 donors of 3 independent experiments. Mean with SEM.

To exclude this possibility, we used Etomoxir, an inhibitor of the carnitine palmitoyltransferase 1 (CPT1) to test if upon prolonged inhibition of glucose uptake NK cells switch to fatty acid metabolism. For this purpose, we incubated long-term treated NK cells (Glupin or DMSO) with or without Etomoxir for 24 h and subsequently stimulated them via plate bound CD16 mAb. CD107a expression was measured after 2 h via flow cytometry and IFN-γ secretion was analyzed after 16 h via ELISA. Inhibition of CPT1 of control NK cells did not change the percentage of $CD107a^+$ NK cells in comparison to the control. Similarly, the comparison of Glupin-treated cells with and without Etomoxir showed no changes in the percentage of degranulation (Figure 26). Analysis of IFN-γ secretion showed a slight trend towards reduction after Etomoxir treatment. In the case of Glupin-treated cells, there was no trend observable with and without inhibition of CPT1 (Figure 26). However, IFN-γ secretion was significantly reduced after long-term treatment with Glupin compared to the control group, confirming the previously obtained data. These data confirm the previous findings regarding SCFA that fatty acids are not the energy source in question.

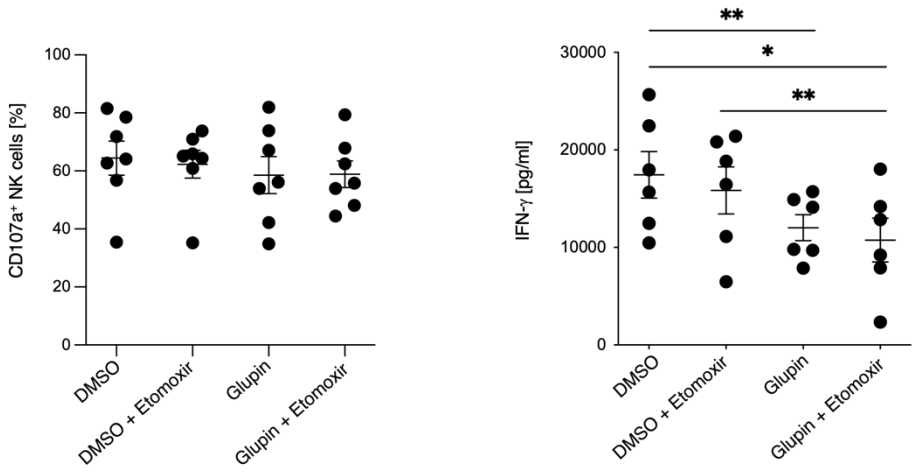

Figure 26: Blocking of fatty acid ß-oxidation did not affect degranulation

Long-term treated NK cells (0.1% DMSO or 100 nM Glupin) were treated with or without 1 µM Etomoxir for 24 h hours followed by a plate-bound stimulation via CD16 for 2 h (CD107a-Assay) or 16 h (IFN-γ). n=7 donors from 4 independent experiments. Mean with SEM. Statistical analysis was performed by Paired t-test. Significant differences are indicated by asterisk *P ≤ 0.05, **P ≤ 0.01, ***P ≤ 0.001

In order to better understand how NK cells continue to perform their normal functions and are not severely limited in proliferation despite insufficient glucose uptake, we analyzed the malate concentration within the cell, since it is already known that the citrate-malate shuttle plays an important role in NK cell metabolism (Guillerey and Smyth 2017). The long-term treatment with Glupin resulted in a slightly lower malate

concentration in direct comparison to the control cells (Figure 27). An equally essential parameter in terms of metabolism is NAD^+, as it plays an important role in many enzymatic reactions of glycolysis, TCA cycle, OxPhos as well as fatty acid oxidation (Navas and Carnero 2021). Long-term treatment with Glupin led to a significantly increased concentration of NAD^+/NADH then control NK cells. (Figure 27).

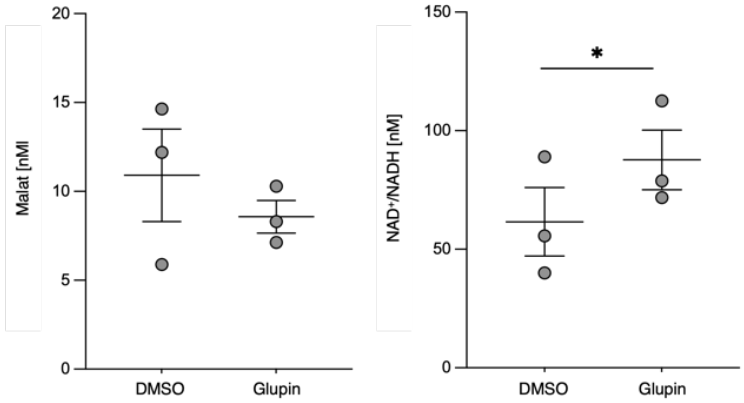

Figure 27: Long-term treatment with Glupin increases NAD/NADH concentration

A) Analysis of malat-concentration of $0.25x10^6$ long-term treated NK cells (100 nM Glupin, 0.1% DMSO). N=3. B) Analysis of NAD/NADH concentration of $0.1x10^6$ long-term treated NK cells (100 nM Glupin, 0.1% DMSO) n=3. Mean with SEM. Statistical analysis was performed using one-way ANOVA. Significant differences are indicated by asterisk *P ≤ 0.05, **P ≤ 0.01, ***P ≤ 0.001

7.2.9 Metabolomic profile of Glupin-treated NK cells

To gain a deeper insight into the various metabolites of NK cells, metabolomics analysis of cells treated with Glupin and DMSO was performed. This can provide initial indications of alternative energy sources, since glutamine, among other things, is considered an important metabolite for energy production. Metabolomics analysis revealed significantly increased concentrations of glutamine and glutamic acid (Figure 28). The amino acids alanine, glycine, aspartic acid as well as threonine were also found in higher concentrations in the NK cells treated with Glupin than in the control cells. In contrast, Glupin-treated NK cells had lower concentrations of glucose, pyruvate, and lactate than control cells. For leucine, valine, taurine, citric acid and serine, no differences could be detected between the Glupin-treated NK cells and the control cells (see Figure 37). The analysis of metabolites showed that NK cells have a high demand for glutamine and that the inhibition of glucose transporters leads to an increased uptake of glutamine.

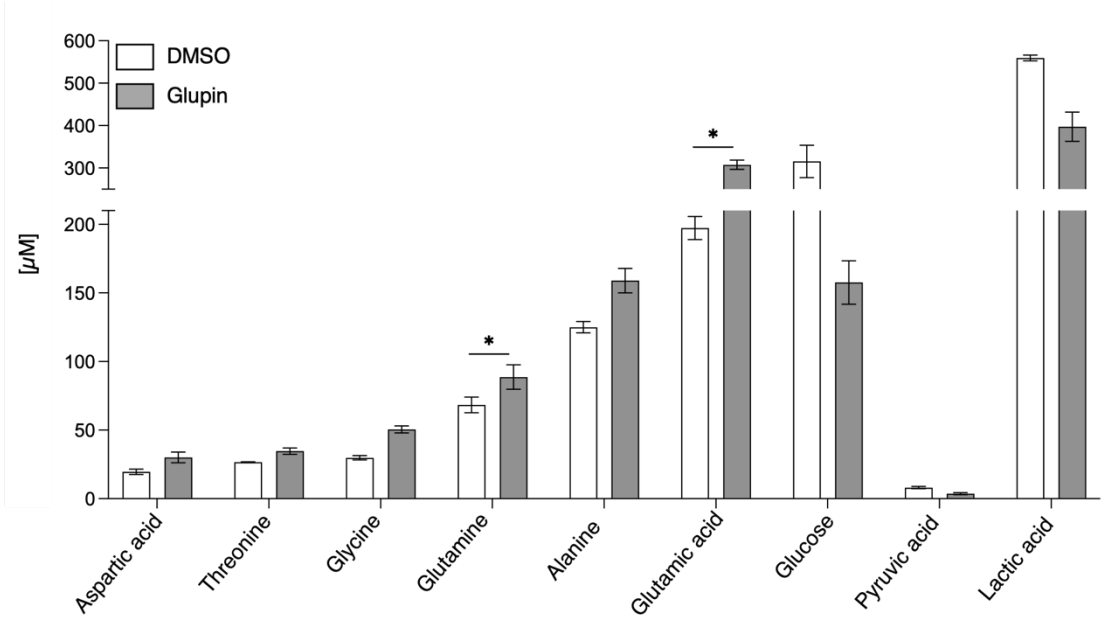

Figure 28: Increased glutamine concentration due to long-term treatment with Glupin

Metabolomics of $10x10^6$ long-term treated NK cells (100 nM Glupin, 0.1% DMSO). n=3. Mean with SEM. Statistical analysis was performed using paired t-test. Significant differences are indicated by asterisk *P ≤ 0.05, **P ≤ 0.01, ***P ≤ 0.001

7.2.10 Inhibition of Glutaminase improved NK cell functions

Based on these data and the finding that tumor cells can also use glutamine to overcome the glucose deficiency (Reckzeh et al. 2019), we wanted to assess the effect of the glutaminase-inhibitor CB839 on NK cell function. Therefore, we generated long-term treated NK cells with Glupin, CB839 or DMSO and treated these cells acutely with Glupin, CB839 or Glupin + CB839 for 72 h. Afterwards, cells were stimulated via plate-bound antibodies against CD16, NKp30 or NKG2D + 2B4 and analyzed for degranulation and IFN-γ secretion. After stimulation via CD16, NKG2D + 2B4 or NKp30 we could not observe any significant changes in the degranulation or IFN-γ secretion of DMSO-long-term treated NK cells, independent of acute treatment with Glupin, CB839 or Glupin + CB839 (Figure 29). Long-term treatment with Glupin showed reduced IFN-γ secretion, whereas degranulation was not affected. The acute inhibition of glutaminase did not change the functions of Glupin-treated NK cells significantly. Long-term treatment with CB839 results in an overall higher degranulation and IFN-γ secretion of NK cells independent of acute treatment with Glupin. This could be observed for all stimulations. (Figure 29).

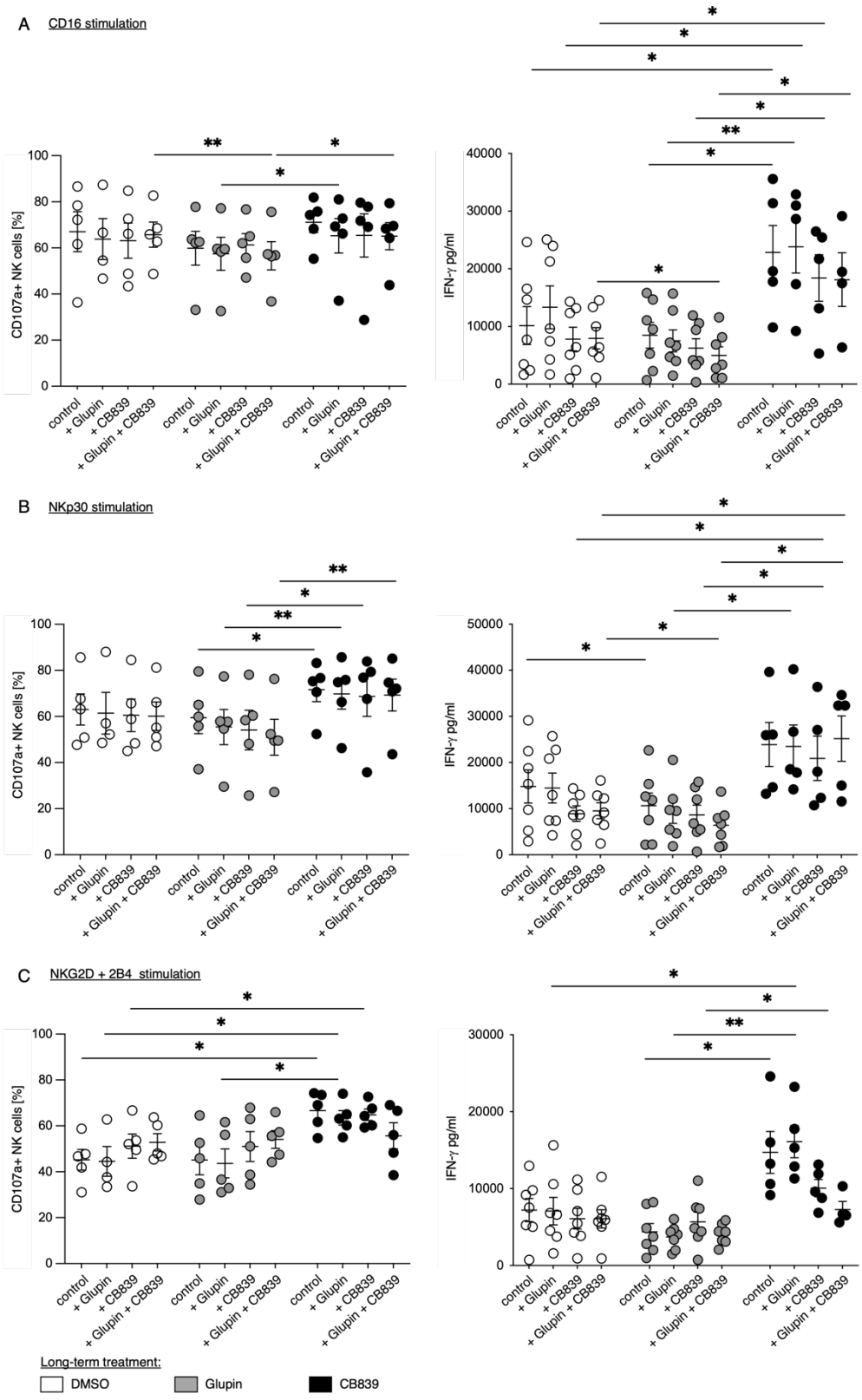

Figure 29: Glutaminase-Inhibition improves NK cell effector functions

Long-term treated NK cells (0.1% DMSO; 100 nM Glupin, 0.5 µM CB839) were acutely treated with 0.1% DMSO, 100 nM Glupin, 0.5 µM CB839 or a combination of 100 nM Glupin + 0.5 µM CB839 for 72 h followed by a stimulation of $0.1x10^6$ treated NK cells via plate-bound antibodies against CD16 (A), NKp30 (B), NKG2D + 2B4 (C) or control IgG as a control. Cells were stimulated for 2 h (CD107a-Assay) or 16 h (IFN-γ). n=5-7 donors of 4 independent experiments. Mean with SEM. Statistical analysis was performed using one-way ANOVA. Significant differences are indicated by asterisk *P ≤ 0.05, **P ≤ 0.01, ***P ≤ 0.001

To better understand these differences between glutaminase inhibition and glucose uptake inhibition, we wanted to investigate whether the metabolic state of the NK cell is altered. We analyzed mitochondrial mass by flow cytometry and observed no changes between NK cells treated with Glupin and DMSO. In contrast, we noticed an increase in MitoTracker fluorescence intensity in CB839-treated NK cells compared with control and concluded that inhibition of glutaminase leads to increased mitochondrial mass (Figure 30).

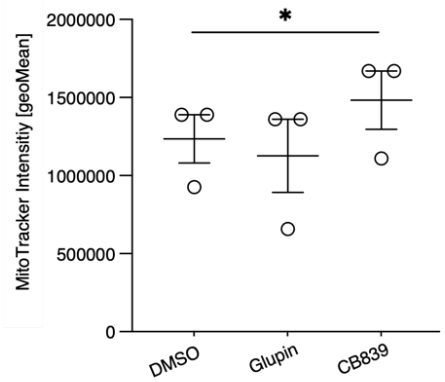

Figure 30: Inhibition of glutaminase increases mitochondrial mass

Flow cytometry analysis of mitochondrial mass of long-term treated NK cells (0.1% DMSO, 100 nM Glupin or 0.5 µM CB839) using MitoTracker DeepRed. n=3. NK cells from 3 independent experiments. Mean with SEM. Statistical analysis was performed by Paired t-test. Significant differences are indicated by asterisk *P ≤ 0.05, **P ≤ 0.01, ***P ≤ 0.001

7.2.11 Transcription analysis by RNA-sequencing

Bulk RNA sequencing was performed to determine transcriptional changes caused by long-term treatment of NK cells with Glutor or Glupin. After normalization to counts per million (CPM), a volcano plot analysis based on log2fold (-1/1) and p-value (cutoff 0.05) identified a total of 1775 differentially expressed genes (DEG) in the Glutor-treated NK cells (Figure 31). A large proportion of these DEGs were up-regulated in Glutor long-term treated NK cells, whereas only a small proportion were down-regulated. These down-regulated genes included the marker for activation and adhesion like *CD38* as well as *CD7* and the mTORC1 regulator *death-associated protein kinase-2* (*DAPK2)*. In contrast, genes associated with glycolysis and hypoxia were up--regulated. Further, genes like *BEN domain containing 5 (BEND5)*, *cytotoxic T-lymphocyte-associated protein 4 (CTLA4), IL-5*, *neural cell adhesion molecule L1 (L1CAM)*, *MAX-interacting protein 1 (MXI1)*, and *platelet-derived growth factor subunit A* (*PDGFA)* were up-regulated (Figure 31). Gene set enrichment analysis (GSEA) showed a similar trend

with respect to DEG. Glutor treatment resulted in increased expression of genes of glycolysis, hypoxia, and the p53 pathway. (Figure 32C). In contrast, genes belonging to the oxidative phosphorylation and fatty acid metabolism gene sets were down-regulated. Thus, increased expression of *protein tyrosine phosphatase receptor type F polypeptide interacting protein α-4*, (PPFIA4), *MXI1*, *Stanniocalcin-2* (*STC2)*, *amyloid beta precursor protein (APP)*, *regulator of G-protein signaling 16* (*RGS16)*, and decreased expression of cyto*chrome c oxidase copper chaperone COX11* (*COX11)* and *ATPase H+ transporting V0 subunit E1 (ATP6V0E1)* were observed (Figure 32A).

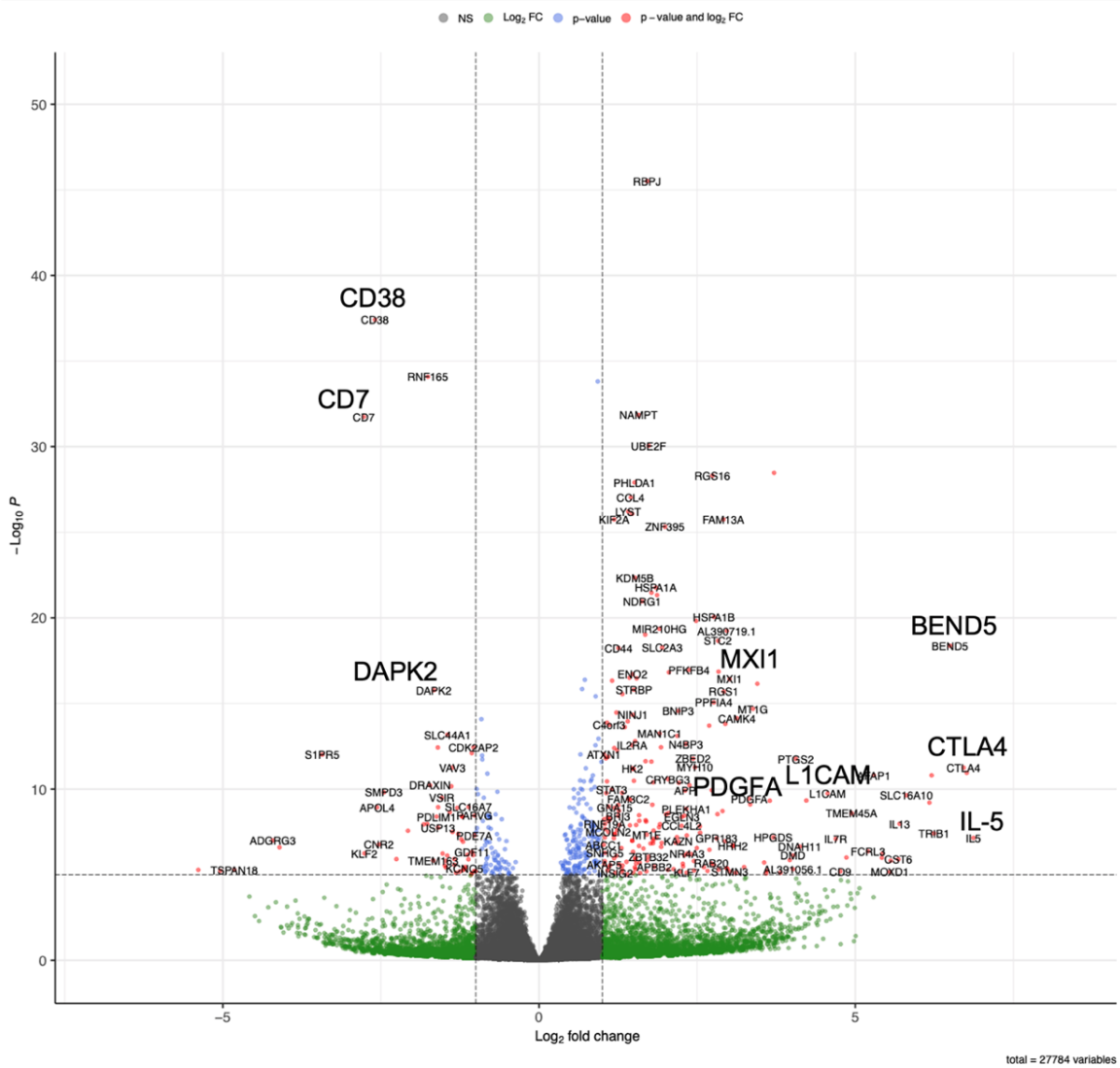

Figure 31: Volcanoplot analysis reveals differences between Glutor and DMSO treatment

Volcano plot of RNA-Sequencing data demonstrating proteins differentially regulated in Glutor-treated NK cells compared to control NK cells. The y-axis represents the -Log10 p value and the x-axis the Log2 fold change in Glutor-treated NK cells. Threshold for significant genes is chosen for fold change > 1 and for p-value cut-off 5.

Since long-term treated NK cells can still take up small amounts of glucose, and hypoxia is known to affect GLUT expression (Macheda et al. 2005), we wanted to

investigate whether other glucose transporters were upregulated after long-term treatment with Glutor. Long-term treatment with Glutor resulted in increased expression of *GLUT-3 (SLC2A3)*, *GLUT-13 (SLC2A13)*, and *GLUT-14 (SLC2A14)* compared to DMSO-treated cells. (Figure 32B). This suggests that Glutor-treated cells attempt to compensate for the lack of glucose uptake by up-regulating glycolysis-related genes. However, the lack of glucose also appears to trigger cell cycle arrest and hypoxia-related genes.

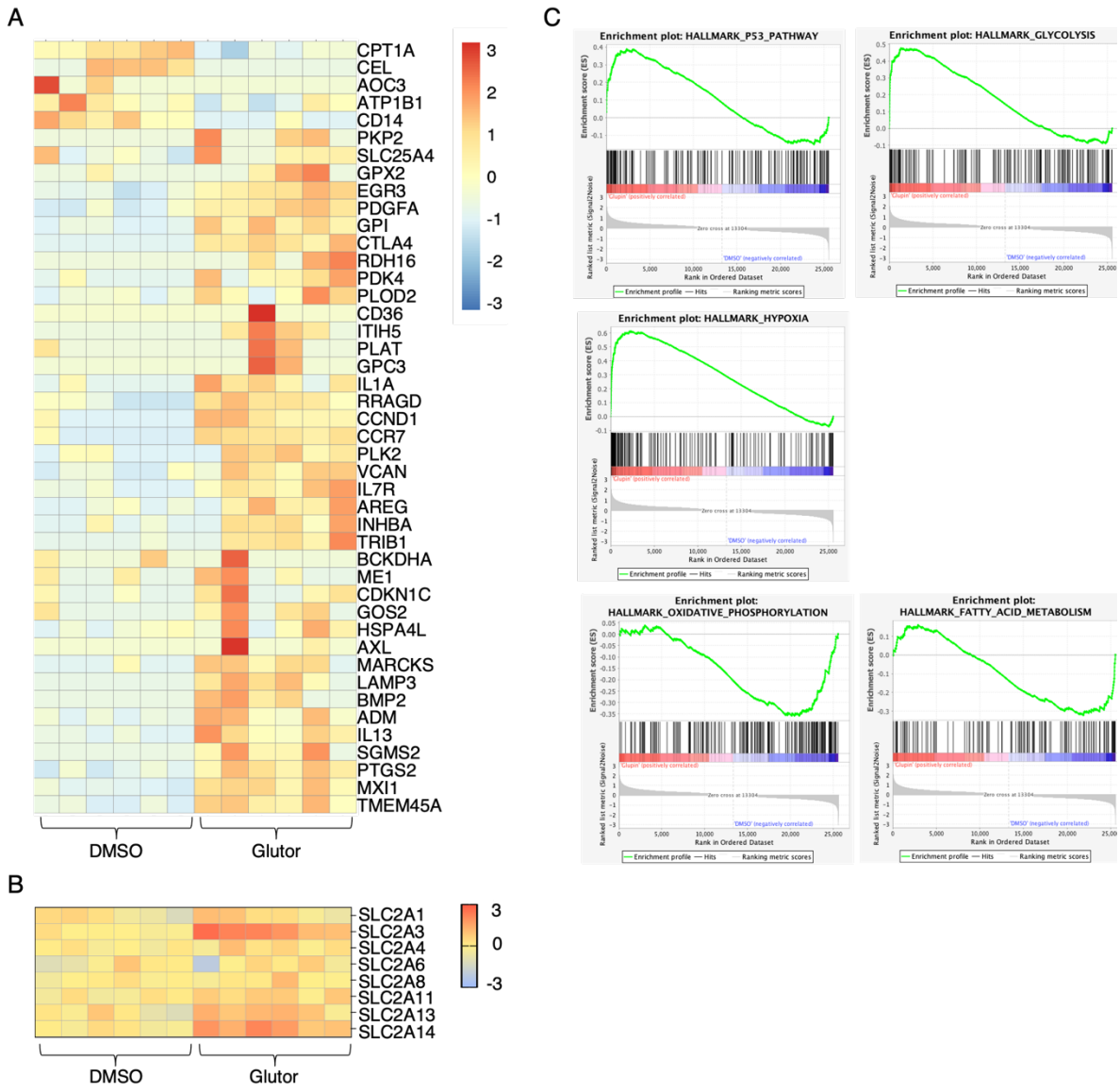

Figure 32:Long-term treatment with Glupin induces a hypoxia phenotype in NK cells

Bulk-RNA-sequencing of long-term treated NK cells (0.1% DMSO, 100 nM Glupin). A) Heatmap of the 49 most differentially expressed genes. Genes with higher expression levels are displayed in red, while genes with lower expression levels are displayed in blue B) GSEA-analysis of the 27784 genes. The 5 most significant Hallmark pathways were shown. Pathways of glycolysis, hypoxia and p53 are enriched in upregulated genes, whereas pathways of OxPhos and fatty acid metabolism are down-regulated. n=6

Volcano plot analysis identified a total of 149 DEG in NK cells treated with Glupin. (Figure 33). Similar to Glutor-treated NK cells, also Glupin-treatment results in a down-regulation of *CD38* and *CD7*, while genes like *BEND5*, *PDGFA*, *L1-CAM*, *MXI1* and *CAVIN1* were up-regulated (Figure 33). The GSEA of NK cells treated with Glupin also showed a similar pattern to that of NK cells treated with Glutor. Thus, there is also an up-regulation of genes belonging to the glycolysis and hypoxia gene sets and a down-regulation of genes belonging to the fatty acid metabolism and oxidative phosphorylation gene sets (Figure 34B).

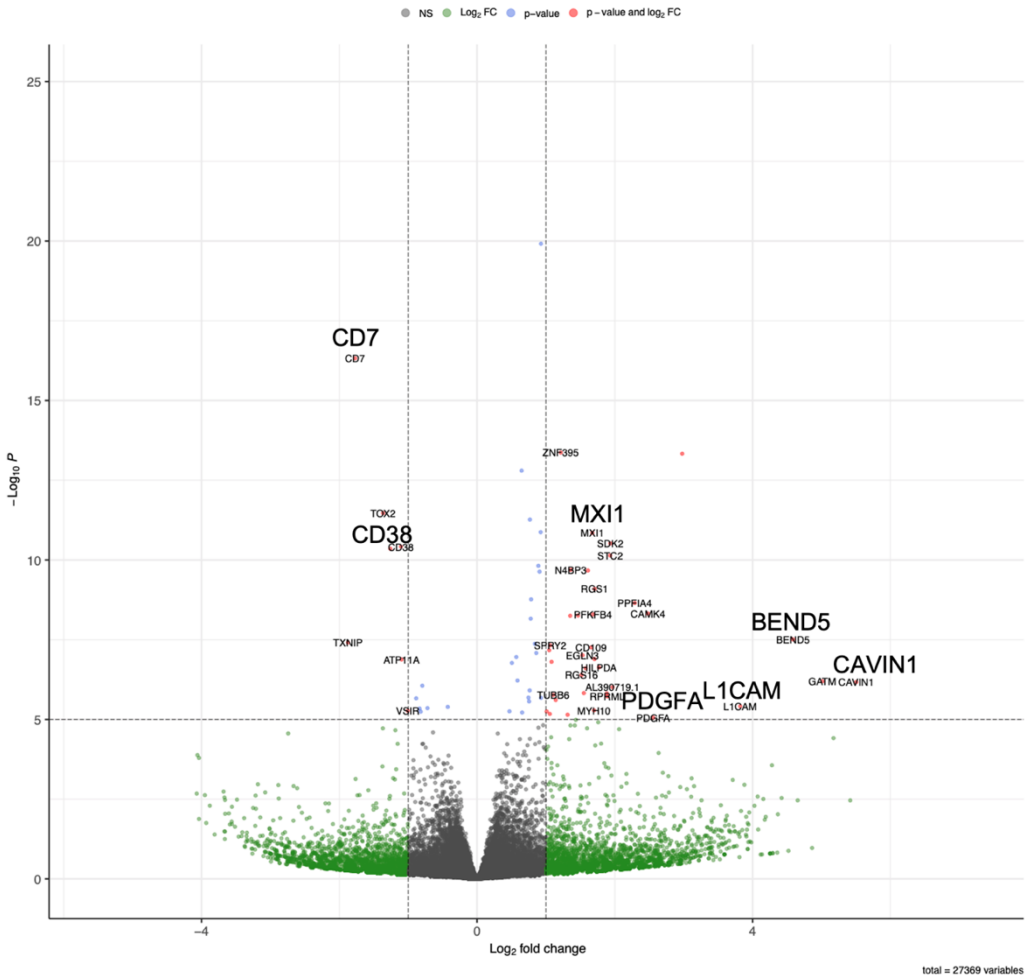

Figure 33: Volcanoplot analysis of Glupin treated NK cells

Volcano plot demonstrating proteins differentially regulated in Glupin-treated NK cells compared to control NK cells. Each data point represents a single quantified gene. The y-axis represents the -Log10 p value and the x-axis the Log2 fold change in Glutor-treated NK cells. Threshold for significant genes is chosen for fold change > 1 and for p-value cut-off 5.

However, there was no significant change in the expression of glucose transporters by Glupin treatment. The direct comparison between Glutor- and Glupin treatment on NK cells displayed a down-regulation of CD38 in Glutor-treated NK cells, whereas SLC2A3 and SLC16A10 were up-regulated (Supplement Figure 37). Glutor- and Glupin-treatment leads to similar changes in gene expression patterns, but Glutor has a higher impact on gene expression.

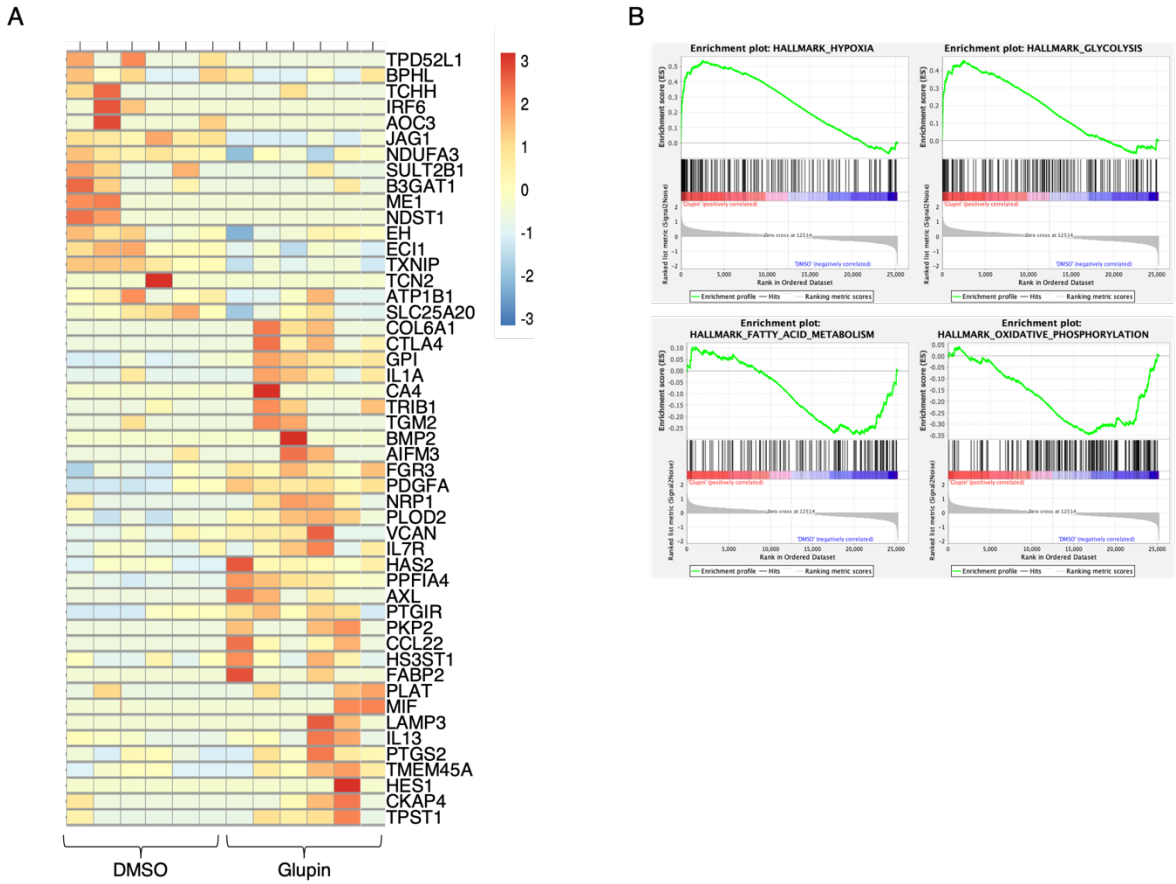

Figure 34:Long-term treatment with Glupin induces a hypoxia phenotype in NK cells

Bulk-RNA-sequencing of long-term treated NK cells (0.1% DMSO, 100 nM Glupin). A) Heatmap of the 49 most differentially expressed genes. Genes with higher expression levels are displayed in red, while genes with lower expression levels are displayed in blue. B) GSEA-analysis of the 27369 genes. The 4 most significant Hallmark pathways were shown. Pathways of glycolysis and hypoxia are enriched in upregulated genes, whereas pathways of OxPhos and fatty acid metabolism are down-regulated. n=6.

8 Discussion

We wanted to investigate the effect of the GLUT-inhibitors Glupin and Glutor on the functional capacity of human NK cells and thus find out whether the use of Glupin or Glutor, in addition to the therapeutic benefit in cancer, does not also restrict NK cell functions, since these play an important role in the killing of tumor cells.

Blocking the glucose transporter by different concentrations of Glupin or Glutor leads to decreased glycolysis and increased OxPhos. In addition, Glutor showed a stronger effect, as little as 50 nM Glutor altered the energetic phenotype of NK cells, whereas these changes were only observed at concentrations of 100 nM or higher with Glupin. This is also demonstrated in the experiments of Waldmann and his group, where it was shown that Glutor with lower concentrations exerted a greater effect on various cell lines than Glupin (Reckzeh et al. 2019; Ceballos et al. 2019). NK cell functions such as cytotoxicity and IFN-γ secretion were not affected by acute treatment with Glutor or Glupin. This could be due to their reliance on alternative sources such as glutamine or fatty acids to meet their energy requirements. In addition, it has been described that the low basal metabolic rate of resting NK cells is sufficient to exert an acute NK cell effector response (Keppel et al. 2015). In this case, short-term inhibition of glucose uptake would have no effect on NK cells and their functions. Furthermore, it is known that the cytotoxic function of NK cells mainly depends on pre-formed effector proteins that are stored in the lytic granules and are mobilized only after NK cell activation (Prager and Watzl 2019). This was confirmed by further analyses, as short-term treatment of NK cells with Glutor or Glupin did not affect the cytotoxicity of NK cells significantly against two different tumor cell lines (HepG2 or MCF7 cells). Indicating that acute alteration of NK cell metabolism has no adverse effects. The time frame involved and the point at which inhibition of glucose uptake may have a negative effect on NK cells is not clear. Nevertheless, it is clear that NK cells are robust to changes in their energy metabolism and can perform their functions normally, at least over a certain period of time.

It is known that activation of NK cells increases their glycolysis to provide sufficient energy and precursors for anabolic processes. (Donnelly et al. 2014; Schafer et al. 2019). We stimulated resting NK cells with cytokines and feeder cells to induce NK cell

proliferation and activation. Both inhibitors resulted in significantly decreased glucose uptake by NK cells after long-term treatment. This was associated with a lack of proliferation of Glutor-treated NK cells. Previous studies have shown, that blocking of glycolysis results in a stop of proliferation in NK cells (Mah et al. 2017). Interestingly, NK cells treated with Glupin show only decreased proliferation within the first 14 days, followed by normal proliferation, thereafter, suggesting that these NK cells change their metabolic profile or become resistant to the inhibitor. But analysis of the NK cells' metabolic profile treated with Glutor or Glupin demonstrated the same trend. Both displayed an increased mitochondrial dependence, whereas the glycolytic capacity is decreased, confirming the sustained inhibition of glucose uptake. However, these data also show that treatment with Glutor appeared to have a stronger effect on the metabolic profile of NK cells than treatment with Glupin, suggesting that it may be the strength of inhibition that leads to the different proliferative outcomes.

Further analysis of key metabolic molecules, such as mTOR, demonstrated that both inhibitor treatments resulted in delayed but persistently increased phosphorylation of mTOR. mTOR plays an essential role in NK cell maturation, activation, and metabolism. Moreover, cytokines such as IL-2 and IL-15 are known to induce mTOR. (Gardiner and Finlay 2017; Yang and Malarkannan 2020). This suggests that NK cells respond longer to stimulation by IL-2 and IL-15, which increases mTOR activity and thus may counteract reduced glucose availability. On the one hand, mTOR can control the translation of cMyc and thus the expression of glucose transporters; on the other hand, mTOR has a direct effect on glycolysis. (Donnelly et al. 2014; Loftus et al. 2018; Takahara et al. 2020). A previous study showed that HK1 expression is regulated by mTORC1-dependent translation and that enhanced expression and activity of HK1 is critical for the consumption of G6P to maintain the elevated glycolytic phenotype required during activation (Moon et al., 2015). This could explain the delayed upregulation of HK1. Long-term treatment with Glupin did not change the expression of cMyc compared to control. This suggests that there is no deficit in the availability of amino acids such as glutamine, as cMyc protein expression can also be regulated by amino acid transport through SLC7A5/SLC3A2 (Loftus et al. 2018). Analysis of CD98 (SLC3A2), which is known to be upregulated on activated and proliferating lymphocytes (Salzberger et al. 2018), showed significant upregulation after long-term Glupin treatment. The same could be observed for CD71 expression, known to be

involved in proliferation and function of lymphocytes (Salzberger et al. 2018). Keating et al. showed that cytokine-stimulated NK cells upregulate their nutrient receptors such as CD71 and CD98 to fulfill their biosynthetic requirements (Keating et al. 2016). Thus, the increased expression of CD71 and CD98 can indicate altered utilization of iron and amino acids as potential energy sources for NK cell activation and proliferation for the highly metabolically active NK cells to ensure their energy supply. Further studies to investigate the role of CD71 and CD98 in NK cells may reveal their effects on NK cell function. Based on the findings on the importance of the citrate-malate shuttle in NK cell metabolism (Assmann et al. 2017), we analyzed the malate concentration in long-term treated NK cells and observed a trend toward lower malate concentration in Glupin-treated NK cells. Previous studies have shown that pyruvate, which is converted to acetyl-CoA, is mainly used for the citrate-malate shuttle, which in turn regulated gene expression and feeds into OxPhos (Assmann et al. 2017). A lack of glucose seems to reduce the activity of the citrate-malate shuttle. Consistent with the metabolomics data, the decreased glucose uptake results in an equally decreased intracellular concentration of pyruvate. As a result, less glucose is used in the TCA cycle and thus reduces the citrate-malate shuttle activity. Another possibility is that the Glupin-treated NK cells produce more lactate to obtain energy as quickly as possible. However, since the Glupin-treated NK cells have less lactate compared to the control cells, this does not seem to be the case.

Glycolysis plays an important role in the synthesis of molecules for the effector functions of NK cells. However, long-term treatment of NK cells with Glupin did not lead to any altered secretion of the pro-inflammatory cytokines IFN-γ, TNF-α and IL-6 as well as the chemokines IL-8 and MCP-1. Interestingly, Glutor treatment leads to significantly increased secretion of these cytokines and chemokines; only the secretion of the anti-inflammatory cytokine IL-10 was decreased. Further, the changes in the chemokine profile of Glutor-treated NK cells resulted in changes in the migratory behavior of various immune cells. Thus, glycolysis after NK cell activation is not only important for proliferation, but also to reduce a pro-inflammatory regulators function of activated NK cells.

In contrast to the spontaneous secretion of IFN-γ, stimulation-dependent secretion of IFN-γ showed a significant reduction of Glutor- or Glupin-treated NK cells stimulated via CD16 or NKp30, whereas stimulation via NKG2D + 2B4 and IL-12 + IL-18 did not show these functional impairments. Similar effects were observed for degranulation when NK cells were treated with Glutor. This could be due to a different metabolic dependence of ITAM-based signaling mediated by CD16 and NKp30, in contrast to ITT- and ITSM-based signaling initiated by NKG2D + 2B4 (Chiesa et al. 2006; Watzl and Long 2010). Another reason might be the less potent activation of NK cells by stimulation with NKG2D + 2B4 compared with CD16 stimulation. In this case, there could be enough energy to fulfill the effector function, while excessive activation strains the NK cell. Furthermore, it could also be that decreased expression of CD16 on the long-term treated NK cells was responsible for these defects, but NKp30 expression was not decreased and showed the same trend towards functional impairment. And at the same time, the cells also showed decreased expression of 2B4, but this did not lead to decreased degranulation nor IFN-γ secretion in the case of NKG2D + 2B4 stimulation. Interestingly, treatment with Glupin had no effect on degranulation, although these NK cells exhibited decreased CD16 expression, ruling out the possibility that decreased expression of CD16 alone was responsible for the reduced response of Glutor-treated NK cells. In turn, this suggests that there are differences in the metabolic dependency of the signaling pathways. So far, however, there are no data or studies that provide information on this.

In addition to the reduced expression of CD16 and 2B4, the altered metabolism of the NK cells led to changes in the NK cell phenotype. The reduced expression of CD57 on Glupin-treated NK cells could mark the less differentiated and more proliferative state of NK cells than the control NK cells. Further, increased expression of CD57 is related to a terminally differentiated and more cytotoxic NK cell population (Nielsen et al. 2013), but in this case the reduced expression of CD57 does not coincide with a reduced cytotoxic function of the NK cells. In addition to downregulation of some markers, long-term treatment with Glutor or Glupin showed increased expression of KLRB1 and HLA-DR in NK cells. KLRB1 primarily labels proinflammatory NK cells and is a marker of NK cell function (Kurioka et al. 2018). Further, Glutor treatment resulted in an increased expression of the exhaustion marker KLRG1 (Alvarez et al. 2019), while NK cells treated with Glupin showed increased expression of the activating receptor NKp44. Overall, the altered expression of these activation and adhesion receptors could be

related to the different functional capabilities of the NK cells, but the cluster analysis did not reveal a clearly distinct NK cell population after long-term treatment.

The cytolytic activity of long-term treated NK cells with Glutor or Glupin against K562 cells in a 4-hour ^{51}Cr release assay was not affected. Although Glutor-treated NK cells exhibited stimulation-dependent deficits in degranulation, these NK cells were still able to kill tumor cells in this bulk assay. This could be due to a few NK cells that are robust enough to this treatment and sufficient to kill the tumor cells. A closer look at the single cell level using time-lapse microscopy to analyze the serial killing capacity of these NK cells revealed some interesting differences between Glutor- and Glupin-treated NK cells. Glutor treatment results in a slightly decreased serial-killing capacity of NK cells compared to the control. Interestingly, the percentage of serial killers as well as the number of kills per NK cell was increased by Glupin treatment. These NK cells as well as the Glutor-treated NK cells showed significantly increased expression of granzyme B. In contrast, there were no differences in perforin expression. However, the increased granzyme B level does not seem to play a decisive role in the increased serial killing capacity of the Glupin-treated NK cells, as the Glutor-treated NK cells showed the same trend. Another possibility for the increased serial-killing capacity could be the decreased CD16 expression in Glupin-treated NK cells, as this leads to faster detachment from opsonized target cells and thus contributes to increased NK cell survival (Srpan et al. 2018). However, this is in contrast to the also decreased CD16 expression on the Glutor-treated NK cells, which did not show increased serial-killing. On the other hand, no significant differences between Glupin-treated NK cells and control cells were found in the analysis of attachment and detachment times (data not shown). Based on recent findings that short-chain fatty acids (SCFA) increase the cytotoxic activity of T cells (Luu et al. 2018), we wanted to investigate whether treatment with Glupin leads to increased use of SCFA. However, treatment of NK cells with both SCFA butyrate and pentanoate had no effect on NK cell cytotoxic activity or phosphorylation of mTOR, suggesting that these two SCFA do not appear to be responsible for this effect. This was confirmed by inhibition of the CPT1, which showed no changes in degranulation or IFN-γ secretion of long-term treated NK cells. This is consistent with previous findings on the independence of IFN-γ secretion from fatty acid metabolism (Keppel et al. 2015). Furthermore, Michelet et al. show a negative effect of fatty acid metabolism on NK cell function (Michelet et al. 2018). This indicates

that NK cells do not use fatty acids to meet their metabolic needs even under glucose starvation. Another explanation for the results of Glupin-treated NK cells could be increased utilization of glutamine, which is known to be an important fuel for NK cell activation and proliferation (Loftus et al. 2018). This is also supported by our metabolomics data, which revealed a significantly increased concentration of glutamine and glutamine acid in Glupin-treated NK cells. Long-term treatment with the glutaminase inhibitor CB839 significantly increases cytotoxic function as well as IFN-γ secretion by NK cells, which is associated with increased mitochondrial mass. Moreover, acute treatment of Glupin-treated NK cells with CB839 showed no functional impairment, indicating that glutamine does not appear to be responsible for the changes induced by Glupin-treatment. Similar results are shown in T cells, where Varghese et al. demonstrated enhanced anti-melanoma activity of CB839-treated T cells (Varghese et al. 2021). One possible explanation for the continued proliferation of NK cells during treatment with Glupin could be the increased consumption of glutamine, as metabolomics revealed higher glutamine levels in Glupin-treated NK cells. And the combination of Glupin with the glutaminase inhibitor CB839 stops NK cell proliferation completely, suggesting that glutamine can compensate for glucose deficiency during proliferation, but not for increased effector function. This could be because Glutamine is also a precursor to proline, which is known to play an important role in modulating cell signaling and epigenetic changes (Patriarca et al. 2021). Further investigation into the mechanism of why NK cells exhibit increased functional activity due to CB839 treatment could perhaps contribute to a deeper understanding of glutamine metabolism in NK cells and its effects on NK cell function.

Our transcriptional analysis confirmed differences between Glutor and Glupin treatment. NK cells treated with Glutor showed increased expression of *GLUT-3*, *GLUT-13*, and *GLUT-14*, whereas Glupin did not significantly alter their GLUT expression. Reckzeh et al. also demonstrated increased GLUT-3 expression in tumor cells during glucose starvation (Reckzeh et al. 2019), which appears to be a counter-response of the cells. The expression of GLUT-13 and GLUT-14 has not been further described in NK cells. Apart from these differences, treatment with Glutor as well as Glupin increased the expression of genes related to glycolysis and hypoxia, indicating that these cells are trying to counteract the strong inhibition of glucose uptake. Hypoxia is an important factor related to the tumor microenvironment. This, together with the

reduced availability of nutrients such as glucose and glutamine, can affect immune cell function. Thus, it has been shown that NK cells are sensitive to a hypoxic environment and consequently switch their metabolism. The transcription factor HIF1α plays an important role in the context of hypoxia, as it regulates immune responses to reduced oxygen concentrations and regulates gene expression of glucose transporters. Both inhibitor treatments led to a small increase in HIF1α compared to the control. It is known that NK cells upregulate HIF1α under hypoxic conditions and that HIF1α can increase the expression of glycolytic enzymes. (Macheda et al. 2005; Chambers and Matosevic 2019; Solocinski et al. 2020; Kierans and Taylor 2021). However, the exact significance of HIF1α in NK cells has so far been contradictory. On the one hand, it was shown that the deletion of HIF1α led to a reduction in cell number, on the other hand, it was shown that HIF1α suppresses the cytotoxic activity of NK cells (Hasmim et al. 2015; Victorino et al. 2021). Further it is known, that HIF1α regulates the transcription of L1-CAM and that the glycolytic energy metabolism in tumor cells affects the expression of L1-CAM. (Zhang et al. 2012; Mrazkova et al. 2018). L1-CAM plays an important role in cell adhesion and signal transduction, and it is mostly associated with an increased proliferation and migration in tumor cells (Finas et al. 2008; Zhang et al. 2022). Both Inhibitor-treatments displayed up-regulation of *L1-CAM* in comparison to the control, demonstrating the influence of *HIF1α* and glycolysis on proliferation and migration in NK cells.

Nevertheless, since genes related to hypoxia and to glycolysis were up-regulated in both Glutor and Glupin-treated NK cells, this does not seem to be responsible for the increased serial-killing capacity. However, Glutor-treatment of NK cells has a stronger influence on their gene expression than Glupin treatment. An important finding in this regard was the increased expression of genes related to the p53 pathway in Glutor-treated NK cells, suggesting cell cycle arrest, which may explain their lack of proliferation compared with control NK cells and Glupin-treated NK cells. Moreover, in accord with decreased surface expression of CD38, glucose arrest also down-regulates *CD38* gene expression. CD38 has multiple functions, such as NADase activity, which contributes to the regulation of NAD^+ levels. Analysis of NAD^+/NADH revealed increased levels after Glupin treatment, which may be due to decreased *CD38* expression. Previous studies have shown that this interaction is an important factor in tumor progression by inhibiting the anti-tumor activity of lymphocytes invading the tumor (Chini 2009; Navas and Carnero 2021). In addition, knockout of CD38 leads

to increased levels of NAD^+, which is associated with increased cytotoxicity of T cells (Morandi et al. 2021). This increased NAD^+ activity may explain the enhanced serial killing capacity of long-term treated NK cells. Further experiments on the direct effect of NAD^+ should be investigated to evaluate its functional role in NK cell cytotoxicity.

Long-term inhibition of glucose uptake by Glutor negatively affects NK cell proliferation, which is associated with increased mitochondrial dependence and changes in NK cell phenotype. Stimulation-induced degranulation and IFN-γ secretion were also significantly impaired, whereas overall cytotoxic activity showed no defects, indicating that the cytotoxic machinery appears to be robust. However, halting NK cell proliferation would also impair NK cell-mediated tumor control. This highlights the importance of evaluating the effect of potential tumor therapeutics on immune cells. In addition, tumor cells are known to overcome glucose deprivation by using glutamine as their main energy source. In this case, a combination therapy of a glucose uptake inhibitor and glutaminase inhibitor must be used. In our experiments, we observed that this combination leads to apoptosis of NK cells, suggesting that this needs to be optimized. Accordingly, the therapeutic benefit of long-term administration of Glutor would be low since the proliferation and certain functions of the NK cells are impaired. However, there was no direct restriction of the tumor cell killing capacity of the long-term treated NK cells. The use of Glupin shows similarities to Glutor treatment in NK cell phenotype and stimulation-dependent decreased IFN-γ secretion. In contrast, Glupin treatment do not affect degranulation or proliferation and, interestingly, increase the serial killing ability of NK cells. This finding is interesting and should be further investigated as to why these NK cells have a higher capacity for serial killing. A limitation could be that Glupin treatment has no effect on tumor cells because some tumor cells are resistant to these concentrations, but even in this case it would be beneficial to increase NK cell activity. Treatment with Glupin would both stop tumor cell proliferation and increase the anti-tumor activity of NK cells, which is the best outcome for therapy, suggesting that Glupin is a potent and effective anticancer drug in several ways.

9 Graphical conclusion

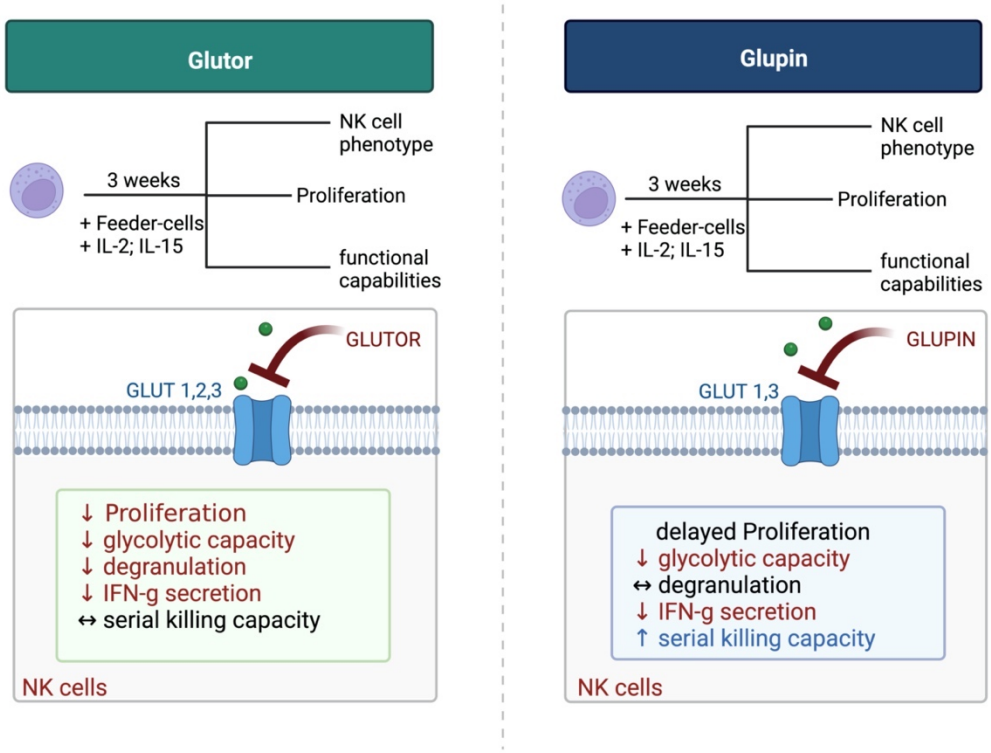

Figure 35: Graphical conclusions

Long-term treatment with Glutor impairs proliferation, reduce the glycolytic capacity and negatively affected degranulation and IFN-γ secretion, whereas serial-killing capacity is not affected. Long-term treatment with Glupin leads to a delayed proliferation and diminish the glycolytic capacity as well as the IFN-γ secretion, whereas degranulation is not affected by Glupin. Interestengly, Glupin-treatment enhance the serial-killing capacity of NK cells.

10 References

Airley RE, Mobasheri A (2007) Hypoxic regulation of glucose transport, anaerobic metabolism and angiogenesis in cancer: Novel pathways and targets for anticancer therapeutics. Chemotherapy 53:233–256

Alvarez M, Simonetta F, Baker J, et al (2019) Regulation of murine NK cell exhaustion through the activation of the DNA damage repair pathway. JCI Insight 4:. https://doi.org/10.1172/jci.insight.127729

Angela M, Endo Y, Asou HK, et al (2016) Fatty acid metabolic reprogramming via mTOR-mediated inductions of PPARγ directs early activation of T cells. Nat Commun 7:1–15. https://doi.org/10.1038/ncomms13683

Argüello RJ, Combes AJ, Char R, et al (2020) SCENITH: A Flow Cytometry-Based Method to Functionally Profile Energy Metabolism with Single-Cell Resolution. Cell Metab 32:1063-1075.e7. https://doi.org/10.1016/j.cmet.2020.11.007

Assmann N, O'Brien KL, Donnelly RP, et al (2017) Srebp-controlled glucose metabolism is essential for NK cell functional responses. Nat Immunol 18:1197–1206. https://doi.org/10.1038/ni.3838

Bryceson YT, March ME, Ljunggren HG, Long EO (2006) Synergy among receptors on resting NK cells for the activation of natural cytotoxicity and cytokine secretion. Blood 107:159–166. https://doi.org/10.1182/blood-2005-04-1351

Caligiuri MA (2008) Human natural killer cells. Blood 112:461–469. https://doi.org/10.1182/blood-2007-09-077438

Ceballos J, Schwalfenberg M, Karageorgis G, et al (2019) Synthesis of Indomorphan Pseudo-Natural Product Inhibitors of Glucose Transporters GLUT-1 and -3. Angewandte Chemie International Edition 58:17016–17025. https://doi.org/10.1002/anie.201909518

Chambers AM, Matosevic S (2019) Immunometabolic Dysfunction of Natural Killer Cells Mediated by the Hypoxia-CD73 Axis in Solid Tumors. Front Mol Biosci 6:60

Chester C, Fritsch K, Kohrt HE (2015) Natural killer cell immunomodulation: Targeting activating, inhibitory, and co-stimulatory receptor signaling for cancer immunotherapy. Front Immunol 6

Chiesa S, Mingueneau M, Fuseri N, et al (2006) Multiplicity and plasticity of natural killer cell signaling pathways. Blood 107:2364–2372. https://doi.org/10.1182/blood-2005-08-3504

Chini E (2009) CD38 as a Regulator of Cellular NAD: A Novel Potential Pharmacological Target for Metabolic Conditions. Curr Pharm Des 15:57–63. https://doi.org/10.2174/138161209787185788

Cooper MA, Fehniger TA, Turner SC, et al (2001) Human natural killer cells: A unique innate immunoregulatory role for the CD56bright subset. Blood 97:3146–3151. https://doi.org/10.1182/blood.V97.10.3146

Covarrubias AJ, Perrone R, Grozio A, Verdin E (2021) NAD+ metabolism and its roles in cellular processes during ageing. Nat Rev Mol Cell Biol 22:119–141

Donnelly RP, Loftus RM, Keating SE, et al (2014) mTORC1-Dependent Metabolic Reprogramming Is a Prerequisite for NK Cell Effector Function. The Journal of Immunology 193:4477–4484. https://doi.org/10.4049/jimmunol.1401558

Feron O (2009) Pyruvate into lactate and back: From the Warburg effect to symbiotic energy fuel exchange in cancer cells. Radiotherapy and Oncology 92:329–333

Finas D, Huszar M, Agic A, et al (2008) L1 cell adhesion molecule (L1CAM) as a pathogenetic factor in endometriosis. Human Reproduction 23:1053–1062. https://doi.org/10.1093/humrep/den044

Freud AG, Caligiuri MA (2006) Human natural killer cell development. Immunol Rev 214:56–72. https://doi.org/10.1111/j.1600-065X.2006.00451.x
Ganapathy V, Thangaraju M, Prasad PD (2009) Nutrient transporters in cancer: Relevance to Warburg hypothesis and beyond. Pharmacol Ther 121:29–40
Gardiner CM (2019) NK cell metabolism. J Leukoc Biol 105:1235–1242. https://doi.org/10.1002/JLB.MR0718-260R
Gardiner CM, Finlay DK (2017) What fuels natural killers? Metabolism and NK cell responses. Front Immunol 8:367. https://doi.org/10.3389/FIMMU.2017.00367/BIBTEX
Guillerey C, Smyth MJ (2017) Cytokine-driven role of Srebps in killer cell metabolism. Nat Immunol 18:1183–1184
Hasmim M, Messai Y, Ziani L, et al (2015) Critical role of tumor microenvironment in shaping NK cell functions: Implication of hypoxic stress. Front Immunol 6:482
Husain Z, Huang Y, Seth P, Sukhatme VP (2013) Tumor-Derived Lactate Modifies Antitumor Immune Response: Effect on Myeloid-Derived Suppressor Cells and NK Cells. The Journal of Immunology 191:1486–1495. https://doi.org/10.4049/jimmunol.1202702
Jensen H, Potempa M, Gotthardt D, Lanier LL (2017) Cutting Edge: IL-2–Induced Expression of the Amino Acid Transporters SLC1A5 and CD98 Is a Prerequisite for NKG2D-Mediated Activation of Human NK Cells. The Journal of Immunology 199:1967–1972. https://doi.org/10.4049/jimmunol.1700497
Juelke K, Killig M, Luetke-Eversloh M, et al (2010) CD62L expression identifies a unique subset of polyfunctional CD56 dim NK cells. Blood 116:1299–1307. https://doi.org/10.1182/blood-2009-11-253286
Keating SE, Zaiatz-Bittencourt V, Loftus RM, et al (2016) Metabolic Reprogramming Supports IFN-γ Production by CD56 bright NK Cells . The Journal of Immunology 196:2552–2560. https://doi.org/10.4049/jimmunol.1501783
Keppel MP, Saucier N, Mah AY, et al (2015) Activation-Specific Metabolic Requirements for NK Cell IFN-γ Production. The Journal of Immunology 194:1954–1962. https://doi.org/10.4049/jimmunol.1402099
Kidani Y, Elsaesser H, Hock MB, et al (2013) Sterol regulatory element-binding proteins are essential for the metabolic programming of effector T cells and adaptive immunity. Nat Immunol 14:489–499. https://doi.org/10.1038/ni.2570
Kierans SJ, Taylor CT (2021) Regulation of glycolysis by the hypoxia-inducible factor (HIF): implications for cellular physiology. J Physiol 599:23–37. https://doi.org/10.1113/JP280572
Kobayashi T, Lam PY, Jiang H, et al (2020) Increased lipid metabolism impairs NK cell function and mediates adaptation to the lymphoma environment. Blood 136:3004–3017. https://doi.org/10.1182/blood.2020005602
Krzeslak A, Wojcik-Krowiranda K, Forma E, et al (2012) Expression of GLUT1 and GLUT3 glucose transporters in endometrial and breast cancers. Pathology and Oncology Research 18:721–728. https://doi.org/10.1007/s12253-012-9500-5
Kurioka A, Cosgrove C, Simoni Y, et al (2018) CD161 defines a functionally distinct subset of pro-inflammatory natural killer cells. Front Immunol 9:486. https://doi.org/10.3389/FIMMU.2018.00486/BIBTEX
Lanier LL, Yu G, Phillips JH (1991) Analysis of Fc gamma RIII (CD16) membrane expression and association with CD3 zeta and Fc epsilon RI-gamma by site-directed mutation. J Immunol 146:1571–6
Li JL, Lin TY, Chen PL, et al (2021) Mitochondrial Function and Parkinson's Disease: From the Perspective of the Electron Transport Chain. Front Mol Neurosci 14:315

Loftus RM, Assmann N, Kedia-Mehta N, et al (2018) Amino acid-dependent cMyc expression is essential for NK cell metabolic and functional responses in mice. Nat Commun 9:1–15. https://doi.org/10.1038/s41467-018-04719-2
Long EO, Sik Kim H, Liu D, et al (2013) Controlling natural killer cell responses: Integration of signals for activation and inhibition. Annu Rev Immunol 31:227–258
Luetke-Eversloh M, Killig M, Romagnani C (2013) Signatures of human NK cell development and terminal differentiation. Front Immunol 4
Luu M, Weigand K, Wedi F, et al (2018) Regulation of the effector function of CD8+ T cells by gut microbiota-derived metabolite butyrate. Sci Rep 8:. https://doi.org/10.1038/s41598-018-32860-x
Macheda ML, Rogers S, Best JD (2005) Molecular and cellular regulation of glucose transporter (GLUT) proteins in cancer. J Cell Physiol 202:654–662. https://doi.org/10.1002/jcp.20166
Mah AY, Rashidi A, Keppel MP, et al (2017) Glycolytic requirement for NK cell cytotoxicity and cytomegalovirus control. JCI Insight 2:. https://doi.org/10.1172/jci.insight.95128
Martínez-Reyes I, Chandel NS (2020) Mitochondrial TCA cycle metabolites control physiology and disease. Nat Commun 11:1–11
Michelet X, Dyck L, Hogan A, et al (2018) Metabolic reprogramming of natural killer cells in obesity limits antitumor responses. Nat Immunol 19:1330–1340. https://doi.org/10.1038/s41590-018-0251-7
Morandi F, Horenstein AL, Malavasi F (2021) The Key Role of NAD+ in Anti-Tumor Immune Response: An Update. Front Immunol 12:1221. https://doi.org/10.3389/fimmu.2021.658263
Mrazkova B, Dzijak R, Imrichova T, et al (2018) Induction, regulation and roles of neural adhesion molecule L1CAM in cellular senescence. Aging 10:434–462. https://doi.org/10.18632/aging.101404
Navale AM, Paranjape AN (2016) Glucose transporters: physiological and pathological roles. Biophys Rev 8:5–9
Navas LE, Carnero A (2021) NAD+ metabolism, stemness, the immune response, and cancer. Signal Transduct Target Ther 6:1–20
Nielsen CM, White MJ, Goodier MR, Riley EM (2013) Functional significance of CD57 expression on human NK cells and relevance to disease. Front Immunol 4
Patriarca EJ, Cermola F, D'Aniello C, et al (2021) The Multifaceted Roles of Proline in Cell Behavior. Front Cell Dev Biol 9:2236
Poznanski SM, Ashkar AA (2019) What Defines NK Cell Functional Fate: Phenotype or Metabolism? Front Immunol 10:1414. https://doi.org/10.3389/FIMMU.2019.01414
Poznanski SM, Lee AJ, Nham T, et al (2017) Combined Stimulation with Interleukin-18 and Interleukin-12 Potently Induces Interleukin-8 Production by Natural Killer Cells. J Innate Immun 9:511–525. https://doi.org/10.1159/000477172
Prager I, Liesche C, van Ooijen H, et al (2019) NK cells switch from granzyme B to death receptor–mediated cytotoxicity during serial killing. J Exp Med 216:2113. https://doi.org/10.1084/JEM.20181454
Prager I, Watzl C (2019) Mechanisms of natural killer cell-mediated cellular cytotoxicity. J Leukoc Biol 105:1319–1329. https://doi.org/10.1002/JLB.MR0718-269R
Raulet DH (2006) Missing self recognition and self tolerance of natural killer (NK) cells. Semin Immunol 18:145–150

Reckzeh ES, Karageorgis G, Schwalfenberg M, et al (2019) Inhibition of Glucose Transporters and Glutaminase Synergistically Impairs Tumor Cell Growth. Cell Chem Biol 26:1214-1228.e25. https://doi.org/10.1016/j.chembiol.2019.06.005
Salzberger W, Martrus G, Bachmann K, et al (2018) Tissue-resident NK cells differ in their expression profile of the nutrient transporters Glut1, CD98 and CD71. PLoS One 13:. https://doi.org/10.1371/journal.pone.0201170
Schafer JR, Salzillo TC, Chakravarti N, et al (2019) Education-dependent activation of glycolysis promotes the cytolytic potency of licensed human natural killer cells. Journal of Allergy and Clinical Immunology 143:346-358.e6. https://doi.org/10.1016/j.jaci.2018.06.047
Semenza GL (2008) Tumor metabolism: Cancer cells give and take lactate. Journal of Clinical Investigation 118:3835–3837
Solocinski K, Padget MR, Fabian KP, et al (2020) Overcoming hypoxia-induced functional suppression of NK cells. J Immunother Cancer 8:e000246. https://doi.org/10.1136/jitc-2019-000246
Srpan K, Ambrose A, Karampatzakis A, et al (2018) Shedding of CD16 disassembles the NK cell immune synapse and boosts serial engagement of target cells. Journal of Cell Biology 217:3267–3283. https://doi.org/10.1083/jcb.201712085
Surace L, Doisne JM, Escoll P, et al (2021) Polarized mitochondria as guardians of NK cell fitness. Blood Adv 5:26–38. https://doi.org/10.1182/bloodadvances.2020003458
Takahara T, Amemiya Y, Sugiyama R, et al (2020) Amino acid-dependent control of mTORC1 signaling: A variety of regulatory modes. J Biomed Sci 27:87
Terrén I, Orrantia A, Vitallé J, et al (2019) NK cell metabolism and tumor microenvironment. Front Immunol 10
Thorens B, Mueckler M (2010) Glucose transporters in the 21st Century. Am J Physiol Endocrinol Metab 298:E141
Varghese S, Pramanik S, Williams LJ, et al (2021) The glutaminase inhibitor CB-839 (Telaglenastat) enhances the antimelanoma activity of T-cell-mediated immunotherapies. Mol Cancer Ther 20:500–511. https://doi.org/10.1158/1535-7163.MCT-20-0430
Victorino F, Bigley TM, Park E, et al (2021) Hif1α is required for nk cell metabolic adaptation during virus infection. Elife 10:. https://doi.org/10.7554/eLife.68484
Wang F, Zhang S, Jeon R, et al (2018) Interferon Gamma Induces Reversible Metabolic Reprogramming of M1 Macrophages to Sustain Cell Viability and Pro-Inflammatory Activity. EBioMedicine 30:303–316. https://doi.org/10.1016/j.ebiom.2018.02.009
Wang KS, Frank DA, Ritz J (2000) Interleukin-2 enhances the response of natural killer cells to interleukin-12 through up-regulation of the interleukin-12 receptor and STAT4. Blood 95:3183–3190. https://doi.org/10.1182/blood.v95.10.3183
Warburg O (1925) über den Stoffwechsel der Carcinomzelle. Klin Wochenschr 4:534–536. https://doi.org/10.1007/BF01726151
Watzl C (2014) How to trigger a killer: Modulation of natural killer cell reactivity on many levels. In: Advances in Immunology. Academic Press Inc., pp 137–170
Watzl C, Long EO (2010) Signal Transduction During Activation and Inhibition of Natural Killer Cells. In: Current Protocols in Immunology. John Wiley & Sons, Inc.
Watzl C, Urlaub D (2012) Molecular mechanisms of natural killer cell regulation. Frontiers in Bioscience 17:1418–1432. https://doi.org/10.2741/3995
Werner C, Doenst T, Schwarzer M (2016) Metabolic Pathways and Cycles. In: The Scientist's Guide to Cardiac Metabolism. Elsevier, pp 39–55

Yang C, Ko B, Hensley CT, et al (2014) Glutamine oxidation maintains the TCA cycle and cell survival during impaired mitochondrial pyruvate transport. Mol Cell 56:414–424. https://doi.org/10.1016/j.molcel.2014.09.025
Yang C, Malarkannan S (2020) Transcriptional Regulation of NK Cell Development by mTOR Complexes. Front Cell Dev Biol 8:1280. https://doi.org/10.3389/FCELL.2020.566090/BIBTEX
Zhang H, Wong CCL, Wei H, et al (2012) HIF-1-dependent expression of angiopoietin-like 4 and L1CAM mediates vascular metastasis of hypoxic breast cancer cells to the lungs. Oncogene 31:1757–1770. https://doi.org/10.1038/onc.2011.365
Zhang J, Guo Z, Xie Q, et al (2022) Tryptophan hydroxylase 1 drives glioma progression by modulating the serotonin/L1CAM/NF-κB signaling pathway. BMC Cancer 22:457. https://doi.org/10.1186/s12885-022-09569-2
Zheng X, Qian Y, Fu B, et al (2019) Mitochondrial fragmentation limits NK cell-based tumor immunosurveillance. Nat Immunol 20:1656–1667. https://doi.org/10.1038/s41590-019-0511-1

11 Table of Figures

12 Table of Tables

13 List of abbreviations

5

^{51}Cr *Chromium-51*

A

AAO *amino acid oxidation*
ACLY *ATP citrate lyase*
ADCC *antibody mediated cellular cytotoxicity*
ATP *adenosine triphosphate*

B

BSA *bovine serum albumine*

C

CD *cluster of differentiation*
CI *cell index*
CO_2 *carbon dioxide*
CPM *counts per million*
CPT1 *carnitine palmitoyltransferase-1*

D

DAP12 *DNAX activating protein of 12 kDa*
DEG *differentially expressed genes*
DG *2-desoxy-D-glucose*
DMEM *Dulbecco's Modified Eagle's Medium*
DMSO *Dimethyl sulfoxide*
DNA *Deoxyribonucleic acid*
DPBS *Dulbecco's Phosphate-Buffered Saline*

E

E:T *effector to target ratio*
EAT-2 *Ewing's sarcoma-associated transcript-2*
ECAR *Extracellular acidification rate*
EDTA *Ethylenediaminetetraacetic acid*
eIF-4E *eukaryotic translation initiation factor 4E*
ETC *electron transport chain*

F

FA *fatty acid*
FACS *fluorescence-activated cell sorting*
FADH2 *dihydroflavin adenine dinucleotide*
FAO *fatty acid oxidation, fatty acid oxidation*
FasL *Fas-Ligand*
FCS *fetal calf serum*

G

G6P *glucose-6-phosphate*
GLUTs *glucose transporters with facilitated diffusion*
GSEA *gene set enrichment analysis*

H

h *hours*
HIF1α *hypoxia-inducible factor-1 alpha*
HK *hexokinases, hexokinase*

I

IFN-γ *interferon-gamma*
IgG *immunoglobulin G*
IL *interleukin*
IMDM *Iscove's Modified Dulbecco's Media*
ITAM *immunoreceptor tyrosine-based activation motif*
ITSM *immunoreceptor tyrosine-based switch motifs*

J

JAK2 *Janus kinase 2*

L

LAT *Linker for activation of T cells*
LC-MS *Liquid chromatography–mass spectrometry*
LSM *Lymphocyte Separation Medium*
LST8 *lethal with sec thirteen 8*

M

MCP-1 *monocyte chemoattractant protein-1*
MHC *major histocompatibility complex*
MIC *major histocompatibility complex class 1 (MHC 1) chain-related protein*
min *minutes*
mL *milliliters*
mLST8/GβL *mammalian LST8/G-protein □-subunit like protein*
MRM *multiple reaction monitoring*
mTOR *mammalian target of rapamycin*

N

NADPH *nicotinamide adenine dinucleotide phosphate*
NCRs *natural cytotoxicity receptors*
NEAA *Non-essential amino acids*
ng *nanogram*
NK *Natural killer*
NKG2D *activating receptor NK group member D*
nM *nanomolar*
NPH *3-nitrophenylhydrazine*

O

O_2 *oxygen*
OCR *oxygen consumption rate*
OxPhos *oxidative phosphorylation*

P

PBMC *peripheral blood mononuclear cells*
PDH *pyruvate dehydrogenase*
PFA *paraformaldehyde*
PI3K *phosphatidyl-inositol-3-OH-kinase*
PLC *phospholipase C*
PMSF *Phenylmethylsulfonyl fluoride*
PPP *pentose phosphate pathway*

R

RNA *Ribonucleic acid*
RPMI *Roswell Park Memorial Institute*
RT *rommtemperature*

S

S6K1 *protein S6 kinase 1*
SAP *SLAM-associated protein*
SCENITH *Single-cell energetic metabolism by profiling translation inhibition*
SCFA *short chain fatty acids*
SGLTs *sodium-glucose-linked transporters*
SLAM *signaling lymphocyte activation molecule*
SLC25A1 *Solute Carrier Family 25 Member 1*
SLP-76 *SH2 domain-containing leukocyte protein of 76 kDa*
SREBP *sterol regulatory element-binding protein*
STAT4 *signal transducer and activator of transcription 4*

T

TCA *tricarboxylic acid*
TNF *tumor necrosis factor*
TRAIL *TNF-related apoptosis-inducing ligand*

U

ULBP *UL16 binding protein*

V

Vav *vav guanine nucleotide exchange factor*

Y

YINM *tyrosine-based signaling motif*

Z

ZAP70 *Zeta-chain-associated protein kinase 70*

µ

µl *microliters*

α

α-KG *alpha-ketoglutarate*

14 Supplement

14.1 Gating Strategy

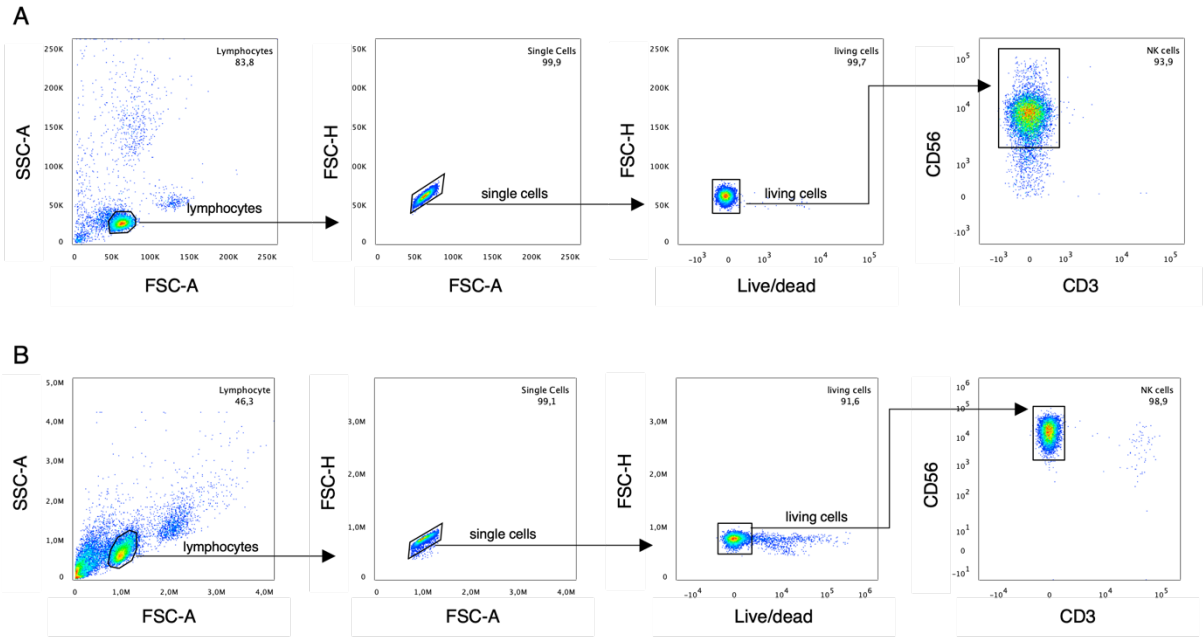

Figure 36: Gating strategy of resting and pre-activated NK cells

Gating strategy of flow cytometric analysis of resting (A) or pre-activated (B) NK cells.

14.2 Metabolomics data

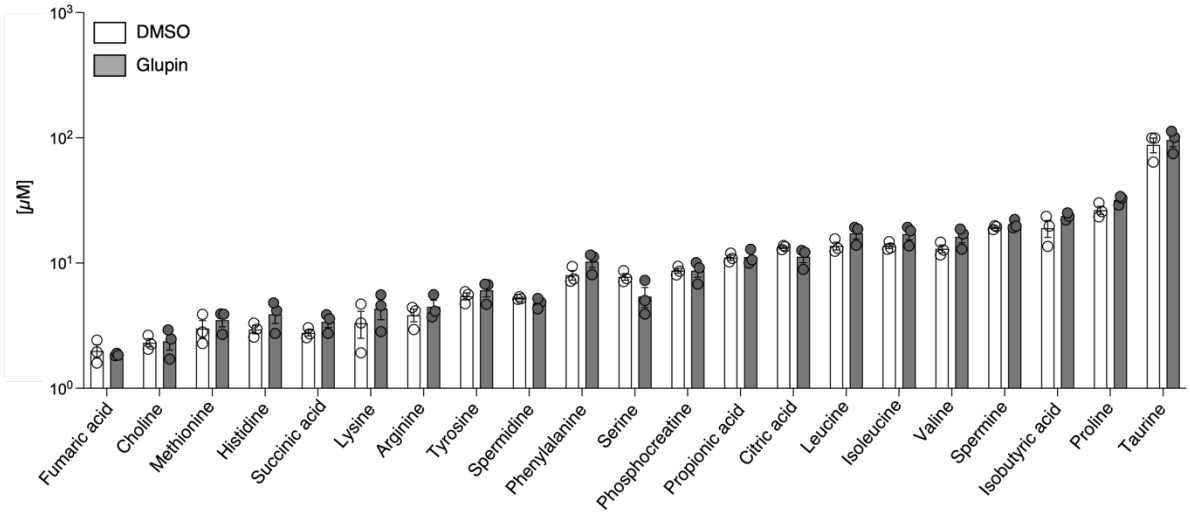

Figure 37: Metabolomics data of long-term treated NK cells
Metabolomics of $10x10^6$ long-term treated NK cells (100 nM Glupin, 0.1% DMSO). n=3. Mean with SEM.

14.3 RNA-Sequencing – comparison between Glutor and Glupin treatment

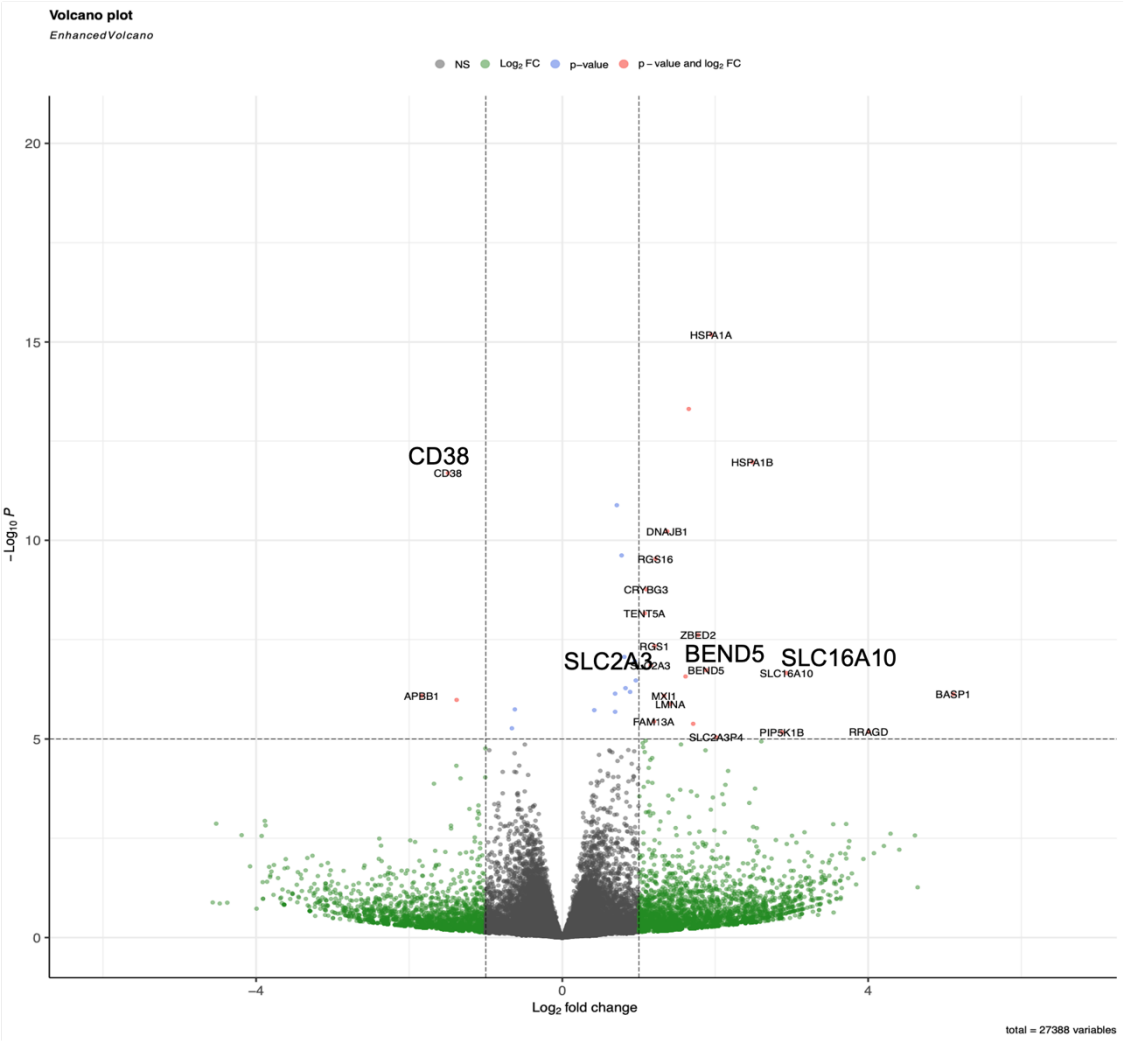

Figure 38: small differences between long-term treatment with Glupin and Glutor
Volcano plot demonstrating proteins differentially regulated in Glutor-treated NK cells compared to Glupin-treated NK cells. Each data point represents a single quantified gene. The y-axis represents the -Log10 p value and the x-axis the Log2 fold change in Glutor-treated NK cells. Threshold for significant genes is chosen for fold change > 1 and for p-value cut-off 5.

14.4 Raw data

Table 14: CD107a-Assay-short term treatment

CD107a$^+$ NK cells CD16 stimulation	Control for Glutor	Glutor	Control for Glupin	Glupin
Resting NK cells	17.57	16.97	44.15	49.27
Pre-activated NK cells	65.3	79.46	65.3	70.46

Table 15: IFN-γ secretion of CD16 stimulated NK cells after short term treatment

IFN-γ [pg/ml] CD16 stimulation	Control for Glutor	Glutor	Control for Glupin	Glupin
Resting NK cells	1115.80	1340.33	893.51	1151.87
Pre-activated NK cells	3250.82	3340.99	4090.67	4382.37

Table 16: IFN-γ secretion of IL-12/IL-18 stimulated NK cells after short term treatment

IFN-γ [pg/ml] IL12/IL18 stimulation	Control for Glutor	Glutor	Control for Glupin	Glupin
Resting NK cells	6600.83	6052.66	1191.85	1025.59

Table 17: Impedance-based analysis of MCF7 cells in the presence or absence of NK cells w/o Glutor or Glupin

	Cell Index
MCF7	3,28
MCF7 + NK cells	2,22
MCF7 + Glutor	2,4
MCF7 + Glutor + NK cells	1,59
MCF7	2,89
MCF7 + NK cells	1,18
MCF7 + Glupin	2.,93
MCF7 + Glupin + NK cells	0,91

Table 18: Impedance-based analysis of HepG2 cells in the presence or absence of NK cells w/o Glutor or Glupin

	Cell Index
HepG2	3,02
HepG2 + NK cells	2,06
HepG2 + Glutor	2,76
HepG2 + Glutor + NK cells	1,96
HepG2	3,08
HepG2 + NK cells	2,09
HepG2 + Glupin	2,86
HepG2 + Glupin + NK cells	2,10

Table 19: Absolute cell count on day 21 of long term treated NK cells

	Absolute cell count (day 21)
Control for Glutor	$1.73x10^7$
Glutor	$1.21x10^6$
Control for Glupin	$2.67x10^7$
Glupin	$2.17x10^7$

Table 20: Analysis of HK1 and pmTOR during long-term treatment with Glutor

Analysis of	Treatment	Day 0	Day 2	Day 4	Day 7
Glut1 expression [%]	DMSO	0	27%	72.5%	0
	Glutor	0	27%	72.5%	0
HK1 expression [MFI]	DMSO	2868,8	3823,2	11697	13212
	Glutor	2807,8	3610,2	9595	14604
pmTOR expression [MFI]	DMSO	325,8	1302,4	2695	1165
	Glutor	304,8	1046,8	2003	2047

Table 21: Analysis of HK1 and pmTOR during long-term treatment with Glupin

Analysis of	Treatment	Day 0	Day 2	Day 4	Day 7
Glut1 expression [%]	DMSO	0%	31.2%	69.75%	0%
	Glupin	0%	1.41%	4.5%	0%
HK1 expression [MFI]	DMSO	2868,8	3823,2	11697	13212
	Glupin	2795,2	3850	10144	14303
pmTOR expression [MFI]	DMSO	325,8	1302,4	2695	1165
	Glupin	302,8	1146	2227	1797

Table 22: Analysis of CD71, CD98 and cMyc during long-term treatment with Glupin

Analysis of	Treatment	Day 3	Day 5	Day 21
CD71 expression [MFI]	DMSO	2398	1843	1016
	Glupin	2623	2106	1867
CD98 expression [MFI]	DMSO	73303	51222	38221
	Glupin	67003	50615	51095
cMyc expression [MFI]	DMSO	8470	11528	9641
	Glupin	8272	10333	9880

Table 23: SCENITH of long-term treated NK cells

SCENITH [%]	Control for Glutor	Glutor	Control for Glupin	Glupin
Glycolytic dependence	59% +/- 4%	59% +/- 4%	59% +/- 4%	59% +/- 4%
Mitochondrial dependence	0	77.39%	0	36.47%
Glycolytic capacity	144.1%	22.6%	144.1%	63.52%
FAO and AAO capacity	39% +/- 4%	39% +/- 4%	39% +/- 4%	39% +/- 4%

Table 24: Glucose-uptake Assay

	Control for Glutor	Glutor	Control for Glupin	Glupin
Glucose uptake	8.97 µM	2.88 µM	8.96 µM	0.53 µM

Table 25: NK cell phenotype after long-terrm treatment with Glutor or Glupin

NK cell phenotype	Control for Glutor	Glutor	Control for Glupin	Glupin
2B4 [geoMean]	16529,2	9296,8	16529,2	12026
NKp30 [geoMean]	23877,4	15959,6	23877,4	21747,4
NKG2D [geoMean]	8944,8	8625,6	8944,8	8940,6
NKp44 [geoMean]	2706	4545,8	2706	5682,4
CD38 [geoMean]	21319	5543,6	21319	8655,2
HLA-DR [geoMean]	7497,2	10738,8	7497,2	8503,6
DNAM-1 [geoMean]	48388,2	53528,8	48388,2	47156,4
NKp46 [geoMean]	20150,6	17558,2	20150,6	17344
CD11a [geoMean]	146301,8	106408	146301,8	127507,6
CD18 [geoMean]	93896,2	69610,8	93896,2	85969,2
NKG2C [geoMean]	8992,8	7743,4	8992,8	8506,2
CD16 [geoMean]	107572	46203,8	107572	46203,8
KLRB1 [%]	52,86	70,94	52,86	66,58
TIGIT [%]	78,22	58,74	78,22	73,1
CD8 [%]	41,08	26,08	41,08	28,976
NKG2A [%]	70,78	68,92	70,78	71,4
TRAIL [%]	83,42	76,52	83,42	90,72
41BB [%]	2,382	4,518	2,382	2,196
KLRG1 [%]	0,886	16,912	0,886	4,354
CD62L [%]	9,03	1,99	2,67	1,12
CD57 [%]	4,85	2,08	4,85	1,48

Table 26: Analysis of Granzyme B and Perforin of ling-term treated NK cells

Analysis of	Control for Glutor	Glutor	Control for Glupin	Glupin
Perforin [MFI]	2646	1908	2646	2483
Granzyme [MFI]	5581	8006	5581	7920

Table 27: Cytokine- and chemokine profile of long-term treated NK cells

[pg/ml]	Control for Glutor	Glutor	Control for Glupin	Glupin
IFN-γ	440,90	805,42	440,90	570,58
TNF-α	20,39	53,04	20,39	54,91
IL-6	1,03	3,4	1,03	1.09
IL-10	5,2	1,8	5,2	1,5
IL-8	58,74	144,05	58,74	129,11
MCP-1	1,34	11,16	1,34	2,00

Table 28: Migration-Assay

Absolute cell count	Control for Glutor	Glutor	Control for Glupin	Glupin
NK cells	9.472	11.119	9.472	10.088
NKT cells	754	1.039	754	894
Monocytes	2.026	936	2.026	1.761
Dendritic cells	1.826	1.375	1.826	2.039
T cells	8.227	10.078	8.227	9.028
B cells	1.089	1.703	1.089	1.206
Granulocytes	7.620	4.912	7.620	7.120

Table 29: CD107a-Assay of long-term treated NK cells

$CD107a^+$ NK cells [%]	Control for Glutor	Glutor	Control for Glupin	Glupin
CD16	66,63%	41,67%	60% +/- 2%	60% +/- 2%
NKp30	71,34%	45,64%	70% +/- 1%	70% +/- 1%
NKG2D + 2B4	21,96%	28,06%	38% +/- 2%	38% +/- 2%

Table 30: IFN-γ secretion of long-term treated NK cells

IFN-γ [pg/ml]	Control for Glutor	Glutor	Control for Glupin	Glupin
CD16	14.440	7.532	14.440	13.770
NKp30	10.098	6.603	9.559	5.941
NKG2D + 2B4	2.625	4.024	3.300	3.500
IL-12 + IL-18	24.723	12.957	24.723	19.629

Table 31: serial-killing assay of long-term treated NK cells

Serial-killing assay	Control for Glutor	Glutor	Control for Glupin	Glupin
Kills/NK cells	1,89	1,46	1,93	2,45
% serial killers	53,73	43,73	56,16	70,59

Table 32: Effect of SCFA on NK cells

	pmTOR [geomean]	CD107a [%]
DMSO	791,83	72,48
0.5 mM Butyrate	772,16	72,86
0.75 mM Butyrate	754,66	75,25
1mM Butyrate	739,5	75,18
2.5mM Pentanoate	767,83	77,43
5mM Pentanoate	788,33	77,33
7.5 mM Pentanoate	785,83	72,15

Table 33: Influence of Etomoxir on NK cell function after long-term treatment with Glupin

$CD107a^+$ NK cells	Without Etomoxir	With Etomoxir
DMSO	64,43%	62,32%
Glupin	58,57%	58,88%

IFN-γ [pg/ml]	Without Etomoxir	With Etomoxir
DMSO	15.264	13.855
Glupin	10.628	9.425

Table 34: Metabolomics

[µM]	DMSO	Glupin
Aspartic acid	19,56	30,03
Threonine	26,63	34,73
Glycine	29,83	50,53
Glutamine	68,33	88,7
Alanine	125	159
Glutamic acid	197,33	307,66
Glucose	315,66	157,66
Pyruvic acid	8,09	3,72
Lactic acid	559,33	397,33
Fumaric acid	1,98	1,85
Choline	2,31	2,37
Methionine	3	3,51
Histidine	2,94	3,90
Succinic acid	2,76	3,4
Lysine	3,31	4,33
Arginine	3,84	4,48
Tyrosine	5,42	6,06
Spermidine	5,23	4,8
Phenylalanine	8,01	10,29
Serine	7,77	5,40
Phosphocreatine	8,69	8,68
Propionic acid	11,03	11,16
Citric acid	13,36	11,23
Leucine	13,7	17,3
Isoleucine	13,63	17,033
Valine	13	16,23
Spermine	19,3	20,36
Isobutyric acid	18,96	23,66
Proline	26,43	32
Taurine	87,73	96,23

Eidesstattliche Versicherung (Affidavit)

_____ _____

Name, Vorname
(Surname, first name)

Matrikel-Nr.
(Enrolment number)

Belehrung:

Wer vorsätzlich gegen eine die Täuschung über Prüfungsleistungen betreffende Regelung einer Hochschulprüfungsordnung verstößt, handelt ordnungswidrig. Die Ordnungswidrigkeit kann mit einer Geldbuße von bis zu 50.000,00 € geahndet werden. Zuständige Verwaltungsbehörde für die Verfolgung und Ahndung von Ordnungswidrigkeiten ist der Kanzler/die Kanzlerin der Technischen Universität Dortmund. Im Falle eines mehrfachen oder sonstigen schwerwiegenden Täuschungsversuches kann der Prüfling zudem exmatrikuliert werden, § 63 Abs. 5 Hochschulgesetz NRW.

Die Abgabe einer falschen Versicherung an Eides statt ist strafbar.

Wer vorsätzlich eine falsche Versicherung an Eides statt abgibt, kann mit einer Freiheitsstrafe bis zu drei Jahren oder mit Geldstrafe bestraft werden, § 156 StGB. Die fahrlässige Abgabe einer falschen Versicherung an Eides statt kann mit einer Freiheitsstrafe bis zu einem Jahr oder Geldstrafe bestraft werden, § 161 StGB.

Die oben stehende Belehrung habe ich zur Kenntnis genommen:

Official notification:

Any person who intentionally breaches any regulation of university examination regulations relating to deception in examination performance is acting improperly. This offence can be punished with a fine of up to EUR 50,000.00. The competent administrative authority for the pursuit and prosecution of offences of this type is the chancellor of the TU Dortmund University. In the case of multiple or other serious attempts at deception, the candidate can also be unenrolled, Section 63, paragraph 5 of the Universities Act of North Rhine-Westphalia.

The submission of a false affidavit is punishable.

Any person who intentionally submits a false affidavit can be punished with a prison sentence of up to three years or a fine, Section 156 of the Criminal Code. The negligent submission of a false affidavit can be punished with a prison sentence of up to one year or a fine, Section 161 of the Criminal Code.

I have taken note of the above official notification.

_____ _____

Ort, Datum
(Place, date)

Unterschrift
(Signature)

Titel der Dissertation:
(Title of the thesis):

_____

_____

_____

Ich versichere hiermit an Eides statt, dass ich die vorliegende Dissertation mit dem Titel selbstständig und ohne unzulässige fremde Hilfe angefertigt habe. Ich habe keine anderen als die angegebenen Quellen und Hilfsmittel benutzt sowie wörtliche und sinngemäße Zitate kenntlich gemacht.
Die Arbeit hat in gegenwärtiger oder in einer anderen Fassung weder der TU Dortmund noch einer anderen Hochschule im Zusammenhang mit einer staatlichen oder akademischen Prüfung vorgelegen.

I hereby swear that I have completed the present dissertation independently and without inadmissible external support. I have not used any sources or tools other than those indicated and have identified literal and analogous quotations.

The thesis in its current version or another version has not been presented to the TU Dortmund University or another university in connection with a state or academic examination.*

*Please be aware that solely the German version of the affidavit ("Eidesstattliche Versicherung") for the PhD thesis is the official and legally binding version.

_____ _____

Ort, Datum
(Place, date)

Unterschrift
(Signature)